CarbonTracker-CH_4 Documentation

CT-CH_4 2025 release

Published on April 1, 2025

Youmi Oh[1,2], Lori Bruhwiler[1], Xin Lan[1,2], Kenneth Schuldt[1,2], Sourish Basu[3], Kirk Thoning[1], Sylvia Englund Michel[4], Reid Clark[4], John B. Miller[1], Arlyn Andrews[1], Tuula Aalto[5], Marcos Andrade[3], Shuji Aoki[6], Francesco Apadula[7], Jgor Arduini[8], Sabrina Arnold[9], Bianca Baier[1], Lukas Bäni[10], Jakub Bartyzel[11], Gilles Bentz[12], Tobias Biermann[13], Sebastien C. Biraud[14], Pierre-Eric Blanc[15], Harald Boenisch[16], Gordon Brailsford[17], Willi A. Brand[18], Dominik Brunner[19], Thao Paul V. Bui[20], Pim van den Bulk[21], Benoit Burban[22], Francescopiero Calzolari[23], Cecilia S. Chang[20], Huilin Chen[24], Lukasz Chmura[11], Yonghoon Choi[25], Jason M. St. Clair[26], Sites Climadat[27], Julian Della Coletta[28], Aurelie Colomb[29], Lino Condori[30], Franz Conen[31], Sébastien Conil[32], Cédric Couret[33], Monica Crippa[34], Paolo Cristofanelli[23], Emilio Cuevas[35], Roger Curcoll[27], Bruce Daube[36], Kenneth J. Davis[37], Jonathan M. Dean-Day[20], Marc Delmotte[12], Ankur Desai[38], Elizabeth DiGangi[39], Glenn S. Diskin[25], Joshua P. DiGangi[25], Michael Elsasser[33], Lukas Emmenegger[19], Gulzhan Esenzhanova[40], Giuseppe Etiope[41], Marc L. Fischer[14], Grant Forster[42], Arnoud Frumau[21], Marta Fuente-Lastra[12], Ryo Fujita[43], Michal Galkowski[11], Luciana V. Gatti[44], Torsten Gehrlein[16], Christoph Gerbig[18], Francois Gheusi[45], Emanuel Gloor[46], Daisuke Goto[47], Samuel Hammer[28], Thomas F. Hanisco[26], László Haszpra[48], Juha Hatakka[5], Martin Heimann[18], Michal Heliasz[13], Daniela Heltai[7], Stephan Henne[19], Arjan Hensen[21], Christian Hermans[49], Ove Hermansen[50], Antje Hoheisel[28], Jutta Holst[51], Tatiana Di Iorio[52], Laura T. Iraci[20], Viktor Ivakhov[53], Daniel A Jaffe[54], Armin Jordan[18], Warren Joubert[55], Hui-Yun Kang[56], Anna Karion[57], Victor Kazan[12], Ralph F. Keeling[58], Petri Keronen[59], Bert Kers[60], Jooil Kim[58], Jörg Klausen[61], Tobias Kneuer[62], Mi-Young Ko[56], Pasi Kolari[59], Katerina Kominkova[63], Eric Kort[64], Elena Kozlova[65], Paul B. Krummel[66], Dagmar Kubistin[62], Susan S. Kulawik[20], Nicolas Kumps[49], Casper Labuschagne[55], Ray L. Langenfelds[66], Andrea Lanza[7], Eric Larmanou[13], Olivier Laurent[12], Tuomas Laurila[5], Thomas Lauvaux[67], Jost Lavric[18], Choong-Hoon Lee[56], Soojeong Lee[56], Haeyoung Lee[17], John Lee[68], Irene Lehner[13], Kari Lehtinen[5], Reimo Leppert[18], Ari Leskinen[69], Markus Leuenberger[70], Ingeborg Levin[28], Janne Levula[59], Matthias Lindauer[62], Mikaell Ottosson Löfvenius[71], Zoe M. Loh[66], Morgan Lopez[12], David Lowry[72], Timothy J. Lueker[58], Chris René Lunder[50], Toshinobu Machida[73], Ivan Mammarella[59], Giovanni Manca[34], Alistair Manning[74], Michal V. Marek[75], Per Marklund[71], Josette E. Marrero[20], Melissa Yang

Martin[76], Damien Martin[77], Giordane A. Martins[78], Hidekazu Matsueda[43], Martine De Mazière[49], Kathryn McKain[1], Frank Meinhardt[33], Malika Menoud[79], Jean-Marc Metzger[80], N. Mihalopoulos[81], Natasha L. Miles[37], Charles E. Miller[82], Meelis Mölder[83], Vanessa Monteiro[37], Stephen Montzka[1], Fred Moore[1], Heiko Moossen[18], Caisa Moreno[84], Eric Morgan[58], Josep-Anton Morgui[27], Shinji Morimoto[6], Jennifer Müller-Williams[62], Mathew Mutuku[85], Cathrine Lund Myhre[50], Jaroslaw Necki[11], Sylvia Nichol[17], Euan Nisbet[72], Yosuke Niwa[73], David Murithi Njiru[85], Steffen Manfred Noe[86], Florian Obersteiner[16], Simon ODoherty[87], Nina Paramonova[53], Caroline L. Parworth[20], Olli Peltola[5], Carole Philippon[12], Salvatore Piacentino[52], Jean Marc Pichon[29], Penelope Pickers[88], Joseph Pitt[74], Jasna Pittman[36], Christian Plass-Dülmer[62], Stephen Matthew Platt[50], Maria Elena Popa[79], Ben Pouter[26], Steve Prinzivalli[39], Michel Ramonet[12], James Randerson[89], Scott J. Richardson[37], Ludwig Ries[33], Louis-Jeremy Rigouleau[12], Pedro P. Rivas[35], Thomas Röckmann[79], Michael Rothe[18], Ju-Mee Ryoo[20], Greg Santoni[36], Alcide Giorgio di Sarra[52], Motoki Sasakawa[73], Bert Scheeren[24], Martina Schmidt[12], Tanja Schuck[90], Marcus Schumacher[18], Thomas Seifert[18], Mahesh Kumar Sha[49], Paul Shepson[91], Owen Sherwood[92], Daegeun Shin[56], Christopher D. Sloop[39], Dan Smale[17], Paul D. Smith[93], Lise Lotte Sørensen[94], Rodrigo A. F. de Souza[95], Gerard Spain[77], Kieran M. Stanley[74], David Steger[19], Martin Steinbacher[19], Britton Stephens[96], Colm Sweeney[1], Risto Taipale[97], Shinya Takatsuji[98], Kirk Thoning[1], Helder Timas[99], Gaston Torres[100], Pamela Trisolino[23], Jocelyn Turnbull[101], Karin Uhse[33], Taku Umezawa[73], Carina van der Veen[79], Alex Vermeulen[51], Brian Viner[102], Gabriela Vitkova[75], Marcel de Vries[60], Andrew Watson[65], Ray Weiss[58], Guido van der Werf[103], Dietmar Weyrauch[62], Steven C. Wofsy[104], Justin Worsey[65], Doug Worthy[105], Irène Xueref-Remy[106], Emma L. Yates[20], Dickon Young[74], Camille Yver-Kwok[12], Sönke Zaehle[18], Andreas Zahn[16], Giulia Zazzeri[72], Christoph Zellweger[19], Zhen Zhang[107], Miroslaw Zimnoch[11]

1 NOAA Global Monitoring Laboratory, USA
2 University of Colorado, Boulder, USA
3 University of Maryland, USA
4 Institute of Arctic and Alpine Research, University of Colorado, USA
5 Finnish Meteorological Institute, Climate System Research, Helsinki, Finland
6 Tohoku University, Japan
7 Ricerca sul Sistema Energetico, Milano, Italy
8 University of Urbino, Italy
9 Deutsches Zentrum für Luft- und Raumfahrt (DLR), Institut für Physik der Atmosphäre, Germany
10 University of Bern, Switzerland
11 AGH University of Krakow, Poland
12 Laboratoire des Sciences du Climat et de l'Environnement, (LSCE-IPSL), CEA-CNRS-UVSQ, Université Paris-Saclay, France
13 Lund University, Centre for Environmental and Climate Science, Sweden
14 Lawrence Berkeley National Laboratory, USA
15 Observatoire Des Sciences De Lunivers Institut Pythéas, France
16 Institute of Meteorology and Climate Research (IMK), Karlsruhe Institute of Technology (KIT), Germany

17 National Institute of Water and Atmospheric Research, New Zealand
18 Max-Planck-Institute for Biogeochemistry, Germany
19 Empa, Swiss Federal Laboratories for Materials Science and Technology, Switzerland
20 NASA Ames Research Center, USA
21 Netherlands Organisation for Applied Scientific Research
22 Joint Research Unit Ecology of Guianan Forests, France
23 The Institute of Atmospheric Sciences and Climate (CNR-ISAC), Italy
24 Centre for Isotope Research, Energy and Sustainability Research Institute Groningen, University of Groningen, Netherlands
25 NASA Langley Research Center, USA
26 NASA Goddard Space Flight Center, USA
27 Institut de Ciencia i Tecnologia Ambientals, Universitat Autonoma de Barcelona, Spain
28 Universitaet Heidelberg, Germany
29 Observatoire de Physique du Globe de Clermont Ferrand, France
30 Servicio Meteorologico Nacional, Argentina
31 University of Basel, Switzerland
32 Agence nationale pour la gestion des déchets radioactifs, France
33 Umweltbundesamt, Germany
34 European Commission, Joint Research Centre, Ispra, Italy
35 State Meteorological Agency of Spain, Spain
36 Harvard University, USA
37 Penn State University, USA
38 University of Wisconsin, USA
39 Earth Networks, an AEM brand
40 The Agency On Hydrometeorology Under The Ministry Of Emergency Situation Of The Kyrgyz Republic, Kyrgyzstan
41 Istituto Nazionale di Geofisica e Vulcanologia, Italy
42 National Centre for Atmospheric Science, UK
43 Meteorological Research Institute, Japan
44 National Institute for Space Research (INPE), Center of Terrestrial System Science (CCST), Greenhouse Gas Laboratory (LaGEE), Brazil
45 Observatoire Midi-Pyrenees, France
46 University of Leeds, UK
47 National Institute of Polar Research, Japan
48 Research Centre for Astronomy and Earth Sciences, Hungary
49 Royal Belgian Institute for Space Aeronomy, Belgium
50 NILU, Kjeller, Norway
51 Lund University, Dept. Phys. Geography & Ecosystem Science, Sweden
52 Italian National agency for new technologies, Energy and sustainable economic development, laboratory UTMEA-TER Earth Observations and Analyses, Italy
53 Voeikov Main Geophysical Observatory, Russia
54 University of Washington, USA
55 South African Weather Service, South Africa
56 Korea Meteorological Administration, South Korea
57 National Institute of Standards and Technology, USA
58 Scripps Institution of Oceanography, USA
59 Institute for Atmospheric and Earth System Research/Physics, Faculty of Sciences, University of Helsinki, Finland
60 University of Groningen, Centre for Isotope Research, Netherlands
61 Federal Office of Meteorology and Climatology MeteoSwiss, Switzerland
62 Hohenpeißenberg Meteorological Observatory, Germany
63 Global Change Research Institute of the Czech Academy of Sciences, Czech Republic
64 University of Michigan, USA
65 University of Exeter, Centre for Environmental Data Analysis, UK
66 Commonwealth Scientific and Industrial Research Organisation, Environment, Aspendale, Victoria, Australia

67 *University of Reims Champagne-Ardenne, France*
68 *University of Maine, USA*
69 *University of Eastern Finland, Finland*
70 *Climate and Environmental Physics, Physics Institute, University of Bern, Switzerland*
71 *Unit for Field-based Forest Research, Swedish University of Agricultural Sciences, Sweden*
72 *Royal Holloway University London, UK*
73 *National Institute for Environmental Studies, Japan*
74 *University of Bristol, UK*
75 *CzechGlobe -Global Change Research Institute CAS, Czech Republic*
76 *NASA Suborbital Research Center, USA*
77 *National University of Ireland - Galway, Ireland*
78 *Fundação Amazônica de Defesa da Atmosfera, Brazil*
79 *Utrecht University, Netherlands*
80 *Observatoire de Physique de lAtmosphère de la Réunion, France*
81 *Environmental and Chemical Processes Laboratory, University of Crete, Heraklion, Greece*
82 *NASA Jet Propulsion Laboratory, USA*
83 *Lund University , Department of Physical Geography and Ecosystem Science, Sweden*
84 *Laboratorio de Física de la Atmósfera, Bolivia*
85 *Kenya Meteorological Department, Kenya*
86 *Estonian University of Life Sciences, Institute of Forestry and Engineering, Estonia*
87 *Atmospheric Chemistry Research Group School of Chemistry, University of Bristol, UK*
88 *University of East Anglia, UK*
89 *University of California, Irvine, California, USA*
90 *University of Frankfurt, Germany*
91 *Purdue University, USA*
92 *Dalhousie University, Canada*
93 *Swedish University of Agricultural Sciences, Sweden*
94 *Aarhus University, Denmark*
95 *State University of Amazonas, Brazil*
96 *National Center for Atmospheric Research, USA*
97 *University of Helsinki, Finland*
98 *Japan Meteorological Agency, Japan*
99 *Instituto Nacional de Meteorologia e Geofisica, Cape Verde*
100 *Direccion Meteorologica de Chile, Chile*
101 *GNS Science, New Zealand*
102 *Atmospheric Technologies Group, Savannah River National Laboratory, USA*
103 *Wageningen University and Research, Netherlands*
104 *Department of Earth and Planetary Sciences, Harvard University*
105 *Environment and Climate Change Canada, Canada*
106 *Aix-Marseille University, France*
107 *Institute of Tibetan Plateau Research, Chinese Academy of Sciences, China*

Contents

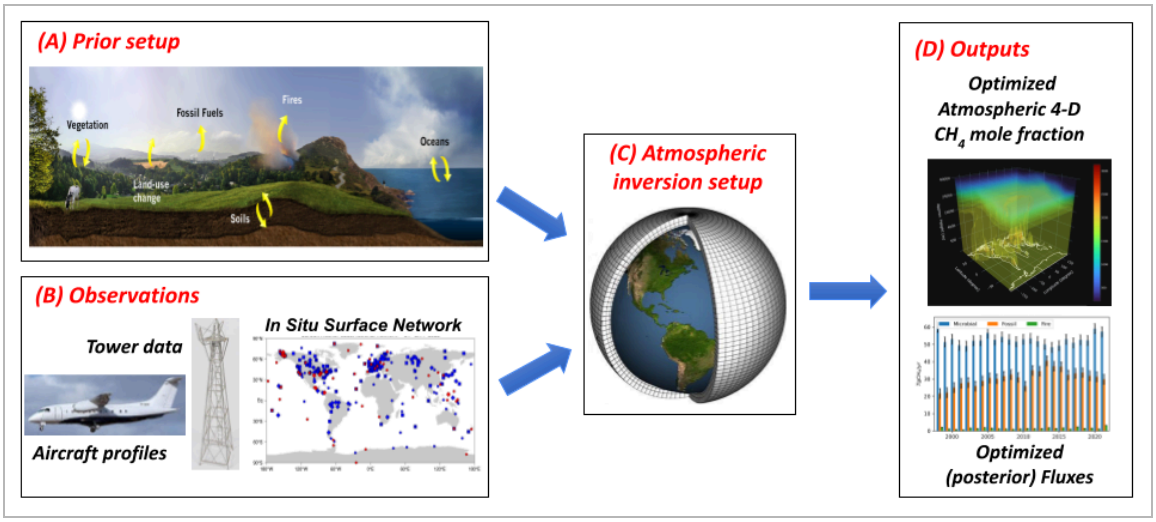
(A) Prior setup
Vegetation
Fossil Fuels
Fires
Oceans
Land-use change
Soils
(B) Observations
Tower data
In Situ Surface Network
Aircraft profiles
(C) Atmospheric inversion setup
(D) Outputs
Optimized Atmospheric 4-D CH_4 mole fraction
Optimized (posterior) Fluxes

The goal of the CarbonTracker-CH_4 is to produce quantitative estimates of methane (CH_4) emissions at the Earth's surface that are consistent with observed patterns of CH_4 and its stable carbon isotope ratios ($\delta^{13}C$-CH_4) in the atmosphere. CarbonTracker-CH_4 is an dual-tracer inverse model of atmospheric CH_4 and $\delta^{13}C$-CH_4, which means that it produces model predictions of atmospheric CH_4 and $\delta^{13}C$-CH_4, to be compared with the observed atmospheric CH_4 and $\delta^{13}C$-CH_4 (**Section B**). The difference between them is attributed to differences in the emissions used to make the prediction (prior) and emissions affecting the true atmospheric CH_4. Using numerical techniques (**Section C**), these differences are used to solve for a set of emissions that most closely matches the observed CH_4 and $\delta^{13}C$-CH_4 in the atmosphere (posterior). CarbonTracker-CH_4 has a representation of atmospheric transport based on meteorological analyses, modules representing emissions from microbial, fossil, and pyrogenic sources, and oxidation by atmospheric chemical reactions and soil microbes (**Section A**). The outputs include global 3-D mole fraction of atmospheric CH_4, monthly estimation of microbial, fossil, and pyrogenic sources, and pre-processed observations of atmospheric CH_4 and $\delta^{13}C$-CH_4 used for CarbonTracker-CH_4 (**Section D**). CarbonTracker-CH_4 is updated on an approximately annual basis, and the current release, CT-CH_4 2025, provides results from 1997 through the end of 2023.

A. Prior setup

1. Prior emissions

For CarbonTracker-CH_4 2025, we updated anthropogenic emissions to EDGAR v8.0 (European Commission et al. 2023), revised global wetland emissions based on (Zhang et al. 2025), revised tropospheric chlorine sinks based on (Wang et al. 2019), and revised geologic seep emissions based on (Hmiel et al. 2020) (Table 2). Prior estimates of emissions from microbial, fossil, and pyrogenic sources are based on bottom-up inventories and process-based models (Figure 1 and Table 2). **Our current inversion approach is to estimate fluxes from total microbial, fossil, and pyrogenic sources, rather than estimating each source sector separately** (Basu et al. 2022)**. Our use of atmospheric isotope data allows observational constraints on the partitioning between fossil and microbial emissions, but little information on how emissions are distributed among the source sectors (e.g. anthropogenic and natural microbial sources).** Based on the posterior mean estimates of global methane (CH_4) emissions, about 35% of CH_4 emissions is from anthropogenic microbial sources, 30% is from natural microbial sources, 30% is from fossil sources, and 5% is from pyrogenic sources (Figure 1). Detailed information on each source sector can be found in the following sections.

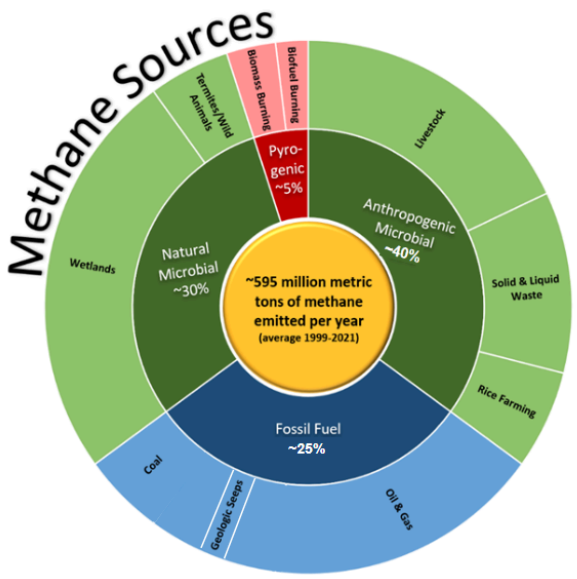

Figure 1. Piechart of estimated mean global CH_4 emissions from microbial, fossil, and pyrogenic source sectors. Credit: Amy Leibrand.

1.1. Microbial

1.1.1. Anthropogenic microbial (e.g. ruminants, waste, and rice)

Agriculture is the most significant source of CH_4 emitted by human activity (200-240 $TgCH_4$/yr) (Saunois et al. 2020). Ruminants, such as cattle, goats, sheep, and buffalo can convert hard-to-digest forage to energy through a process called enteric fermentation, in which microbes produce easily digested material inside the animal's gut. Most of the CH_4 produced in this way exits the animal via belching, however, a small portion emerges from flatulence. CH_4 emissions from animals can be reduced by the use of more easily digested feed, and research to develop dietary supplements targeted at reducing these emissions is ongoing (Abbott et al. 2020). Emissions from enteric fermentation are expected to increase as the global population and affluence grows.

Animal waste, wastewater, and landfills produce CH_4 when conditions favor anaerobic decomposition. This is the process by which organic material decomposes in low oxygen conditions by chains of microbial processes that produce mostly CH_4 and carbon dioxide (CO_2). CH_4 produced in landfills or waste treatment facilities can be captured and used as fuel rather than being vented into the atmosphere (Themelis & Bourtsalas 2021).

Rice agriculture is also a significant source of CH_4 in the atmosphere. This is because warm, waterlogged rice paddies are ideal for the development of anaerobic conditions

and methanogenesis. Bottom-up estimates of emissions from rice agriculture are about 25-40 $TgCH_4$/yr (Saunois et al. 2020), and emissions can be significantly reduced by drainage of paddies between harvests, application of fertilizer, and development of varieties of rice that tolerate drier conditions.

This release of CarbonTracker-CH_4 uses the 1x1 degree gridded emissions from EDGAR v8.0 as prior emission estimates for emissions from rice agriculture, enteric fermentation, animal waste management, wastewater, and landfills (European Commission et al. 2023)(Janssens-Maenhout et al. 2019).

1.1.2. Natural microbial (wetlands, wild animals, termites, and other aquatic sources)

The largest source of CH_4 from natural sources is wetlands. Wetlands are defined as regions that are permanently or seasonally waterlogged, and they can be broadly categorized into marshes, swamps, bogs and fens. Wetlands include both high-latitude peat bogs and typically low-latitude tropical swamps. Saturated soils in warm tropical environments tend to produce the most CH_4, however, warming Arctic temperatures raise concern for increasing output from high-latitude wetlands and future decomposition of carbon that is currently stored in the frozen soils of the Arctic (Schuur et al. 2022; Zhang et al. 2023).

CH_4 is easily oxidized in overlying aerobic water columns or wetlands. Because of this, for a wetland to be most productive, the water table must be at or near the surface or the depth of overlying water must be shallow, or plants with aerenchyma acts as a rapid path to bypass the oxic surface layers (Le Mer & Roger 2001; McNicol et al. 2023). Over time, wetland plants have adapted to low oxygen environments with hollow stems to allow the delivery of oxygen and other gases to their root systems. These hollow stems also allow transport of CH_4 directly to the atmosphere, which along with bubbles, accounts for most of the CH_4 transport into the atmosphere. Diffusion also occurs but is thought to be significantly smaller. Estimates of global emissions from wetlands are about 100-200 $TgCH_4$/yr with most coming from tropics (Saunois et al. 2020), which we hope to narrow with CarbonTracker-CH_4. Most of this occurring in tropical regions. Because emissions are sensitive to temperature and precipitation, they exhibit significant seasonal cycles (especially at high latitudes) and inter-annual variability (Zhang et al. 2017).

Other natural sources of CH_4 include enteric fermentation in insects (mainly termites) and wild animals. Both of these sources are thought to be much smaller than that from wetlands (10-25 $TgCH_4$/yr) (Bergamaschi et al. 2007; Lan et al. 2021).

Recent studies found that CH_4 emissions from aquatic ecosystem sources are largely underestimated (Rosentreter et al. 2021). Since the estimation of aquatic sources is highly uncertain (25 to more than 200 $TgCH_4$/yr) (Saunois et al. 2020; Zhuang et al. 2023), the aquatic sources were not considered for this release of CarbonTracker-CH_4.

CH_4 emissions from wetlands are difficult to quantify for two reasons; their global spatial distribution is difficult to accurately pinpoint and there is large variability in conditions that lead to CH_4 production. This release of CarbonTracker-CH_4 uses the 1x1 degree gridded wetland emissions of CH_4 from a process-based model, a LPJ-wsl (Zhang et al. 2025). The terrestrial ecosystem model LPJ-wsl is a process-based land surface model developed for simulating the fully coupled water and carbon budget of the terrestrial biosphere based on the development of the LPJ dynamic global vegetation model (Calle & Poulter 2020). Inundation is simulated by a TOPMODEL hydrological framework (Zhang et al. 2015), which determines the area fraction with soil water saturation from the knowledge of the mean watershed water table depth and a probability density function of combined topographic and soil properties.

1.2. Fossil

Humans first began influencing the carbon cycle by adapting their environment to fit their needs. Early humans used fire to control animals and later cleared forests for agriculture. Over the last two centuries, following the industrial and technical revolutions as well as a significant increase in global population, fossil fuel combustion is now the largest anthropogenic source of CO_2 (Crippa et al. 2020). Coal, oil, and natural gas are the most common energy sources.

CH_4 is the principal component of natural gas. It leaks to the atmosphere during natural gas production and transport, and these leaks contribute a considerable amount to atmospheric CH_4 levels. Natural gas can also be a side product of oil production that is flared, or vented to the atmosphere. Together, anthropogenic emissions from oil and gas production are thought to contribute about 70-100 $TgCH_4$/yr (~10% of the global annual CH_4 sources) based on bottom-up inventories (Saunois et al. 2020). CH_4 is also associated with coal deposits and can be released when pulverizing coal, an important step in preparing coal for power production. However, the largest contribution from coal production is venting directly to the atmosphere from coal mines. Emissions from coal may contribute an additional 30-60 $TgCH_4$/yr.

As of 2022, coal supplied only about 20% to the U.S. electricity generation, and its share has been dropping as natural gas and renewables have become less expensive (https://www.eia.gov/tools/faqs). Coal has high environmental costs; leveling of

mountaintops, pollution of waterways, emissions of sulfur and nitrogen oxides, as well as mercury are all associated with coal production and combustion. In addition, the amount of CO_2 emitted per unit of energy produced is about twice that of natural gas, making coal an environmentally costly choice for energy production (Ren & Patel 2009). China is the world's largest consumer of coal, followed by India and the U.S. In China, coal supplied about 55% of China's total energy consumption in 2021, and China's fossil consumption has increased by more than a factor of three over the last two decades (https://www.eia.gov/international/analysis/country/CHN).

Combustion of natural gas currently generates 60% of electricity in the U.S in 2022 (https://www.eia.gov/tools/faqs/faq.php?id=427&t=3). Its popularity as a fuel has grown due to its efficiency and lower air quality and climate impacts. Advances in recovery of natural gas, principally hydraulic fracturing, have led to increases in reserve estimates. It is now thought that the U.S. has a large enough natural gas supply to last nearly a century based on current consumption. U.S. shale gas production accounted for 80% of the global shale gas production in 2022 (https://www.eia.gov/tools/faqs/faq.php?id=907&t=8).

Lastly, natural fossil CH_4 can be emitted from geologic seeps in shallow coastal waters (Hmiel et al. 2020). In order for this to happen, the overlying water column must be shallow since CH_4 is efficiently removed by anaerobic microbial processes. This means that the water column must be shallow enough for bubbles to deliver CH_4 directly to the air at the surface, called ebullition. Fossil CH_4 can also be emitted from terrestrial seeps and other features such as mud volcanoes and hot springs. Estimates of the contribution of geologic emissions vary from negligible to 40-60 Tg CH_4/yr or more, making this process highly uncertain (Judd 2004; Saunois et al. 2020).

This release of CarbonTracker-CH_4 uses the 1x1 degree gridded emissions from the EDGAR v8.0 as prior emission estimates for anthropogenic fossil fuel emissions (European Commission et al. 2023)(Janssens-Maenhout et al. 2019). We use natural fossil emissions reported by (Hmiel et al. 2020).

1.3. Pyrogenic (biomass and biofuel burning)

Fire is an important part of the carbon cycle. Even before human civilization began to use fire to clear land for agricultural purposes, most ecosystems were subject to natural wildfires. These fires rejuvenated old forests in various ways including reintroducing important minerals to the soils. As fires consume a landscape, in either controlled or natural burning, CO_2, CO, and CH_4 (among many other gasses and aerosols) are released in significant quantities. Each year, vegetation fires emit around 2 PgC as CO_2

into the atmosphere, mostly in the tropics (Van Der Werf et al. 2017). Fires are a relatively small part of the atmospheric CH_4 budget: ~30 $TgCH_4$/yr, however, they are an important contribution to the inter-annual variability of CH_4 (Randerson et al. 2018). A large fraction of present-day fires are started by humans, with most started intentionally to clear land for agriculture, or to re-fertilize soils before a new growing season.

For biomass and biofuel burning emissions of this CarbonTracker-CH_4 release, we use the Global Fire Emission Database (GFED) 4.1s for 1997–2023 (Van Der Werf et al. 2017).

2. Isotopic signatures of emission sources

The stable carbon isotopic ratios (in delta notation, $\delta^{13}C\text{-}CH_4$) describes the ratio of the heavy isotope to the light isotope in the sample ($R_{sam}=(^{13}C/^{12}C)_{sam}$) relative to a known standard ratio, R_{std}, which is Vienna Pee Dee Belemnite (VPDB) for carbon (Equation below). The deviation of this ratio-of-ratios from one is multiplied by 1000 to express isotope variations in parts per thousand (‰, permil).

$$\delta^{13}C = (R_{sam}/R_{std})-1$$

Measurements of atmospheric CH_4 abundance and $\delta^{13}C\text{-}CH_4$, in combination with isotopic signatures of sources and sinks, allow partitioning of CH_4 budgets into different source categories. This is because isotopic signatures of source categories differ significantly, where the $\delta^{13}C\text{-}CH_4$ of microbial sources (−61.7±6.2‰) is isotopically more depleted (i.e. more of the lighter carbon isotope) than fossil (−44.8±10.7‰) and biomass burning (−26.2±4.8‰) sources (Sherwood et al. 2021). When the isotopic signature is weighted by spatiotemporal-varying flux in each emi sector, the mean isotopic signature between microbial, fossil, and pyrogenic sources becomes more separable (Figure 2). More information on our source isotopic signature can be found in (Lan et al. 2021).

Instead of optimizing the source signatures, we fix the signatures based on our best understanding from bottom-up inventories and modeling to reduce the degrees of freedom in our inversion system. In principle, it is possible to estimate both CH_4 fluxes and $\delta^{13}C\text{-}CH_4$ source signatures in a dual tracer inversion. However, this makes the problem non-linear and the inversion convergence slow. It is also difficult to construct a prior covariance for $\delta^{13}C\text{-}CH_4$ source signatures since much of the uncertainty stems from extrapolating a limited number of $\delta^{13}C\text{-}CH_4$ signature measurements to the entire domain of CH_4 sources, resulting in errors that are systematic and non-Gaussian. Therefore, we explore the impact of $\delta^{13}C\text{-}CH_4$ signature

uncertainty on our results by running inversions with alternate specifications of δ^{13}C-CH_4signature maps. Please see details in Basu et al. 2022.

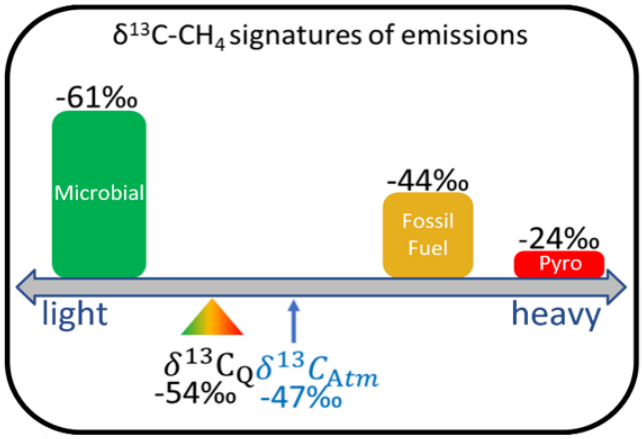

Figure 2. Global mean flux-weighted CH_4 isotopic signature (δ^{13}C-CH_4) of microbial, fossil, and pyrogenic sources. Approximate values of global mean source signatures are shown. Credit. Xin Lan.

2.1. Microbial

For wetland emissions, the spatial map of δ^{13}C-CH_4 from (Ganesan et al. 2018) is used, that is based on global C3/C4 vegetation map and soil pH. We use globally averaged δ^{13}C-CH_4 source signatures for waste/landfills, termites, and rice given insufficient measurement sample size to develop spatial source signature distributions (Sherwood et al. 2017; Sherwood et al. 2021). Ruminant and wild animal source signatures depend strongly on the locally available mix of C3- and C4-based biomass material (Chang et al. 2019). We used the averages of two different global maps of biomass C3/C4 ratios (Randerson et al. 2012; Still et al. 2003) in combination with measurements of C3- and C4-based δ^{13}C-CH_4 source signatures to create global source signature maps at 1°×1° resolution.

2.2. Fossil

The fossil source δ^{13}C-CH_4 signatures are also from the datasets by (Sherwood et al. 2021). In these datasets, fossil signatures were categorized by (1) coal gas, (2) conventional gas, and (3) shale gas (Lan et al. 2021). The global gridded map of fossil isotopic signatures is created based on the spatial distribution of available δ^{13}C-CH_4

signatures. For the U.S. region, we calculate the oil and gas $\delta^{13}C\text{-}CH_4$ mean signature year by year as the average of shale gas and conventional gas signatures for major basins weighted by their respective basin-level gas production volumes at 1°×1° resolution (Lan et al. 2021). For countries without available fossil $\delta^{13}C\text{-}CH_4$ signature data, global average $\delta^{13}C\text{-}CH_4$ values (weighted by country-level production) are used. The other energy/industry category includes small fossil sources, such as the power industry, combustion for manufacturing, aviation, ground transportation and shipping, and iron and steel production, and we use the global weighted average fossil fuel isotopic signature for this category. A spatially resolved global map of $\delta^{13}C\text{-}CH_4$ signatures from geological seepage was developed by (Etiope et al. 2019) and used in this project.

2.3. Pyrogenic

Biomass burning and biofuel burning $\delta^{13}C\text{-}CH_4$ is dependent strongly on the locally available mix of C3- and C4-based biomass material (for combustion or as a food source). Here, we used the averages of two different global maps of biomass C3/C4 ratios (Randerson et al. 2012; Still et al. 2003) in combination with measurements of C3- and C4-based $\delta^{13}C\text{-}CH_4$ source signatures to create global source signature maps at 1° × 1° resolution.

3. Chemical and Soil Sinks of Methane

3.1. Distribution and magnitude

Atmospheric CH_4 has three loss mechanisms: atmospheric oxidation by OH and Cl throughout the atmosphere, destruction by $O(^1D)$ in the stratosphere, and surface uptake in aerobic soils (Figure 3) (Basu et al. 2022; Lan et al. 2021). Atmospheric oxidation of CH_4 in the tropospheric OH and Cl is the largest portion of CH_4 sources (87%), and the atmospheric oxidation in the stratosphere accounts for about 7% of the total CH_4 sinks. A small fraction of CH_4 is consumed by aerobic bacteria in upland soils (6%). **Note: we are not adjusting the chemical sink in this version of Carbontracker-CH_4.**

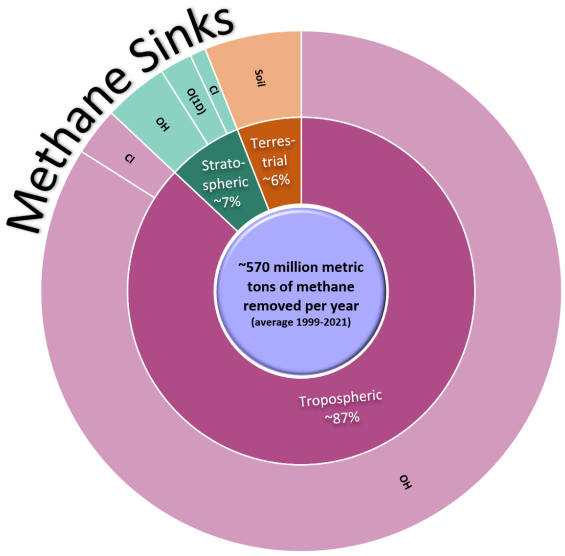

Figure 3. Piechart of global mean CH_4 sinks from atmospheric chemical reactions and soil sinks. Credit: Amy Leibrand.

3.1.1. Atmospheric chemical reactions

CH_4 is removed from the atmosphere primarily by its reaction with the hydroxyl radical (OH), but also by its reaction with atomic chlorine (Cl) and excited-state oxygen (O^1D) in the stratosphere. Methane is also removed in the troposphere by Cl, but this is a small sink comprising ~3% of total global loss. The distribution of Cl in the troposphere is highly uncertain, but because its reaction with CH_4 is strongly fractionating it can have a large effect on the isotopic composition of atmospheric CH_4 (Strode et al. 2020; Gromov et al. 2018). The chemical loss of CH_4 over a year is roughly equal to the total input from its sources (~570 $TgCH_4$/yr), causing the average lifetime of CH_4 in the troposphere to be much shorter (about 9 years) than CO_2 (> 100 years). However, small differences in the total emissions and losses of CH_4, lead to changes in observed CH_4 levels (Figures 1 and 3).

It is difficult to characterize the global distribution of OH because it is extremely reactive as well as it has a short lifespan within the atmosphere. Instead, observations of atmospheric species that have relatively well-known anthropogenic sources and are destroyed only by reaction with OH, such as methyl chloroform (CH_3CCl_3), are used to estimate the abundance of atmospheric OH. Utilizing an empirical approach, (Montzka et al. 2011) noted that the inter-annual variability in atmospheric OH is likely to be within about ~2%. Errors in OH distributions arise from uncertainty in the sources of CH_3CCl_3 used to estimate OH, as well as uncertainties in transport models (Krol et al. 1998) estimate that the uncertainty of OH distribution is 10%.

About 7% of the total chemical loss of CH_4 is due to transport and breakdown in the stratosphere. A small amount of this CH_4-depleted air is returned to the troposphere and has the potential to influence the interpretation of high-altitude (aircraft) measurements of CH_4 (Zhou et al. 2023). In addition, errors in simulating stratosphere-troposphere transport have the potential to produce biases for long-term model simulations.

Errors in the chemical loss of CH_4, and the inability to adequately resolve inter-annual variability of OH, make the estimation of CH_4 fluxes challenging. A 2% variation in the global CH_4 sink is equivalent to ~10 $TgCH_4$/yr, roughly the size of estimated inter-annual variability in CH_4 sources. Currently, the best approach is to use OH fields that are as consistent as possible with existing records of species whose chemistry is significantly linked with OH. Examples include carbon monoxide (CO) and methyl chloroform (CH_3CCl_3) (Patra et al. 2014).

This release of CarbonTracker-CH_4 prescribes and does not optimize methane sinks. Monthly climatological CH_4 loss rates in the stratosphere due to OH, Cl, and $O(^1D)$ were constructed from a run of the ECHAM5/MESSy1 chemistry transport model (Jöckel et al. 2006). Loss due to tropospheric Cl is simulated using a recent model-derived estimate of tropospheric Cl (Wang et al. 2019). For tropospheric OH, we use the monthly OH climatology of (Spivakovsky et al. 2000) after scaling by 0.9 to match the declining atmospheric abundance of methyl chloroform in the early 2000s (Montzka et al. 2011; Basu et al. 2022).

3.1.2. Soil sink of atmospheric CH_4

A natural sink of atmospheric CH_4 is oxidation by microbes in dry soils (~40 $TgCH_4$/yr), but the total size of global soil sinks is uncertain due to undetermined key environmental parameters (Oh et al. 2020; Lee et al. 2023). Wetlands that undergo dry and wet seasons can switch between being sources and sinks of CH_4 as well. This release of CarbonTracker-CH_4 uses the 1x1 degree gridded soil consumption of CH_4 from a process-based model, a Terrestrial Ecosystem Model (TEM) (Zhuang et al. 2013; Liu et al. 2020).

3.2. Fractionation

Each CH_4 sink process has a different preference for reacting with the light ^{12}C over the heavier ^{13}C (Figure 4). The fractionation between ^{12}C and ^{13}C for each of the sink reactions is modeled as the equation below (Saueressig et al. 2001), where *T* is the air temperature in Kelvin. Coefficients *C* and *D* that we used are tabulated in Table 1.

$$k_{12}/k_{13}=1/\alpha=Ce^{D/T}$$

Compared to ((Basu et al. 2022), we changed the OH fractionation factor from 1.0039 (Saueressig et al. 2001) to 1.0054 (Cantrell et al. 1990), because the simulation with the latter fractionation improves representation of the seasonality and latitudinal gradients of observed CH_4 isotopes.

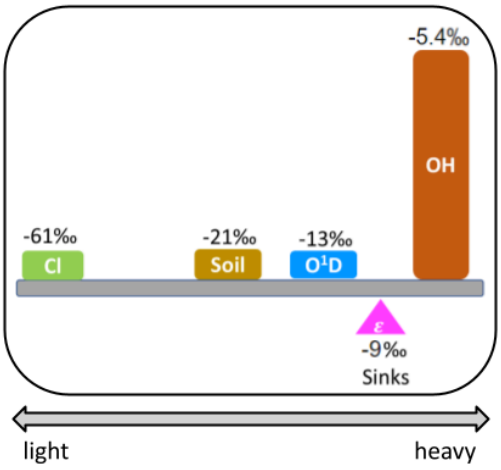

Figure 4. The global mean process-weighted isotopic signature of atmospheric chemical sinks and soil sinks. Credit. Xin Lan.

Table 1. Fractionation parameters for CH_4 sink processes

Loss reaction	**C**	**D(K)**	**Reference**
Loss of OH	1.0054	0.00	(Cantrell et al. 1990)
Loss of Cl	1.0430	6.46	(Saueressig et al. 2001)
Loss of O^1D	1.0130	0.00	(Saueressig et al. 2001)
Soil sink	1.0215	0.00	(King S. L. Quay P. D. Lansdown J. 1989)

4. Global mass balance

Modeling $\delta^{13}C\text{-}CH_4$ in the atmosphere requires special care to spin up the model to a quasi-steady state to avoid initial condition artifacts during the analysis period (Tans,

1997). The time required for atmospheric $\delta^{13}C\text{-}CH_4$ to reach a steady state can be significantly longer than even the CH_4 lifetime of ~9 years, depending on the size of the atmospheric CH_4 burden and how far off the initial $\delta^{13}C\text{-}CH_4$ is. Thus, we spun up our model for 14 years from 1984 to 1997, and selected 1998–2021 as the analysis period. To further avoid the initial condition artifacts, we adjust our prior to satisfy global mass balance requirements for CH_4 and $\delta^{13}C\text{-}CH_4$ (Lan et al. 2021).

The sum of the bottom-up CH_4 emission estimates described above is not consistent with top-down estimates of global total emissions based on observed atmospheric CH_4 growth and estimated loss, which requires a 67 Tg yr^{-1} increase in the annual global emission in 2021 compared to the 1999–2006 when atmospheric growth was small. In addition, the $\delta^{13}C\text{-}CH_4$ mass balance requires 145 Tg yr^{-1} emissions from fossil sources (including natural geological seeps) to be consistent with observed averaged $\delta^{13}C\text{-}CH_4$ in the atmosphere. Therefore, we (i) scale the oil and gas emissions from EDGAR v8.0 to reach a total of 140 Tg yr^{-1} from all fossil sources, and (ii) impose a linear trend on microbial emissions to achieve an increase of 67 Tg yr^{-1} in total 2021 emissions compared to 1999–2006. This ensures that our global CH_4 and $\delta^{13}C\text{-}CH_4$ budgets approximate the long-term trends in atmospheric CH_4 and $\delta^{13}C\text{-}CH_4$ during our simulation period. We kept the prior flux of 2022-2023 same as 2021.

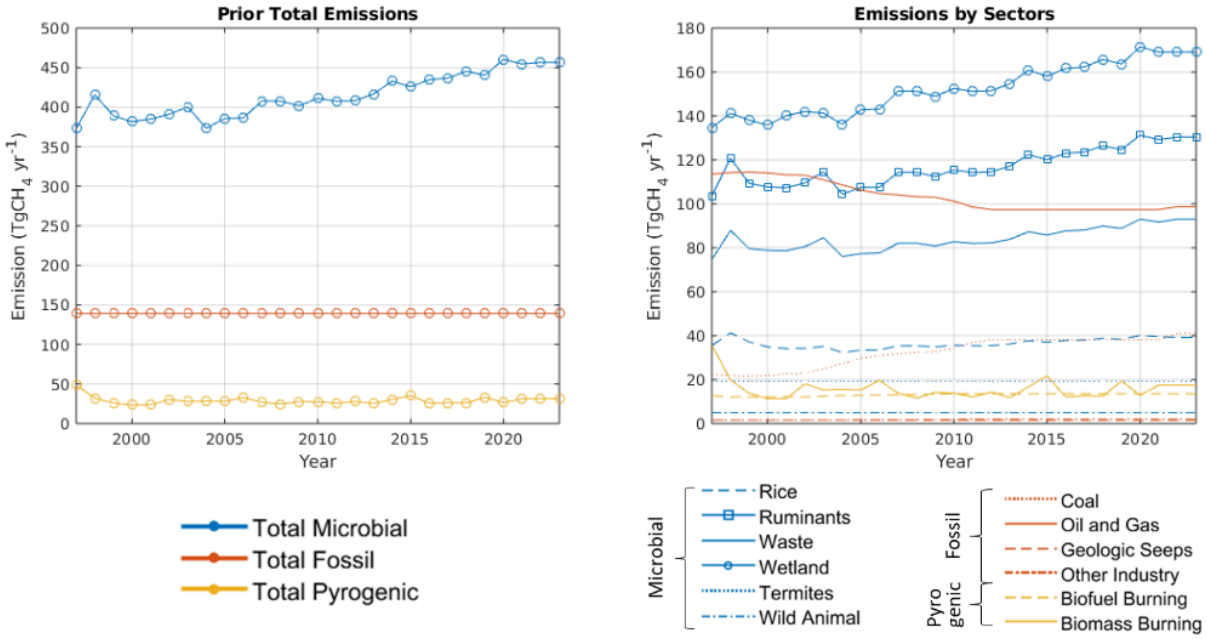

Figure 5. Long-term annual emissions of total microbial, fossil, and pyrogenic sources (left) and each source sector (right) after the global mass balance of atmospheric CH_4 and $\delta^{13}C\text{-}CH_4$.

5. Summary table of data sources for prior sources and sinks

Table 2 summarizes data sources for different CH_4 sources and their source signatures, and table 3 summarizes data sources for different CH_4 sinks and their fractionation factors, that we used for this release of Carbontracker-CH_4.

Table 2. Data sources for total source emissions and δ^{13}C-CH_4 source signatures for this version of CarbonTracker-CH_4.

Source	**Source sector**	**Total emissions**	***δ^{13}C-CH_4 source signatures***
Fossil Emission	Coal, oil and natural gas, and other energy/industry	EDGAR v8.0 (European Commission et al. 2023)	(Sherwood et al. 2021)
	Geological seeps	(Hmiel et al. 2020)	(Etiope et al. 2019)
Biomass and biofuel burning	Biomass burning fluxes	GFED 4.1s (Randerson et al. 2018; Van Der Werf et al. 2017)	(Randerson et al. 2012; Still et al. 2003)
	Biofuel fluxes	EDGAR v8.0 (European Commission et al. 2023)	(Randerson et al. 2012; Still et al. 2003)
Microbial Emission	Ruminants fluxes	EDGAR v8.0 (European Commission et al. 2023)	(Randerson et al. 2012; Still et al. 2003)
	Waste and landfills fluxes		(Sherwood et al. 2021)
	Rice fluxes		
	Wild animals and termites fluxes	(Bergamaschi et al. 2007)	

	Wetland and soil sink	LPJ-wsl (Zhang et al. 2025)	(Ganesan et al. 2018)

Table 3. Data sources for sink strength/distribution and fractionation for this version of CarbonTracker-CH_4.

Sink	Location	Distribution	Fractionation
Loss of OH	Troposphere	(Spivakovsky et al. 2000); (Montzka et al. 2011)	(Cantrell et al. 1990)
	Stratosphere	(Jöckel et al. 2006)	
Loss of Cl	Troposphere	(Wang et al. 2019)	(Saueressig et al. 1995)
	Stratosphere	(Jöckel et al. 2006)	
Loss of O1D	stratosphere	(Jöckel et al. 2006)	(Saueressig et al. 2001)
Soil sink	Terrestrial	(Zhuang et al. 2013; Liu et al. 2020)	(King et al. 1989)

B. Observations

1. Atmospheric CH_4 measurement dataset

For the CarbonTracker-CH_4 version 2025, we incorporated NOAA GML's GLOBALVIEWplus products to reduce duplication in efforts to collecting datasets. Specifically, we used version 'obspack_ch4_1_GLOBALVIEWplus_v7.0_2024-10-29' for CH_4 datasets(Fig. 6). This significantly increased our total CH_4 data points from 9 to 20 million. The GLOBALVIEW product is constructed using the Observation Package (ObsPack) framework (Masarie et al. 2014). The framework is designed to bring together atmospheric greenhouse gas (GHG) observations from a variety of sampling platforms, prepare them with specific applications in mind, and package and distribute them in a self-consistent and well-documented product. ObsPack products are intended to support GHG budget studies and represent a new generation of cooperative value-added GHG data products. This product includes 479 atmospheric methane datasets derived from observations made by 66 laboratories from 27 countries. Data for the period 1983-2023 (where available) are included. For more details on the GLOBALVIEWplus (GV+) datasets, please refer to: https://gml.noaa.gov/ccgg/obspack/index.html.

2. Atmospheric *$\delta^{13}C$-CH_4 measurement dataset*

We used *$\delta^{13}C$-CH_4* data from the Institute for Arctic and Alpine Research (INSTAAR) as well as other isotope laboratories making precise measurements of atmospheric CH_4 with isotope ratio mass spectrometers (Fig. 6). The INSTAAR *$\delta^{13}C$-CH_4* data were measured in a subset of air samples collected from NOAA's Global Greenhouse Gas Reference Network (GGGRN). Because different labs have independent ties to primary reference materials which may not agree, we calculated offsets to bring the *$\delta^{13}C$-CH_4* data onto the INSTAAR realization of the Vienna Pee Dee Belemnite (VPDB) scale (Miller et al. 2002). These offsets were based on measurements of cylinders, flasks filled from cylinders, or co-located sample data, and are all described in (Umezawa et al. 2012). When there was not a direct comparison, we used comparisons between each of these labs and the Institute for Marine and Atmospheric research Utrecht (IMAU). Each comparison had an uncertainty associated with it, and these were combined in quadrature to account for uncertainty in the offset correction. The total measurement uncertainty in assimilated *$\delta^{13}C$-CH_4* datasets was typically less than 0.15‰. This internal product includes 82 atmospheric methane isotope datasets derived from observations made by 6 laboratories from 5 countries, and data for the period 1991-2023 (where available) are included.

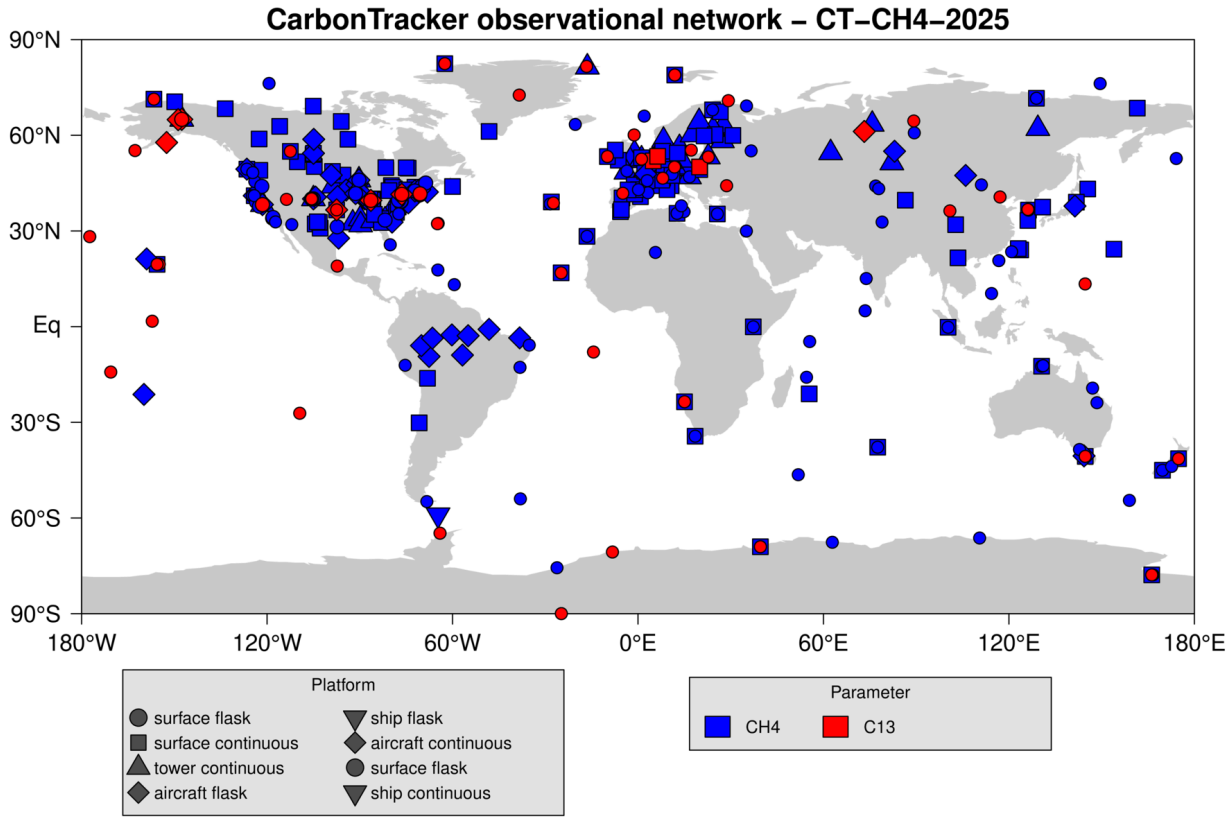
CarbonTracker observational network – CT–CH4–2025
90°N
60°N
30°N
Eq
30°S
60°S
90°S
180°W
120°W
60°W
0°E
60°E
120°E
180°E
Platform
surface flask
surface continuous
tower continuous
aircraft flask
ship flask
aircraft continuous
surface flask
ship continuous
Parameter
CH4
C13

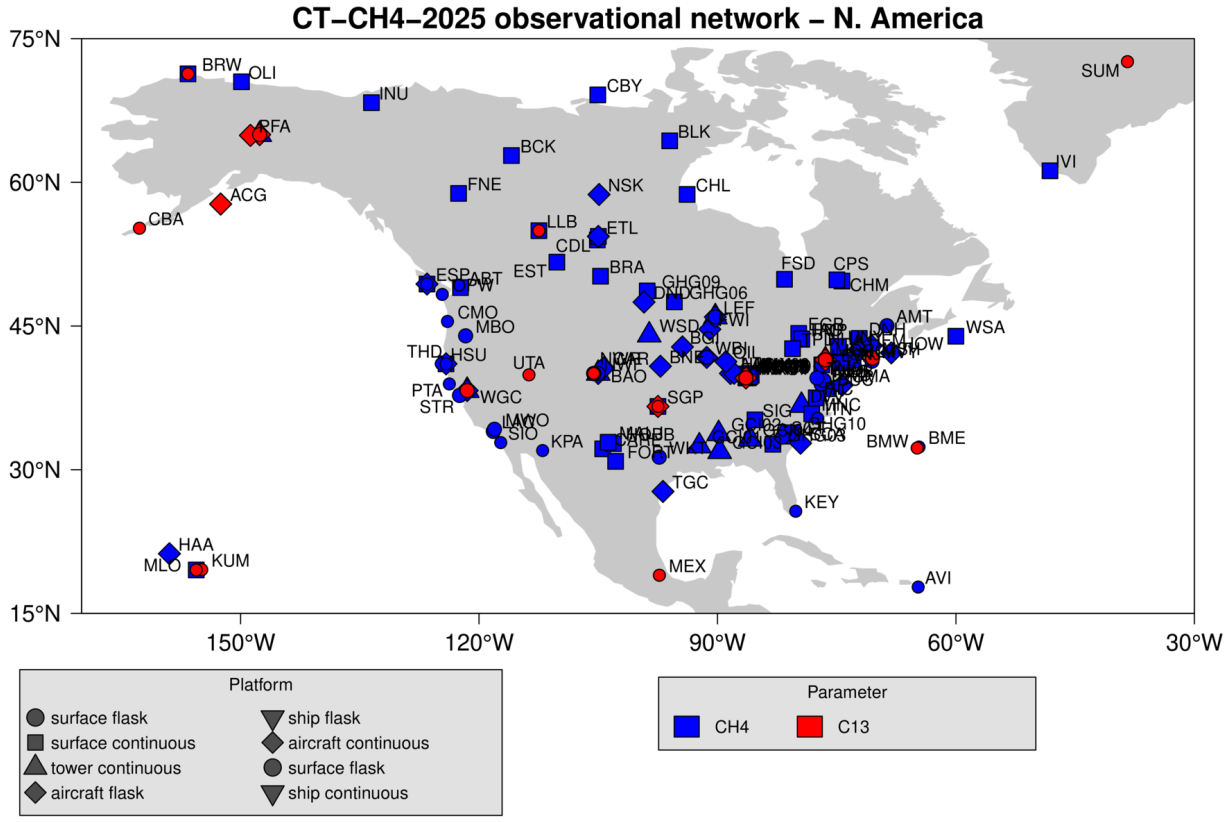
CT–CH4–2025 observational network – N. America
75°N
60°N
45°N
30°N
15°N
150°W
120°W
90°W
60°W
30°W
BRW
OLI
INU
CBY
SUM
IVI
BLK
BCK
FNE
NSK
CHL
ACG
CBA
LLB
ETL
CDL
EST
BRA
FSD
CPS
CHM
GHG09
GHG06
LEF
CMO
MBO
WSD
AMT
WSA
THD
HSU
UTA
BAO
PTA
STR
WGC
SGP
SIC
KPA
BMW
BME
TGC
KEY
HAA
MLO
KUM
MEX
AVI
Platform
surface flask
surface continuous
tower continuous
aircraft flask
ship flask
aircraft continuous
surface flask
ship continuous
Parameter
CH4
C13

Figure 6. Locations of CarbonTracker-CH4 (top) global and (bottom) North American observation sites.

3. *Selection of filtering, withholding, matching, and assimilating dataset*

For CarbonTracker-CH_4 version 2025, we added 3 steps for rigorous filtering, matching, withholding, and assimilating selection before incorporating the dataset into the inversion framework (Figure 7).

First, for each site, we decide if the day time or nighttime observations for a particular site will be assimilated. In addition we decide whether to apply an elevation limit to avoid assimilating data at low elevation due to the local source influence. See Tables 4-5 for information about how data at each site are used. Using site specific criteria, we further filter out sites with a strong source influence ('obs_flag' = 0). We also do not assimilate timeseries that are less than one year in length to avoid assimilation shock from adding limited data.

Second, to avoid data that was not filtered from Step 1, we used the CCG-curve fitting method to filter out outliers more than 3 standard deviations from the monthly mean (including a long-term trend) of that site. More info on the curve fitting is available at: https://gml.noaa.gov/ccgg/mbl/crvfit/crvfit.html. We applied this fitting for 0-5 LST for mountain tower continuous sites, 11-16 LST for all other tower continuous sites, and all hours for other sites. Based on the first and second steps, we only assimilate data points that passed both filters. As a result, only 7.5% of the CH_4 data is assimilated, and 60% of the $\delta^{13}C\text{-}CH_4$ data is assimilated.

As a third step, we added withholding and matching criteria for CH_4 and $\delta^{13}C\text{-}CH_4$ data and created GV+CTCH$_4$ datasets that have additional parameters CTCH4_assim and CTCH4_match. Data are withheld for evaluation of posterior results, while matching refers to making sure that CH_4 and $\delta^{13}C\text{-}CH_4$ data are coincident in space and time. We withheld 5% of the assimilable data and incorporated the temporal dependency, but not the dependency across the sites yet. Based on this, we set the 'CTCH4_assim' parameter to be 0=not assimilated based on the above filetering steps, 1=assimilated, 2=withheld. For each CH_4 dataset, we also assign the number for 'CTCH4_match' to use this parameter when matching it with $\delta^{13}C\text{-}CH_4$ data. After applying the matching algorithm, the final matching rates for $\delta^{13}C\text{-}CH_4$ data was > 90%.

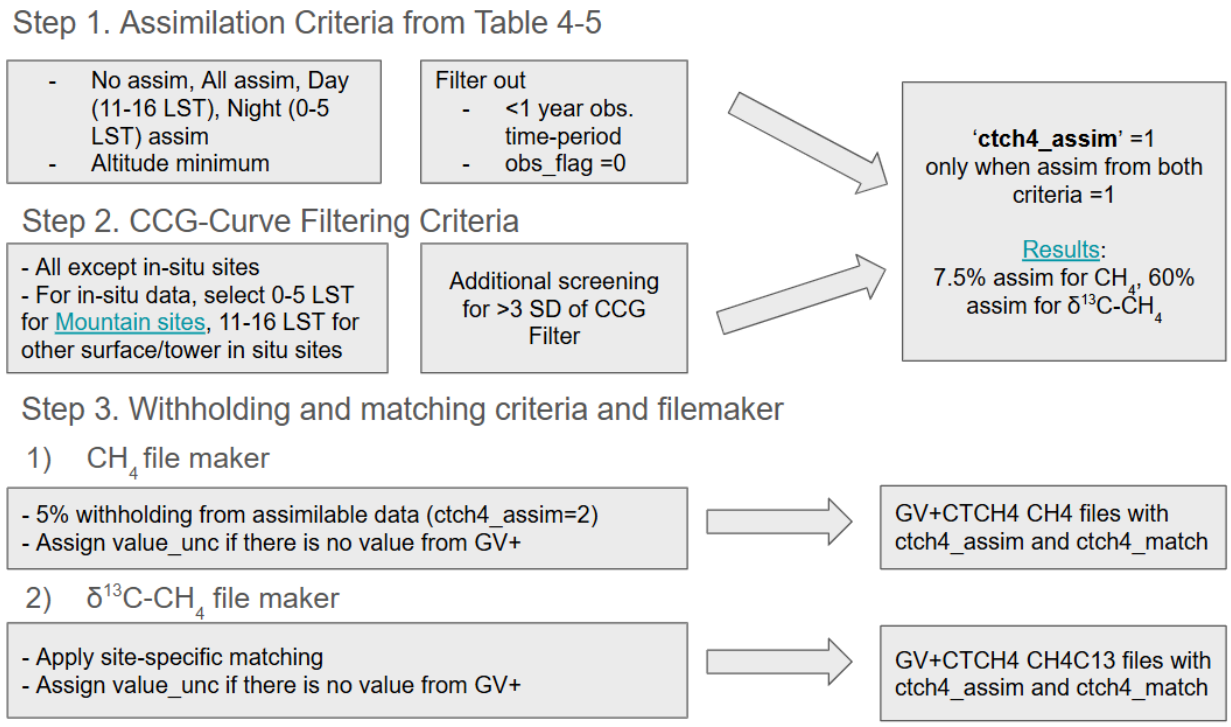

Figure 7. Diagram of data filtering and selection

4. *Model-data mismatch setup*

We set model-data mismatch for CH_4 and $\delta^{13}C\text{-}CH_4$ differently. For CH_4, we followed the method from (Bruhwiler et al. 2014). Specifically, the model–data mismatch values for CH_4 were based on the evaluation of forward simulation with prior fluxes by selecting the one standard deviation of prior bias (prior - observed) for each surface site. For aircraft profiles, model-data mismatch was determined using the one standard deviation of the prior bias at every 1 km vertical interval. We forced the assimilation to closely match remote marine background sites while some sites were given a very large model–data mismatch because they are likely influenced by strong local sources. A complete list of sites and their model–data mismatches for CH_4 sites is shown in Table 6.

For $\delta^{13}C\text{-}CH_4$, we followed the method from (Bergamaschi et al. 2005; Basu et al. 2022). In specific, the model-data mismatch is calculated as the quadrature sum of measurement errors and model errors. We calculated model error by calculating the spatial gradient of modeled $\delta^{13}C\text{-}CH_4$ at the monitoring sites, using horizontally and vertically adjacent model grid cells. A complete list of sites and their model–data mismatches for $\delta^{13}C\text{-}CH_4$ sites is shown in Table 7.

Table 4. Summary of site selection for assimilation and filtering for CH_4.

[Download Here]

	Filename	Assimnighttime	Assimdaytime	Minaltitude		Filename	Assimnighttime	Assimdaytime	Minaltitude		Filename	Assimnighttime	Assimdaytime	Minaltitude
1	ch4_aao_aircraft-pfp_1_allvalid	0	0		**201**	ch4_inx07_surface-insitu_60_allhours-21magl	0	0		**401**	ch4_spo_surface-flask_2_representative	1	1	
2	ch4_above_aircraft-insitu_1_allvalid	0	0		**202**	ch4_inx07_surface-insitu_60_allhours-58magl	0	0		**402**	ch4_ssl_tower-insitu_23_allvalid-12magl	0	0	
3	ch4_abp_surface-flask_1_representative	1	1		**203**	ch4_inx08_surface-insitu_60_allhours-41magl	0	0		**403**	ch4_ssl_tower-insitu_23_allvalid-35magl	0	1	
4	ch4_abt_surface-insitu_6_allvalid	0	1		**204**	ch4_inx09_surface-insitu_60_allhours-130magl	0	0		**404**	ch4_start08_aircraft-insitu_59_allvalid	0	0	
5	ch4_acg_aircraft-pfp_1_allvalid	0	1	1000	**205**	ch4_inx10_surface-insitu_60_allhours-40magl	0	0		**405**	ch4_ste_tower-insitu_147_allvalid-127magl	0	0	
6	ch4_act_aircraft-insitu_428_allvalid-b200	0	0		**206**	ch4_inx11_surface-insitu_60_allhours-130magl	0	0		**406**	ch4_ste_tower-insitu_147_allvalid-187magl	0	0	
7	ch4_act_aircraft-insitu_428_allvalid-c130	0	0		**207**	ch4_inx13_surface-insitu_60_allhours-87magl	0	0		**407**	ch4_ste_tower-insitu_147_allvalid-252magl	0	1	
8	ch4_act_aircraft-pfp_1_allvalid	0	0		**208**	ch4_inx14_surface-insitu_60_allhours-76magl	0	0		**408**	ch4_ste_tower-insitu_147_allvalid-32magl	0	0	
9	ch4_act_aircraft-pfp_1_allvalid-b200	0	0		**209**	ch4_inx15_surface-insitu_60_allhours-75magl	0	0		**409**	ch4_ste_tower-insitu_147_allvalid-82magl	0	0	
10	ch4_act_aircraft-pfp_1_allvalid-c130	0	0		**210**	ch4_inx_aircraft-pfp_1_allvalid	0	0		**410**	ch4_stm_surface-flask_1_representative	1	1	
11	ch4_aia_aircraft-flask_2_representative	0	1		**211**	ch4_inx_surface-pfp_1_allvalid-121magl	0	1		**411**	ch4_str_surface-pfp_1_allvalid-232magl	0	1	
12	ch4_aircorenoaa_aircore_1_allvalid	0	0		**212**	ch4_inx_surface-pfp_1_allvalid-125magl	0	0		**412**	ch4_sum_surface-flask_1_representative	1	1	
13	ch4_ajax_aircraft-insitu_429_allvalid	0	0		**213**	ch4_inx_surface-pfp_1_allvalid-129magl	0	0		**413**	ch4_svb_tower-insitu_440_allvalid-150magl	0	1	
14	ch4_alf_aircraft-pfp_433_representative	0	1	1000	**214**	ch4_inx_surface-pfp_1_allvalid-130magl	0	0		**414**	ch4_svb_tower-insitu_440_allvalid-35magl	0	0	
15	ch4_alt_surface-flask_1	1	1		**215**	ch4_inx_surface-pfp_1_allv	0	0		**415**	ch4_svb_tower-insitu_440	0	0	

	_representative					alid-137magl					_allvalid-85magl			
16	ch4_alt_surface-flask_2_representative	1	1		**216**	ch4_inx_surface-pfp_1_allvalid-39magl	0	0		**416**	ch4_svv_tower-insitu_20_allvalid-27magl	0	0	
17	ch4_alt_surface-flask_45_representative	1	1		**217**	ch4_inx_surface-pfp_1_allvalid-40magl	0	0		**417**	ch4_svv_tower-insitu_20_allvalid-52magl	0	1	
18	ch4_alt_surface-insitu_6_allvalid	0	1		**218**	ch4_inx_surface-pfp_1_allvalid-54magl	0	0		**418**	ch4_syo_surface-flask_1_representative	1	1	
19	ch4_ams_surface-flask_1_representative	1	1		**219**	ch4_ipr_tower-insitu_103_allvalid-100magl	0	1		**419**	ch4_syo_surface-insitu_8_representative	1	1	
20	ch4_amt_surface-flask_1_representative	1	1		**220**	ch4_ipr_tower-insitu_103_allvalid-40magl	0	0		**420**	ch4_tab_aircraft-pfp_433_representative	0	1	1000
21	ch4_amt_surface-pfp_1_allvalid-107magl	0	1		**221**	ch4_ipr_tower-insitu_103_allvalid-60magl	0	0		**421**	ch4_tac_surface-flask_1_representative	0	1	
22	ch4_amy_surface-flask_1_representative	0	1		**222**	ch4_ivi_surface-insitu_11_allvalid	0	1		**422**	ch4_tac_tower-insitu_160_allvalid-100magl	0	0	
23	ch4_amy_surface-insitu_61_allvalid	0	0		**223**	ch4_izo_surface-flask_1_representative	1	1		**423**	ch4_tac_tower-insitu_160_allvalid-185magl	0	1	
24	ch4_aoa_aircraft-flask_19_allvalid	0	0		**224**	ch4_izo_surface-insitu_27_allvalid	1	0		**424**	ch4_tac_tower-insitu_160_allvalid-54magl	0	0	
25	ch4_ara_surface-flask_2_representative	0	1		**225**	ch4_jar_tower-insitu_475_allvalid-110magl	0	1		**425**	ch4_tao_surface-insitu_6_allvalid	0	0	
26	ch4_asc_surface-flask_1_representative	1	1		**226**	ch4_jar_tower-insitu_475_allvalid-30magl	0	0		**426**	ch4_tap_surface-flask_1_representative	0	1	
27	ch4_ask_surface-flask_1_representative	1	1		**227**	ch4_jar_tower-insitu_475_allvalid-50magl	0	0		**427**	ch4_tef_aircraft-pfp_433_representative	0	1	1000
28	ch4_avi_surface-flask_1_representative	1	1		**228**	ch4_jar_tower-insitu_475_allvalid-70magl	0	0		**428**	ch4_tgc_aircraft-pfp_1_allvalid	0	1	1000
29	ch4_azr_surface-flask_1_representative	1	1		**229**	ch4_jar_tower-insitu_475_allvalid-90magl	0	0		**429**	ch4_thd_aircraft-pfp_1_allvalid	0	1	1100
30	ch4_azv_tower-insitu_20_allvalid-29magl	0	0		**230**	ch4_jfj_surface-flask_45_representative	1	1		**430**	ch4_thd_surface-flask_1_representative	0	1	
31	ch4_azv_tower-insitu_20_allvalid-50magl	0	1		**231**	ch4_jfj_surface-insitu_5_allvalid	1	0		**431**	ch4_thd_surface-insitu_112_allvalid	0	1	
32	ch4_bal_surface-flask_1_representative	0	1		**232**	ch4_jfj_tower-insitu_49_allvalid-13magl	1	0		**432**	ch4_tik_surface-flask_1_representative	1	1	
33	ch4_bao_surface-pfp_1_allvalid-300magl	0	1		**233**	ch4_jfj_tower-insitu_49_allvalid-5magl	0	0		**433**	ch4_tik_surface-insitu_55_allvalid	0	1	
34	ch4_bck_surface-insitu_6_allvalid	0	1		**234**	ch4_jue_tower-insitu_147_allvalid-120magl	0	1		**434**	ch4_toh_tower-insitu_147_allvalid-10magl	0	0	

35	ch4_bgi_aircraft-pfp_1_allvalid	0	1	1300	**235**	ch4_jue_tower-insitu_147_allvalid-50magl	0	0		**435**	ch4_toh_tower-insitu_147_allvalid-110magl	0	0	
36	ch4_bhd_surface-flask_1_representative	1	1		**236**	ch4_jue_tower-insitu_147_allvalid-80magl	0	0		**436**	ch4_toh_tower-insitu_147_allvalid-147magl	0	1	
37	ch4_bhd_surface-insitu_15_baseline	0	1		**237**	ch4_kas_surface-insitu_53_allvalid	1	0		**437**	ch4_toh_tower-insitu_147_allvalid-76magl	0	0	
38	ch4_bik_surface-flask_45_representative	0	1		**238**	ch4_key_surface-flask_1_representative	0	0		**438**	ch4_tom_aircraft-insitu_1_allvalid	0	0	
39	ch4_bik_tower-insitu_45_allvalid-180magl	0	0		**239**	ch4_kit_tower-insitu_147_allvalid-100magl	0	0		**439**	ch4_tom_aircraft-pfp_1_allvalid	0	0	
40	ch4_bik_tower-insitu_45_allvalid-300magl	0	1		**240**	ch4_kit_tower-insitu_147_allvalid-200magl	0	1		**440**	ch4_tpd_surface-insitu_6_allvalid	0	0	
41	ch4_bik_tower-insitu_45_allvalid-30magl	0	0		**241**	ch4_kit_tower-insitu_147_allvalid-30magl	0	0		**441**	ch4_trn_tower-insitu_11_allvalid-100magl	0	0	
42	ch4_bik_tower-insitu_45_allvalid-5magl	0	0		**242**	ch4_kit_tower-insitu_147_allvalid-60magl	0	0		**442**	ch4_trn_tower-insitu_11_allvalid-180magl	0	1	
43	ch4_bik_tower-insitu_45_allvalid-90magl	0	0		**243**	ch4_kjn_surface-flask_45_representative	0	1		**443**	ch4_trn_tower-insitu_11_allvalid-50magl	0	0	
44	ch4_bir_tower-insitu_56_allvalid-10magl	0	0		**244**	ch4_klm_surface-pfp_1_allvalid-4magl	0	0		**444**	ch4_trn_tower-insitu_11_allvalid-5magl	0	0	
45	ch4_bir_tower-insitu_56_allvalid-50magl	0	0		**245**	ch4_korus-aq_aircraft-insitu_428_allvalid-dc8	0	0		**445**	ch4_ugd_aircraft-insitu_1_allvalid	0	0	
46	ch4_bir_tower-insitu_56_allvalid-75magl	0	1		**246**	ch4_kre_tower-insitu_441_allvalid-10magl	0	0		**446**	ch4_ulb_aircraft-pfp_1_allvalid	0	1	2300
47	ch4_bis_surface-insitu_11_allvalid	0	0		**247**	ch4_kre_tower-insitu_441_allvalid-125magl	0	0		**447**	ch4_uld_surface-insitu_61_allvalid	0	1	
48	ch4_bkt_surface-flask_1_representative	0	1		**248**	ch4_kre_tower-insitu_441_allvalid-250magl	0	1		**448**	ch4_uny_surface-insitu_112_allvalid	0	1	
49	ch4_blk_surface-insitu_6_allvalid	0	0		**249**	ch4_kre_tower-insitu_441_allvalid-50magl	0	0		**449**	ch4_ush_surface-flask_1_representative	1	1	
50	ch4_bme_surface-flask_1_representative	1	1		**250**	ch4_krk_surface-insitu_118_allvalid	0	0		**450**	ch4_uta_surface-flask_1_representative	0	1	
51	ch4_bmw_surface-flask_1_representative	1	1		**251**	ch4_krs_tower-insitu_20_allvalid-35magl	0	0		**451**	ch4_uto_surface-insitu_30_allvalid	0	0	
52	ch4_bne_aircraft-pfp_1_allvalid	0	1	1400	**252**	ch4_krs_tower-insitu_20_allvalid-67magl	0	1		**452**	ch4_uum_surface-flask_1_representative	0	1	
53	ch4_bnt_surface-flask_1_representative	1	1		**253**	ch4_kum_surface-flask_1_representative	1	1		**453**	ch4_vac_surface-insitu_431_allvalid	0	1	
54	ch4_bra_surface-insitu_6_allvalid	0	0		**254**	ch4_kzd_surface-flask_1_representative	0	1		**454**	ch4_vgn_tower-insitu_20_allvalid-42magl	0	0	

55	ch4_brm_tower-insitu_49_allvalid-12magl	0	0		**255**	ch4_kzm_surface-flask_1_representative	1	1		**455**	ch4_vgn_tower-insitu_20_allvalid-85magl	0	1	
56	ch4_brm_tower-insitu_49_allvalid-132magl	0	0		**256**	ch4_lef_aircraft-pfp_1_allvalid	0	1	1400	**456**	ch4_vrs_surface-flask_45_representative	1	1	
57	ch4_brm_tower-insitu_49_allvalid-212magl	0	1		**257**	ch4_lef_surface-flask_1_representative	0	1		**457**	ch4_wao_surface-insitu_13_allvalid	0	0	
58	ch4_brm_tower-insitu_49_allvalid-44magl	0	0		**258**	ch4_lef_surface-pfp_1_allvalid-244magl	0	0		**458**	ch4_wbi_aircraft-pfp_1_allvalid	0	1	1200
59	ch4_brm_tower-insitu_49_allvalid-72magl	0	0		**259**	ch4_lef_surface-pfp_1_allvalid-396magl	0	1		**459**	ch4_wbi_surface-pfp_1_allvalid-379magl	0	1	
60	ch4_brw_surface-flask_1_representative	0	0		**260**	ch4_lef_tower-insitu_1_allvalid-122magl	0	0		**460**	ch4_wes_surface-insitu_25_allvalid	0	0	
61	ch4_brw_surface-insitu_1_allvalid	0	0		**261**	ch4_lef_tower-insitu_1_allvalid-30magl	0	0		**461**	ch4_wgc_surface-pfp_1_allvalid-484magl	0	1	
62	ch4_brz_tower-insitu_20_allvalid-20magl	0	0		**262**	ch4_lef_tower-insitu_1_allvalid-396magl	0	1		**462**	ch4_wgc_surface-pfp_1_allvalid-89magl	0	0	
63	ch4_brz_tower-insitu_20_allvalid-40magl	0	0		**263**	ch4_lew_surface-insitu_112_allvalid	0	1		**463**	ch4_wgc_tower-insitu_1_allvalid-30magl	0	0	
64	ch4_brz_tower-insitu_20_allvalid-5magl	0	0		**264**	ch4_lew_surface-pfp_1_allvalid-95magl	0	1		**464**	ch4_wgc_tower-insitu_1_allvalid-483magl	0	1	
65	ch4_brz_tower-insitu_20_allvalid-80magl	0	1		**265**	ch4_lhw_surface-insitu_5_allvalid	0	0		**465**	ch4_wgc_tower-insitu_1_allvalid-91magl	0	0	
66	ch4_bsc_surface-flask_1_representative	0	1		**266**	ch4_lin_tower-insitu_147_allvalid-10magl	0	0		**466**	ch4_wis_surface-flask_1_representative	0	1	
67	ch4_bsd_tower-insitu_160_allvalid-108magl	0	0		**267**	ch4_lin_tower-insitu_147_allvalid-2.5magl	0	0		**467**	ch4_wkt_surface-flask_1_representative	0	1	
68	ch4_bsd_tower-insitu_160_allvalid-248magl	0	1		**268**	ch4_lin_tower-insitu_147_allvalid-40magl	0	0		**468**	ch4_wkt_surface-pfp_1_allvalid-122magl	0	0	
69	ch4_bsd_tower-insitu_160_allvalid-42magl	0	0		**269**	ch4_lin_tower-insitu_147_allvalid-98magl	0	1		**469**	ch4_wkt_surface-pfp_1_allvalid-457magl	0	1	
70	ch4_buc_surface-insitu_112_allvalid	0	0		**270**	ch4_llb_surface-flask_1_representative	0	1		**470**	ch4_wlg_surface-flask_1_representative	1	1	
71	ch4_car_aircraft-pfp_1_allvalid	0	1	2400	**271**	ch4_llb_surface-insitu_6_allvalid	0	0		**471**	ch4_wpc_shipboard-flask_1_representative	1	1	
72	ch4_carl_surface-insitu_60_allvalid-9magl	0	0		**272**	ch4_lln_surface-flask_1_representative	1	1		**472**	ch4_wsa_surface-insitu_6_allvalid	0	0	
73	ch4_cba_surface-flask_1_representative	1	1		**273**	ch4_lmp_surface-flask_1_representative	0	1		**473**	ch4_wsd_tower-insitu_60_allvalid	0	1	
74	ch4_cbw_surface-insitu	0	0		**274**	ch4_lmp_surface-insitu_28	0	1		**474**	ch4_yak_tower-insitu_20_	0	0	

	_118_allvalid					_allvalid					allvalid-11magl			
75	ch4_cbw_tower-insitu_445_allvalid-127magl	0	0		**275**	ch4_lmu_surface-insitu_431_allvalid	0	1		**475**	ch4_yak_tower-insitu_20_allvalid-77magl	0	1	
76	ch4_cbw_tower-insitu_445_allvalid-207magl	0	1		**276**	ch4_lut_surface-insitu_118_allvalid	0	1		**476**	ch4_yon_surface-insitu_19_representative	0	1	
77	ch4_cbw_tower-insitu_445_allvalid-27magl	0	0		**277**	ch4_lut_surface-insitu_44_allvalid	0	1		**477**	ch4_zep_surface-flask_1_representative	1	1	
78	ch4_cbw_tower-insitu_445_allvalid-67magl	0	0		**278**	ch4_maa_surface-flask_2_representative	1	1		**478**	ch4_zep_surface-insitu_56_allvalid	0	1	
79	ch4_cby_surface-insitu_6_allvalid	0	0		**279**	ch4_malj_surface-insitu_60_allvalid-134magl	0	1		**479**	ch4_zot_surface-flask_45_representative	0	1	
80	ch4_cdl_surface-insitu_6_allvalid	0	0		**280**	ch4_man_aircraft-insitu_1_allvalid	0	0		**480**	ch4_zsf_surface-insitu_25_allvalid	1	0	
81	ch4_cfa_surface-flask_2_representative	0	1		**281**	ch4_man_aircraft-pfp_433_representative	0	1	1000	**481**	ch4_abp_surface-flask_433_allvalid	0	1	
82	ch4_cgo_surface-flask_1_representative	1	1		**282**	ch4_mbc_surface-flask_1_representative	0	1		**482**	ch4_agp_surface-flask_1_allvalid	0	0	
83	ch4_cgo_surface-flask_2_representative	1	1		**283**	ch4_mbo_surface-pfp_1_allvalid-11magl	1	0		**483**	ch4_akc_shipboard-flask_1_allvalid	1	1	
84	ch4_cgo_surface-flask_45_representative	1	1		**284**	ch4_mci_aircraft-pfp_1_allvalid	0	0		**484**	ch4_alk_aircraft-flask_8_allvalid	0	1	1000
85	ch4_cgo_surface-insitu_2_allvalid	0	0		**285**	ch4_mex_surface-flask_1_representative	1	1		**485**	ch4_ams_surface-insitu_11_allvalid	1	1	
86	ch4_chl_surface-insitu_6_allvalid	0	0		**286**	ch4_mhd_surface-flask_1_representative	1	1		**486**	ch4_aoc_shipboard-flask_1_allvalid	1	1	
87	ch4_chm_surface-insitu_6_allvalid	0	0		**287**	ch4_mhd_surface-insitu_11_allvalid	0	1		**487**	ch4_arh_surface-flask_15_allvalid	1	1	
88	ch4_chr_surface-flask_1_representative	1	1		**288**	ch4_mid_surface-flask_1_representative	1	1		**488**	ch4_bao_aircraft-pfp_1_allvalid	0	1	2500
89	ch4_cib_surface-flask_1_representative	0	1		**289**	ch4_mkn_surface-flask_1_representative	1	1		**489**	ch4_bao_tower-insitu_1_allvalid	0	1	1870
90	ch4_cma_aircraft-pfp_1_allvalid	0	1	1000	**290**	ch4_mkn_surface-insitu_701_allvalid	1	0		**490**	ch4_bgu_surface-flask_11_allvalid	0	1	
91	ch4_cmn_surface-insitu_106_allvalid	1	0		**291**	ch4_mko_surface-insitu_1_allvalid	1	0		**491**	ch4_bhd_surface-flask_15_allvalid	0	1	
92	ch4_cmn_surface-insitu_443_allvalid	1	0		**292**	ch4_mlh_surface-insitu_468_allvalid	0	1		**492**	ch4_bkt_surface-insitu_5_allvalid	0	1	
93	ch4_cmo_surface-flask_1_representative	0	1		**293**	ch4_mlo_surface-flask_1_representative	1	0		**493**	ch4_bwd_surface-pfp_1_allvalid	0	1	180

94	ch4_cob2003b_aircraft-insitu_59_allvalid	0	0		**294**	ch4_mlo_surface-flask_2_representative	1	0		**494**	ch4_cea_aircraft-flask_20_allvalid	1	1	1000
95	ch4_con_aircraft-flask_42_allvalid	1	1	1000	**295**	ch4_mlo_surface-insitu_1_allvalid	1	0		**495**	ch4_chc_surface-insitu_11_allvalid	1	0	
96	ch4_cpa_surface-flask_2_representative	0	1		**296**	ch4_mnc_surface-insitu_112_allvalid	0	0		**496**	ch4_chs_surface-insitu_1_allvalid	0	1	
97	ch4_cps_surface-insitu_6_allvalid	0	0		**297**	ch4_mnm_surface-insitu_19_representative	0	1		**497**	ch4_cob_aircraft-flask_1_allvalid	0	0	
98	ch4_cpt_surface-flask_1_representative	1	1		**298**	ch4_mqa_surface-flask_2_representative	1	1		**498**	ch4_coi_surface-insitu_20_allvalid	0	1	
99	ch4_cpt_surface-insitu_36_marine	0	1		**299**	ch4_mrc_aircraft-pfp_1_allvalid	0	0		**499**	ch4_cos_surface-flask_1_allvalid	0	0	
100	ch4_cra_tower-insitu_188_allvalid-30magl	0	0		**300**	ch4_mrc_surface-pfp_1_allvalid-east	0	0		**500**	ch4_cpa_surface-insitu_5_allvalid	0	1	
101	ch4_cra_tower-insitu_188_allvalid-60magl	0	1		**301**	ch4_mrc_surface-pfp_1_allvalid-south	0	0		**501**	ch4_deu_surface-insitu_25_allvalid	0	1	
102	ch4_cri_surface-flask_2_representative	0	1		**302**	ch4_mrc_tower-insitu_60_allvalid-south	0	0		**502**	ch4_fam_aircraft-flask_1_allvalid	0	1	1000
103	ch4_crp_surface-insitu_137_allvalid	0	0		**303**	ch4_msh_surface-pfp_1_allvalid-46magl	0	1		**503**	ch4_fkl_surface-flask_11_allvalid	0	1	
104	ch4_crv_aircraft-pfp_1_allvalid	0	0		**304**	ch4_mvy_surface-pfp_1_allvalid-16magl	0	1		**504**	ch4_gif_surface-insitu_11_allvalid	0	1	
105	ch4_crv_surface-pfp_1_allvalid-32magl	0	1		**305**	ch4_mwo_surface-pfp_1_allvalid-46magl	1	0		**505**	ch4_hat_surface-insitu_20_allvalid	0	1	
106	ch4_crv_tower-insitu_1_allvalid-17magl	0	0		**306**	ch4_nam_surface-flask_45_representative	0	1		**506**	ch4_hfm_surface-pfp_1_allvalid	0	1	
107	ch4_crv_tower-insitu_1_allvalid-32magl	0	1		**307**	ch4_nat_surface-flask_1_representative	0	1		**507**	ch4_hle_surface-flask_11_allvalid	1	1	
108	ch4_crv_tower-insitu_1_allvalid-5magl	0	0		**308**	ch4_ndao_surface-insitu_45_allvalid-21magl	0	1		**508**	ch4_how_aircraft-pfp_1_allvalid	0	1	1000
109	ch4_crz_surface-flask_1_representative	1	1		**309**	ch4_nha_aircraft-pfp_1_allvalid	0	1	1000	**509**	ch4_itn_surface-flask_1_allvalid	0	1	400
110	ch4_cvo_surface-flask_45_representative	1	1		**310**	ch4_nmb_surface-flask_1_representative	0	1		**510**	ch4_kco_surface-flask_1_allvalid	1	1	
111	ch4_cvo_surface-insitu_456_allvalid	0	1		**311**	ch4_nor_tower-insitu_424_allvalid-100magl	0	1		**511**	ch4_kmp_surface-insitu_30_allvalid	0	0	
112	ch4_cya_surface-flask_2_representative	1	1		**312**	ch4_nor_tower-insitu_424_allvalid-32magl	0	0		**512**	ch4_kor_shipboard-flask_1_allvalid	1	1	
11	ch4_dec_surface-insitu_	0	0		**313**	ch4_nor_tower-insitu_424_	0	0		**513**	ch4_kpa_surface-flask_1_	1	1	

3	431_allvalid					allvalid-58magl					allvalid			
114	ch4_dem_tower-insitu_20_allvalid-45magl	0	0		**314**	ch4_notr_surface-insitu_60_allvalid-91magl	0	0		**514**	ch4_lac_surface-pfp_1_allvalid	0	0	
115	ch4_dem_tower-insitu_20_allvalid-63magl	0	1		**315**	ch4_noy_tower-insitu_20_allvalid-21magl	0	0		**515**	ch4_lau_surface-flask_15_allvalid	0	1	
116	ch4_dnd_aircraft-pfp_1_allvalid	0	1	1400	**316**	ch4_noy_tower-insitu_20_allvalid-43magl	0	1		**516**	ch4_lau_surface-insitu_15_allvalid	0	1	
117	ch4_dnh_surface-insitu_112_allvalid	0	0		**317**	ch4_nwf_surface-pfp_1_allvalid-23magl	1	1		**517**	ch4_lle_surface-flask_1_allvalid	1	1	
118	ch4_drp_shipboard-flask_1_representative	1	1		**318**	ch4_nwf_surface-pfp_1_allvalid-2magl	0	0		**518**	ch4_lmp_surface-flask_28_allvalid	0	1	
119	ch4_dsi_surface-flask_1_representative	0	1		**319**	ch4_nwr_surface-flask_1_representative	1	1		**519**	ch4_lpo_surface-flask_11_allvalid	1	1	
120	ch4_dvv_tower-insitu_60_allvalid	0	0		**320**	ch4_nwr_surface-pfp_1_allvalid-3magl	1	1		**520**	ch4_mcm_surface-flask_1_allvalid	1	1	
121	ch4_eco_aircraft-insitu_1_allvalid	0	0		**321**	ch4_obn_surface-flask_1_representative	0	1		**521**	ch4_mdm_surface-flask_28_allvalid	0	1	
122	ch4_eec_surface-insitu_431_allvalid	0	0		**322**	ch4_ohp_tower-insitu_468_allvalid-100magl	0	1		**522**	ch4_mhd_surface-flask_11_allvalid	0	1	
123	ch4_egb_surface-insitu_6_allvalid	0	0		**323**	ch4_ohp_tower-insitu_468_allvalid-10magl	0	0		**523**	ch4_neb_surface-pfp_1_allvalid	0	0	
124	ch4_eic_surface-flask_1_representative	1	1		**324**	ch4_ohp_tower-insitu_468_allvalid-50magl	0	0		**524**	ch4_ngm_shipboard-flask_8_allvalid	1	1	
125	ch4_ena_surface-insitu_64_allvalid-10magl	0	0		**325**	ch4_oil_aircraft-pfp_1_allvalid	0	1	1100	**525**	ch4_nov_aircraft-flask_20_allvalid	0	1	1000
126	ch4_ers_surface-insitu_11_allvalid	0	0		**326**	ch4_oli_surface-insitu_64_allvalid-10magl	0	0		**526**	ch4_nsa_aircraft-pfp_1_allvalid	0	1	1000
127	ch4_esp_aircraft-pfp_1_allvalid	0	1	1000	**327**	ch4_ope_tower-insitu_11_allvalid-10magl	0	0		**527**	ch4_nsk_aircraft-pfp_1_allvalid	0	1	1400
128	ch4_esp_surface-flask_2_representative	0	1		**328**	ch4_ope_tower-insitu_11_allvalid-120magl	0	1		**528**	ch4_nwb_surface-pfp_1_allvalid	0	0	
129	ch4_esp_surface-insitu_6_allvalid	0	0		**329**	ch4_ope_tower-insitu_11_allvalid-50magl	0	0		**529**	ch4_nwp_surface-flask_8_allvalid	1	1	
130	ch4_est_surface-insitu_6_allvalid	0	0		**330**	ch4_opw_surface-flask_1_representative	0	1		**530**	ch4_nya_surface-flask_8_allvalid	0	1	
131	ch4_etl_aircraft-pfp_1_allvalid	0	1	1400	**331**	ch4_orc_aircraft-insitu_3_allvalid-merge10	0	0		**531**	ch4_nzl_surface-flask_1_allvalid	0	1	
132	ch4_etl_surface-insitu_6_allvalid	0	0		**332**	ch4_ota_surface-flask_2_representative	0	1		**532**	ch4_orl_aircraft-flask_11_allvalid	0	1	1100

133	ch4_fkl_surface-insitu_11_allvalid	0	1		**333**	ch4_oxk_surface-flask_1_representative	0	1		**533**	ch4_pao_shipboard-flask_1_allvalid	1	1	
134	ch4_fne_surface-insitu_6_allvalid	0	0		**334**	ch4_oxk_surface-flask_45_representative	0	1		**534**	ch4_pco_surface-flask_1_allvalid	1	0	
135	ch4_fort_surface-insitu_60_allvalid-128magl	0	1		**335**	ch4_oxk_tower-insitu_147_allvalid-163magl	0	1		**535**	ch4_pdi_surface-insitu_5_allvalid	0	1	
136	ch4_fsd_surface-insitu_6_allvalid	0	0		**336**	ch4_oxk_tower-insitu_147_allvalid-23magl	0	0		**536**	ch4_pdm_surface-flask_11_allvalid	1	0	
137	ch4_ftl_aircraft-pfp_1_allvalid	0	1	1000	**337**	ch4_oxk_tower-insitu_147_allvalid-90magl	0	0		**537**	ch4_pip_aircraft-flask_8_allvalid	0	1	1000
138	ch4_fwi_aircraft-pfp_1_allvalid	0	1	1300	**338**	ch4_pal_surface-flask_1_representative	0	1		**538**	ch4_poc_surface-flask_15_allvalid	1	1	
139	ch4_gat_tower-insitu_147_allvalid-132magl	0	0		**339**	ch4_pal_surface-insitu_30_allvalid	0	0		**539**	ch4_puy_surface-flask_11_allvalid	1	0	
140	ch4_gat_tower-insitu_147_allvalid-216magl	0	0		**340**	ch4_pal_surface-insitu_30_continental	0	0		**540**	ch4_rrs_shipboard-flask_1_allvalid	1	1	
141	ch4_gat_tower-insitu_147_allvalid-30magl	0	0		**341**	ch4_pal_surface-insitu_30_marine	0	1		**541**	ch4_s2k_aircraft-pfp_1_allvalid	0	0	
142	ch4_gat_tower-insitu_147_allvalid-341magl	0	1		**342**	ch4_pal_surface-insitu_30_nonlocal	0	1		**542**	ch4_sio_surface-flask_1_allvalid	0	1	
143	ch4_gat_tower-insitu_147_allvalid-60magl	0	0		**343**	ch4_pdm_surface-insitu_11_allvalid	1	0		**543**	ch4_sod_surface-insitu_30_allvalid	0	1	
144	ch4_gci01_tower-insitu_60_allvalid	0	0		**344**	ch4_pfa_aircraft-pfp_1_allvalid	0	1	1200	**544**	ch4_sur_aircraft-flask_20_allvalid	0	1	1000
145	ch4_gci02_tower-insitu_60_allvalid	0	0		**345**	ch4_poc_shipboard-flask_1_representative	1	1		**545**	ch4_tda_aircraft-flask_8_allvalid	0	1	1000
146	ch4_gci03_tower-insitu_60_allvalid	0	0		**346**	ch4_prs_surface-insitu_21_allvalid	1	0		**546**	ch4_ter_surface-flask_55_allvalid	0	1	
147	ch4_gci04_tower-insitu_60_allvalid	0	0		**347**	ch4_psa_surface-flask_1_representative	1	1		**547**	ch4_tik_surface-flask_55_allvalid	0	1	
148	ch4_ghg03_surface-insitu_112_allvalid	0	0		**348**	ch4_pta_surface-flask_1_representative	0	1		**548**	ch4_tll_surface-insitu_133_allvalid	1	0	
149	ch4_ghg06_surface-insitu_112_allvalid	0	0		**349**	ch4_pui_tower-insitu_30_allvalid-47magl	0	0		**549**	ch4_tll_surface-insitu_5_allvalid	1	0	
150	ch4_ghg09_surface-insitu_112_allvalid	0	0		**350**	ch4_pui_tower-insitu_30_allvalid-84magl	0	1		**550**	ch4_tmd_surface-pfp_1_allvalid	0	1	
151	ch4_ghg10_surface-insitu_112_allvalid	0	0		**351**	ch4_puy_surface-insitu_11_allvalid	1	0		**551**	ch4_tpi_surface-flask_1_allvalid	1	1	
15	ch4_gic_surface-insitu_	1	0		**352**	ch4_rba-b_aircraft-pfp_433	0	1	10	**552**	ch4_trc_surface-flask_1_a	0	0	

2	431_allvalid					_representative			00		llvalid			
153	ch4_gmi_surface-flask_1_representative	1	1		**353**	ch4_rgl_tower-insitu_160_allvalid-45magl	0	0		**553**	ch4_trm_surface-flask_11_allvalid	1	1	
154	ch4_goz_surface-flask_1_representative	1	1		**354**	ch4_rgl_tower-insitu_160_allvalid-90magl	0	1		**554**	ch4_vkv_surface-insitu_55_allvalid	0	1	
155	ch4_gpa_surface-flask_2_representative	1	1		**355**	ch4_ric_surface-insitu_112_allvalid	0	1		**555**	ch4_wgc_aircraft-pfp_1_allvalid	0	1	1000
156	ch4_gsn_surface-insitu_61_allvalid	0	1		**356**	ch4_roc_tower-insitu_11_allvalid-140magl	0	1		**556**	ch4_zgt_surface-insitu_25_allvalid	0	1	
157	ch4_gvn_surface-flask_45_representative	1	1		**357**	ch4_roc_tower-insitu_11_allvalid-25magl	0	0						
158	ch4_haa_aircraft-pfp_1_allvalid	0	1	1000	**358**	ch4_roc_tower-insitu_11_allvalid-80magl	0	0						
159	ch4_hba_surface-flask_1_representative	1	1		**359**	ch4_rpb_surface-flask_1_representative	1	1						
160	ch4_hct_surface-insitu_112_allvalid	0	0		**360**	ch4_rta_aircraft-pfp_1_allvalid	0	1	10000					
161	ch4_hei_surface-insitu_22_allvalid	0	1		**361**	ch4_run_surface-insitu_472_allvalid	0	1						
162	ch4_hel_surface-insitu_147_allvalid	0	0		**362**	ch4_rvrb_shipboard-insitu_1_allvalid	0	0						
163	ch4_hfm_aircraft-pfp_1_allvalid	0	1	1300	**363**	ch4_ryo_surface-insitu_19_representative	0	1						
164	ch4_hil_aircraft-pfp_1_allvalid	0	1	1200	**364**	ch4_sac_tower-insitu_11_allvalid-100magl	0	1						
165	ch4_hip_aircraft-insitu_59_allvalid	0	0		**365**	ch4_sac_tower-insitu_11_allvalid-15magl	0	0						
166	ch4_hip_aircraft-pfp_1_allvalid	0	0		**366**	ch4_sac_tower-insitu_11_allvalid-60magl	0	0						
167	ch4_hnp_surface-insitu_6_allvalid	0	0		**367**	ch4_sah_aircraft-pfp_433_representative	0	1	10000					
168	ch4_hobb_surface-insitu_60_allvalid-91magl	0	0		**368**	ch4_sam_aircraft-pfp_1_allvalid	0	0						
169	ch4_hpb_surface-flask_1_representative	1	1		**369**	ch4_san_aircraft-pfp_1_allvalid	0	1	10000					
17	ch4_hpb_tower-insitu_1	1	0		**370**	ch4_san_aircraft-pfp_433_r	0	1	1000					

0	47_allvalid-131magl					epresentative			0					
171	ch4_hpb_tower-insitu_147_allvalid-50magl	0	0		**371**	ch4_sca_aircraft-pfp_1_allvalid	0	1	10000					
172	ch4_hpb_tower-insitu_147_allvalid-93magl	0	0		**372**	ch4_scs_shipboard-flask_1_representative	1	1						
173	ch4_hsu_surface-flask_1_representative	0	1		**373**	ch4_sct_surface-pfp_1_allvalid-305magl	0	1						
174	ch4_htm_tower-insitu_424_allvalid-150magl	0	1		**374**	ch4_sct_tower-insitu_1_allvalid-305magl	0	1						
175	ch4_htm_tower-insitu_424_allvalid-30magl	0	0		**375**	ch4_sct_tower-insitu_1_allvalid-31magl	0	0						
176	ch4_htm_tower-insitu_424_allvalid-70magl	0	0		**376**	ch4_sct_tower-insitu_1_allvalid-61magl	0	0						
177	ch4_hun_surface-flask_1_representative	0	1		**377**	ch4_sdz_surface-flask_1_representative	0	1						
178	ch4_hun_tower-insitu_35_allvalid-10magl	0	0		**378**	ch4_seac4rs_aircraft-insitu_428_allvalid-dc8	0	0						
179	ch4_hun_tower-insitu_35_allvalid-115magl	0	1		**379**	ch4_seac4rs_aircraft-insitu_428_allvalid-ER2	0	0						
180	ch4_hun_tower-insitu_35_allvalid-48magl	0	0		**380**	ch4_sey_surface-flask_1_representative	1	1						
181	ch4_hun_tower-insitu_35_allvalid-82magl	0	0		**381**	ch4_sgc_surface-insitu_431_allvalid	0	1						
182	ch4_iagos-caribic_aircraft-flask_457_allvalid	0	0		**382**	ch4_sgi_surface-flask_1_representative	1	1						
183	ch4_iagos-caribic_aircraft-insitu_457_allvalid	0	0		**383**	ch4_sgp_aircraft-pfp_1_allvalid	0	1	13000					
184	ch4_iagos-core_aircraft-insitu_45_allvalid	0	0		**384**	ch4_sgp_surface-flask_1_representative	0	1						
185	ch4_ice_surface-flask_1_representative	1	1		**385**	ch4_sgp_surface-insitu_64_allvalid-60magl	0	1						
186	ch4_igr_tower-insitu_20_allvalid-24magl	0	0		**386**	ch4_sgp_surface-pfp_1_allvalid-60magl	0	1						
187	ch4_igr_tower-insitu_20_allvalid-47magl	0	1		**387**	ch4_sgp_surface-pfp_1_allvalid-9magl	0	0						
188	ch4_inu_surface-insitu_6_allvalid	0	0		**388**	ch4_shm_surface-flask_1_representative	1	1						

189	ch4_inx01_surface-insitu_60_allhours-10magl	0	0		**389**	ch4_sig_surface-insitu_112_allvalid	0	1						
190	ch4_inx01_surface-insitu_60_allhours-121magl	0	1		**390**	ch4_sis_surface-flask_2_representative	1	1						
191	ch4_inx01_surface-insitu_60_allhours-40magl	0	0		**391**	ch4_sis_surface-flask_45_representative	1	1						
192	ch4_inx02_surface-insitu_60_allhours-10magl	0	0		**392**	ch4_smo_surface-flask_1_representative	1	1						
193	ch4_inx02_surface-insitu_60_allhours-136magl	0	0		**393**	ch4_smr_tower-insitu_421_allvalid-125magl	0	1						
194	ch4_inx02_surface-insitu_60_allhours-40magl	0	0		**394**	ch4_smr_tower-insitu_421_allvalid-16magl	0	0						
195	ch4_inx03_surface-insitu_60_allhours-10magl	0	0		**395**	ch4_smr_tower-insitu_421_allvalid-67magl	0	0						
196	ch4_inx03_surface-insitu_60_allhours-20magl	0	0		**396**	ch4_snj_surface-insitu_112_allvalid	0	1						
197	ch4_inx03_surface-insitu_60_allhours-40magl	0	0		**397**	ch4_sno_tower-insitu_464_allvalid-20magl	0	0						
198	ch4_inx03_surface-insitu_60_allhours-54magl	0	0		**398**	ch4_sno_tower-insitu_464_allvalid-50magl	0	0						
199	ch4_inx04_surface-insitu_60_allhours-60magl	0	0		**399**	ch4_sno_tower-insitu_464_allvalid-85magl	0	1						
200	ch4_inx05_surface-insitu_60_allhours-125magl	0	0		**400**	ch4_spo_surface-flask_1_representative	1	1						

Table 5. Summary of site selection for assimilation and filtering for $\delta^{13}C\text{-}CH_4$.

[Download Here]

	Filename	Assim nighttime	Assim daytime	Min altitude		Filename	Assim nighttime	Assim daytime	Min altitude
1	ch4_above_aircraft-pfp_1_allvalid	0	0		**41**	ch4_mcm_surface-flask_1_allvalid	1	1	
2	ch4_abp_surface-flask_433_allvalid	0	1		**42**	ch4_mdm_surface-flask_28_allvalid	0	1	
3	ch4_agp_surface-flask_1_allvalid	0	0		**43**	ch4_mhd_surface-flask_11_allvalid	0	1	
4	ch4_akc_shipboard-flask_1_allvalid	1	1		**44**	ch4_neb_surface-pfp_1_allvalid	0	0	

5	ch4_alk_aircraft-flask_8_allvalid	0	1	1000	**45**	ch4_ngm_shipboard-flask_8_allvalid	1	1	
6	ch4_ams_surface-insitu_11_allvalid	1	1		**46**	ch4_nov_aircraft-flask_20_allvalid	0	1	1000
7	ch4_aoc_shipboard-flask_1_allvalid	1	1		**47**	ch4_nsa_aircraft-pfp_1_allvalid	0	1	1000
8	ch4_arh_surface-flask_15_allvalid	1	1		**48**	ch4_nsk_aircraft-pfp_1_allvalid	0	1	1400
9	ch4_bao_aircraft-pfp_1_allvalid	0	1	2500	**49**	ch4_nwb_surface-pfp_1_allvalid	0	0	
10	ch4_bao_tower-insitu_1_allvalid	0	1	1870	**50**	ch4_nwp_surface-flask_8_allvalid	1	1	
11	ch4_bgu_surface-flask_11_allvalid	0	1		**51**	ch4_nya_surface-flask_8_allvalid	0	1	
12	ch4_bhd_surface-flask_15_allvalid	0	1		**52**	ch4_nzl_surface-flask_1_allvalid	0	1	
13	ch4_bkt_surface-insitu_5_allvalid	0	1		**53**	ch4_orl_aircraft-flask_11_allvalid	0	1	1100
14	ch4_bwd_surface-pfp_1_allvalid	0	1	180	**54**	ch4_pao_shipboard-flask_1_allvalid	1	1	
15	ch4_cea_aircraft-flask_20_allvalid	1	1	1000	**55**	ch4_pco_surface-flask_1_allvalid	1	0	
16	ch4_chc_surface-insitu_11_allvalid	1	0		**56**	ch4_pdi_surface-insitu_5_allvalid	0	1	
17	ch4_chs_surface-insitu_1_allvalid	0	1		**57**	ch4_pdm_surface-flask_11_allvalid	1	0	
18	ch4_cob_aircraft-flask_1_allvalid	0	0		**58**	ch4_pip_aircraft-flask_8_allvalid	0	1	1000
19	ch4_coi_surface-insitu_20_allvalid	0	1		**59**	ch4_poc_surface-flask_15_allvalid	1	1	
20	ch4_cos_surface-flask_1_allvalid	0	0		**60**	ch4_puy_surface-flask_11_allvalid	1	0	
21	ch4_cpa_surface-insitu_5_allvalid	0	1		**61**	ch4_rrs_shipboard-flask_1_allvalid	1	1	
22	ch4_deu_surface-insitu_25_allvalid	0	1		**62**	ch4_s2k_aircraft-pfp_1_allvalid	0	0	
23	ch4_fam_aircraft-flask_1_allvalid	0	1	1000	**63**	ch4_sio_surface-flask_1_allvalid	0	1	
24	ch4_fkl_surface-flask_11_allvalid	0	1		**64**	ch4_sod_surface-insitu_30_allvalid	0	1	
25	ch4_gif_surface-insitu_11_allvalid	0	1		**65**	ch4_sur_aircraft-flask_20_allvalid	0	1	1000

26	ch4_hat_surface-insitu_20_allvalid	0	1		**66**	ch4_tda_aircraft-flask_8_allvalid	0	1	1000
27	ch4_hfm_surface-pfp_1_allvalid	0	1		**67**	ch4_ter_surface-flask_55_allvalid	0	1	
28	ch4_hle_surface-flask_11_allvalid	1	1		**68**	ch4_tik_surface-flask_55_allvalid	0	1	
29	ch4_how_aircraft-pfp_1_allvalid	0	1	1000	**69**	ch4_tll_surface-insitu_133_allvalid	1	0	
30	ch4_itn_surface-flask_1_allvalid	0	1	400	**70**	ch4_tll_surface-insitu_5_allvalid	1	0	
31	ch4_kco_surface-flask_1_allvalid	1	1		**71**	ch4_tmd_surface-pfp_1_allvalid	0	1	
32	ch4_kmp_surface-insitu_30_allvalid	0	0		**72**	ch4_tpi_surface-flask_1_allvalid	1	1	
33	ch4_kor_shipboard-flask_1_allvalid	1	1		**73**	ch4_trc_surface-flask_1_allvalid	0	0	
34	ch4_kpa_surface-flask_1_allvalid	1	1		**74**	ch4_trm_surface-flask_11_allvalid	1	1	
35	ch4_lac_surface-pfp_1_allvalid	0	0		**75**	ch4_vkv_surface-insitu_55_allvalid	0	1	
36	ch4_lau_surface-flask_15_allvalid	0	1		**76**	ch4_wgc_aircraft-pfp_1_allvalid	0	1	1000
37	ch4_lau_surface-insitu_15_allvalid	0	1		**77**	ch4_zgt_surface-insitu_25_allvalid	0	1	
38	ch4_lle_surface-flask_1_allvalid	1	1						
39	ch4_lmp_surface-flask_28_allvalid	0	1						
40	ch4_lpo_surface-flask_11_allvalid	1	1						

Table 6. Summary of statistics of observational Sites for CH_4 used in CarbonTracker-CH_4.

[Download Here]

Assimilated										
	Site Code	Laboratory	Latitude	Longitude	Elevation (MASL)	No. of Observation	Model-data mismatch	Mean bias	Standard deviation of bias	Chi-squared
1	**ch4_abp_surface-flask_1_representative**	1	-12.77	-38.17	6.00	113	5.82	0.48	5.30	0.83
2	**ch4_abp_surface-flask_433_allvalid**	433	-12.77	-38.17	15.00	193	7.98	-2.88	7.70	1.06
3	**ch4_abt_surface-insitu_6_allvalid**	6	49.01	-122.34	93.00	57780	45.95	-32.41	43.55	1.40

4	**ch4_acg_aircraft-pfp_1_allvalid**	1	68.04	-156.70	4140.20	1948	11.40	3.70	10.81	0.89
5	**ch4_alf_aircraft-pfp_433_representative**	433	-8.86	-56.76	2690.71	1920	15.61	-5.78	12.78	0.80
6	**ch4_alt_surface-flask_1_representative**	1	82.45	-62.51	190.00	1932	9.02	0.19	8.23	0.83
7	**ch4_alt_surface-flask_2_representative**	2	82.45	-62.51	210.00	1108	8.86	1.20	7.89	0.81
8	**ch4_alt_surface-flask_45_representative**	45	82.45	-62.51	190.00	489	8.28	0.82	8.04	0.95
9	**ch4_alt_surface-insitu_6_allvalid**	6	82.45	-62.51	195.00	189579	9.34	0.38	8.39	0.81
10	**ch4_amt_surface-flask_1_representative**	1	45.02	-68.67	157.00	268	14.85	-0.04	12.77	0.73
11	**ch4_amt_surface-pfp_1_allvalid-107magl**	1	45.03	-68.68	160.40	2096	18.30	1.79	13.70	0.57
12	**ch4_amy_surface-flask_1_representative**	1	36.54	126.33	87.00	557	47.71	9.79	36.31	0.62
13	**ch4_ara_surface-flask_2_representative**	2	-23.86	148.48	185.00	30	6.33	-5.25	4.87	1.22
14	**ch4_arh_surface-flask_15_allvalid**	15	-77.83	166.66	184.00	189	5.00	-0.45	2.31	0.22
15	**ch4_asc_surface-flask_1_representative**	1	-7.97	-14.40	90.00	2305	7.33	-2.28	5.35	0.63
16	**ch4_ask_surface-flask_1_representative**	1	23.26	5.63	2715.00	1139	8.28	0.60	7.13	0.75
17	**ch4_azr_surface-flask_1_representative**	1	38.76	-27.29	24.00	806	14.05	-0.51	13.80	0.96
18	**ch4_bal_surface-flask_1_representative**	1	55.42	16.97	28.00	1342	25.86	-0.38	24.40	0.89
19	**ch4_bao_surface-pfp_1_allvalid-300magl**	1	40.05	-105.00	1884.00	3105	50.33	-28.77	49.20	1.28
20	**ch4_bck_surface-insitu_6_allvalid**	6	62.80	-115.92	220.00	87504	27.37	-5.19	13.58	0.28
21	**ch4_bgi_aircraft-pfp_1_allvalid**	1	42.82	-94.41	4864.07	339	13.03	1.86	13.08	1.12
22	**ch4_bgu_surface-flask_11_allvalid**	11	41.97	3.23	13.71	593	22.36	-2.14	23.49	1.11
23	**ch4_bhd_surface-flask_1_representative**	1	-41.41	174.87	91.68	355	5.40	1.39	4.38	0.75
24	**ch4_bhd_surface-flask_15_allvalid**	15	-41.41	174.87	85.00	316	5.00	-0.26	3.48	0.48
25	**ch4_bhd_surface-insitu_15_baseline**	15	-41.41	174.87	95.00	2179	6.23	-0.01	4.43	0.51
26	**ch4_bik_surface-flask_45_representative**	45	53.20	22.75	483.00	418	25.30	-6.10	23.04	0.88
27	**ch4_bik_tower-insitu_45_allvalid-300magl**	45	53.23	23.01	483.00	56233	24.57	0.42	20.93	0.73
28	**ch4_bir_tower-insitu_56_allvalid-75magl**	56	58.39	8.25	294.00	27357	14.57	1.97	13.51	0.88
29	**ch4_bkt_surface-flask_1_representative**	1	-0.20	100.32	875.00	887	29.51	3.36	31.74	1.17
30	**ch4_bme_surface-flask_1_representative**	1	32.37	-64.65	17.00	396	14.87	-3.44	14.89	1.05
31	**ch4_bmw_surface-flask_1_representative**	1	32.26	-64.88	55.82	1070	11.85	-0.33	10.82	0.84
32	**ch4_bne_aircraft-pfp_1_allvalid**	1	40.80	-97.18	4383.07	1026	14.35	2.18	13.33	0.90
33	**ch4_brm_tower-insitu_49_allvalid-212magl**	49	47.19	8.18	1009.00	90227	53.91	-11.77	48.03	0.84
34	**ch4_bsc_surface-flask_1_representative**	1	44.18	28.66	5.00	723	48.57	-27.82	46.01	1.22
35	**ch4_bsd_tower-insitu_160_allvalid-248magl**	160	54.36	-1.15	630.00	60692	18.71	-4.97	17.30	0.93
36	**ch4_car_aircraft-pfp_1_allvalid**	1	40.75	-104.55	4537.66	8515	11.20	3.47	10.45	0.97
37	**ch4_cba_surface-flask_1_representative**	1	55.21	-162.72	42.54	2405	10.11	-8.68	9.62	1.66
38	**ch4_cbw_tower-insitu_445_allvalid-207magl**	445	51.97	4.93	207.00	166650	53.87	-17.25	48.68	0.92
39	**ch4_cea_aircraft-flask_20_allvalid**	20	62.06	78.41	10619.85	887	42.22	31.25	42.88	1.53
40	**ch4_cfa_surface-flask_2_representative**	2	-19.28	147.06	5.00	784	6.17	-1.30	5.17	0.74
41	**ch4_cgo_surface-flask_1_representative**	1	-40.68	144.68	164.00	1102	5.32	0.50	3.29	0.39

42	**ch4_cgo_surface-flask_2_representative**	2	-40.68	144.69	164.00	1818	5.00	0.07	3.37	0.45
43	**ch4_cgo_surface-flask_45_representative**	45	-40.68	144.69	164.00	158	5.00	0.72	3.54	0.52
44	**ch4_chr_surface-flask_1_representative**	1	1.70	-157.15	4.97	722	10.45	1.14	9.30	0.80
45	**ch4_chs_surface-insitu_1_allvalid**	1	68.51	161.53	64.40	109083	21.12	-10.96	20.41	1.20
46	**ch4_cib_surface-flask_1_representative**	1	41.81	-4.93	849.99	649	20.81	2.65	19.58	0.91
47	**ch4_cma_aircraft-pfp_1_allvalid**	1	38.83	-74.27	4174.64	3495	14.17	4.26	12.51	0.90
48	**ch4_cmn_surface-insitu_106_allvalid**	106	44.17	10.68	2172.00	78681	25.92	-5.27	23.10	0.84
49	**ch4_cmo_surface-flask_1_representative**	1	45.48	-123.97	35.00	24	21.88	-5.83	16.95	0.63
50	**ch4_coi_surface-insitu_20_allvalid**	20	43.16	145.50	94.00	136493	16.11	-4.14	12.91	0.71
51	**ch4_con_aircraft-flask_42_allvalid**	42	24.41	120.44	10122.79	5763	27.09	-0.30	28.92	1.12
52	**ch4_cpa_surface-flask_2_representative**	2	-12.42	130.57	9.00	92	17.08	-8.10	14.03	0.89
53	**ch4_cpt_surface-flask_1_representative**	1	-34.35	18.49	260.00	444	7.55	0.44	4.00	0.28
54	**ch4_cpt_surface-insitu_36_marine**	36	-34.35	18.49	260.00	176927	8.92	1.57	4.80	0.32
55	**ch4_cra_tower-insitu_188_allvalid-60magl**	188	43.13	0.37	660.00	39427	25.02	-5.86	19.26	0.65
56	**ch4_cri_surface-flask_2_representative**	2	15.08	73.83	66.00	342	39.08	-13.41	40.23	1.17
57	**ch4_crv_surface-pfp_1_allvalid-32magl**	1	64.99	-147.60	643.13	1703	19.25	-1.58	11.61	0.37
58	**ch4_crv_tower-insitu_1_allvalid-32magl**	1	64.99	-147.60	643.13	86430	19.81	-1.50	11.79	0.36
59	**ch4_crz_surface-flask_1_representative**	1	-46.43	51.85	202.00	1053	5.00	0.26	2.59	0.27
60	**ch4_cvo_surface-flask_45_representative**	45	16.86	-24.87	40.00	733	7.72	2.70	7.01	0.95
61	**ch4_cvo_surface-insitu_456_allvalid**	456	16.86	-24.87	40.00	74309	8.15	2.90	6.93	0.85
62	**ch4_cya_surface-flask_2_representative**	2	-66.28	110.52	55.00	857	5.00	-0.86	1.90	0.17
63	**ch4_deu_surface-insitu_25_allvalid**	25	49.77	7.05	480.00	33820	37.65	11.44	33.45	0.88
64	**ch4_dnd_aircraft-pfp_1_allvalid**	1	47.79	-98.59	4213.78	1988	11.32	3.97	10.60	0.99
65	**ch4_drp_shipboard-flask_1_representative**	1	-58.99	-63.53	10.00	301	5.00	-0.37	2.31	0.22
66	**ch4_dsi_surface-flask_1_representative**	1	20.70	116.73	8.00	643	27.13	-12.03	25.65	0.98
67	**ch4_eic_surface-flask_1_representative**	1	-27.15	-109.44	60.86	807	5.02	-3.32	3.23	0.85
68	**ch4_esp_aircraft-pfp_1_allvalid**	1	49.45	-126.44	3222.98	5179	10.65	0.89	9.45	0.79
69	**ch4_esp_surface-flask_2_representative**	2	49.38	-126.53	47.00	78	6.20	-8.75	4.73	2.56
70	**ch4_etl_aircraft-pfp_1_allvalid**	1	54.31	-104.94	3394.23	3427	12.30	1.09	9.94	0.68
71	**ch4_fkl_surface-flask_11_allvalid**	11	35.34	25.67	151.38	390	18.29	4.84	15.70	0.80
72	**ch4_fkl_surface-insitu_11_allvalid**	11	35.34	25.67	265.00	75807	15.02	0.29	11.48	0.58
73	**ch4_fort_surface-insitu_60_allvalid-128magl**	60	30.87	-102.82	1115.00	28552	80.14	6.43	74.83	0.88
74	**ch4_ftl_aircraft-pfp_1_allvalid**	1	-4.15	-38.28	2694.22	159	9.99	-2.11	9.53	0.94
75	**ch4_fwi_aircraft-pfp_1_allvalid**	1	44.69	-90.99	4840.88	361	11.51	0.23	11.30	0.91
76	**ch4_gat_tower-insitu_147_allvalid-341magl**	147	53.07	11.44	411.00	62074	22.80	-3.38	20.78	0.85
77	**ch4_gif_surface-insitu_11_allvalid**	11	48.71	2.15	167.00	51250	24.74	1.55	22.60	0.84
78	**ch4_gmi_surface-flask_1_representative**	1	13.39	144.66	6.29	1697	13.21	0.19	12.36	0.83

79	**ch4_goz_surface-flask_1_representative**	1	36.05	14.89	6.00	26	22.80	4.79	21.54	0.89
80	**ch4_gpa_surface-flask_2_representative**	2	-12.25	131.04	37.00	89	19.56	-20.37	19.87	2.10
81	**ch4_gvn_surface-flask_45_representative**	45	-70.67	-8.27	44.00	208	5.00	-0.66	1.51	0.11
82	**ch4_haa_aircraft-pfp_1_allvalid**	1	21.23	-158.89	4299.03	1776	10.48	2.05	10.00	0.94
83	**ch4_hat_surface-insitu_20_allvalid**	20	24.06	123.81	47.30	134193	18.24	-5.50	16.62	0.92
84	**ch4_hba_surface-flask_1_representative**	1	-75.59	-26.47	35.00	989	5.00	0.15	2.48	0.25
85	**ch4_hei_surface-insitu_22_allvalid**	22	49.42	8.68	143.00	202689	33.67	-5.81	30.38	0.84
86	**ch4_hfm_aircraft-pfp_1_allvalid**	1	42.54	-72.17	4374.04	1593	11.67	2.65	11.32	1.01
87	**ch4_hil_aircraft-pfp_1_allvalid**	1	40.03	-87.94	4541.98	3693	14.15	5.89	13.25	1.06
88	**ch4_hle_surface-flask_11_allvalid**	11	32.78	78.96	4522.00	321	23.01	15.85	17.59	1.06
89	**ch4_hpb_surface-flask_1_representative**	1	47.80	11.02	990.00	901	39.09	-3.29	37.42	0.92
90	**ch4_hsu_surface-flask_1_representative**	1	41.03	-124.62	7.60	87	8.66	-5.60	8.82	1.33
91	**ch4_htm_tower-insitu_424_allvalid-150magl**	424	56.10	13.42	265.00	58127	17.85	-1.99	15.58	0.77
92	**ch4_hun_surface-flask_1_representative**	1	46.96	16.65	344.00	1348	32.59	-5.60	30.94	0.93
93	**ch4_hun_tower-insitu_35_allvalid-115magl**	35	46.96	16.65	363.00	29961	27.42	-2.03	24.78	0.82
94	**ch4_ice_surface-flask_1_representative**	1	63.40	-20.29	125.54	1287	8.43	-3.27	8.33	1.12
95	**ch4_inx01_surface-insitu_60_allhours-121magl**	60	39.58	-86.42	377.30	65995	34.16	-0.57	27.11	0.63
96	**ch4_ipr_tower-insitu_103_allvalid-100magl**	103	45.81	8.64	310.00	51799	65.40	-28.43	60.34	1.04
97	**ch4_itn_surface-flask_1_representative**	1	35.37	-77.39	505.00	117	24.09	-17.67	19.68	1.20
98	**ch4_ivi_surface-insitu_11_allvalid**	11	61.21	-48.17	18.00	22290	14.80	-6.38	14.09	1.09
99	**ch4_izo_surface-flask_1_representative**	1	28.31	-16.49	2377.90	1240	9.80	0.95	9.34	0.92
100	**ch4_jar_tower-insitu_475_allvalid-110magl**	475	58.28	27.31	146.00	67424	26.42	-14.16	19.70	0.84
101	**ch4_jfj_surface-flask_45_representative**	45	46.55	7.99	3570.00	357	12.96	1.54	12.42	0.93
102	**ch4_jue_tower-insitu_147_allvalid-120magl**	147	50.91	6.41	218.00	34987	37.72	4.65	41.19	1.21
103	**ch4_kas_surface-insitu_53_allvalid**	53	49.23	19.98	1994.00	152026	26.14	0.38	22.86	0.76
104	**ch4_kco_surface-flask_1_representative**	1	4.97	73.47	6.00	45	35.29	-1.44	11.27	0.10
105	**ch4_kit_tower-insitu_147_allvalid-200magl**	147	49.09	8.42	310.00	58530	26.55	-5.48	23.17	0.80
106	**ch4_kjn_surface-flask_45_representative**	45	70.85	29.23	10.00	176	12.58	-1.35	12.28	0.96
107	**ch4_kre_tower-insitu_441_allvalid-250magl**	441	49.57	15.08	784.00	48498	21.83	-5.22	18.66	0.79
108	**ch4_kum_surface-flask_1_representative**	1	19.53	-154.84	9.06	2645	8.84	2.77	7.56	0.82
109	**ch4_kzd_surface-flask_1_representative**	1	44.22	76.38	528.38	575	28.55	-10.46	26.59	1.00
110	**ch4_kzm_surface-flask_1_representative**	1	43.25	77.87	2524.00	566	20.84	-2.37	18.54	0.80
111	**ch4_lef_aircraft-pfp_1_allvalid**	1	45.97	-90.20	2614.86	4748	15.55	2.60	13.50	0.77
112	**ch4_lef_surface-flask_1_representative**	1	45.93	-90.27	868.00	1182	22.46	-3.20	23.04	1.07
113	**ch4_lef_surface-pfp_1_allvalid-396magl**	1	45.95	-90.27	868.00	2980	25.07	-1.83	17.46	0.49
114	**ch4_lef_tower-insitu_1_allvalid-396magl**	1	45.95	-90.27	868.00	91353	24.94	-3.18	17.85	0.53

115	**ch4_lew_surface-insitu_112_allvalid**	112	40.94	-76.88	238.24	49151	37.60	-5.31	29.48	0.63
116	**ch4_lew_surface-pfp_1_allvalid-95magl**	1	40.94	-76.88	261.00	998	39.40	-16.80	29.62	0.75
117	**ch4_lin_tower-insitu_147_allvalid-98magl**	147	52.17	14.12	171.00	66197	24.53	2.47	20.91	0.74
118	**ch4_llb_surface-flask_1_representative**	1	54.95	-112.45	571.24	212	62.94	-16.71	61.16	0.95
119	**ch4_lln_surface-flask_1_representative**	1	23.47	120.87	2867.00	903	17.85	-2.64	16.46	0.87
120	**ch4_lmp_surface-flask_1_representative**	1	35.52	12.62	50.00	773	14.71	5.60	12.88	0.91
121	**ch4_lmu_surface-insitu_431_allvalid**	431	41.60	-1.10	3079.00	38650	33.34	-38.48	33.63	2.35
122	**ch4_lpo_surface-flask_11_allvalid**	11	48.80	-3.58	20.00	272	25.87	7.56	28.53	1.30
123	**ch4_lut_surface-insitu_44_allvalid**	44	53.40	6.35	61.00	127584	64.26	-19.88	57.71	0.90
124	**ch4_maa_surface-flask_2_representative**	2	-67.62	62.87	42.00	976	5.00	-1.06	2.47	0.29
125	**ch4_malj_surface-insitu_60_allvalid-134magl**	60	32.87	-103.76	1444.00	10718	69.27	0.24	67.51	0.95
126	**ch4_man_aircraft-pfp_433_representative**	433	-2.49	-59.75	2532.36	587	21.64	-5.48	17.81	0.75
127	**ch4_mbc_surface-flask_1_representative**	1	76.25	-119.35	35.00	35	10.54	-6.11	13.62	1.80
128	**ch4_mbo_surface-pfp_1_allvalid-11magl**	1	43.98	-121.69	2742.30	2177	11.58	-0.77	10.47	0.82
129	**ch4_mex_surface-flask_1_representative**	1	18.98	-97.31	4469.00	570	12.95	-1.61	11.84	0.85
130	**ch4_mhd_surface-flask_1_representative**	1	53.33	-9.90	25.69	1199	10.24	1.69	10.05	0.98
131	**ch4_mhd_surface-flask_11_allvalid**	11	53.33	-9.90	29.47	780	11.43	5.26	11.81	1.31
132	**ch4_mid_surface-flask_1_representative**	1	28.21	-177.37	10.38	1322	9.59	-1.41	9.04	0.90
133	**ch4_mkn_surface-flask_1_representative**	1	-0.06	37.30	3649.00	156	13.85	-11.01	9.95	1.14
134	**ch4_mlo_surface-flask_1_representative**	1	19.53	-155.57	3425.33	2770	6.28	3.55	8.29	1.43
135	**ch4_mlo_surface-flask_2_representative**	2	19.54	-155.58	3435.00	1357	6.57	-1.91	4.70	0.52
136	**ch4_mnm_surface-insitu_19_representative**	19	24.29	153.98	27.10	215383	11.61	2.54	9.68	0.74
137	**ch4_mqa_surface-flask_2_representative**	2	-54.48	158.97	13.00	989	5.00	-1.27	2.59	0.33
138	**ch4_msh_surface-pfp_1_allvalid-46magl**	1	41.66	-70.50	78.30	605	26.12	1.66	21.59	0.69
139	**ch4_mvy_surface-pfp_1_allvalid-16magl**	1	41.33	-70.57	16.00	210	23.41	3.18	17.95	0.60
140	**ch4_mwo_surface-pfp_1_allvalid-46magl**	1	34.22	-118.06	1775.23	4889	25.58	-5.65	24.02	0.93
141	**ch4_nam_surface-flask_45_representative**	45	-23.56	15.05	431.00	310	8.63	-2.05	8.14	0.94
142	**ch4_nat_surface-flask_1_representative**	1	-5.64	-35.23	49.55	385	9.13	-2.31	8.44	0.91
143	**ch4_ndao_surface-insitu_45_allvalid-21magl**	45	-23.56	15.05	429.00	7872	6.28	-0.62	5.40	0.75
144	**ch4_ngm_shipboard-flask_8_allvalid**	8	-1.57	149.66	20.00	629	23.24	-5.17	22.24	0.96
145	**ch4_nha_aircraft-pfp_1_allvalid**	1	42.90	-70.52	3958.18	4378	12.27	4.77	11.21	1.00
146	**ch4_nmb_surface-flask_1_representative**	1	-23.58	15.03	461.00	793	9.09	-2.03	8.11	0.84
147	**ch4_nor_tower-insitu_424_allvalid-100magl**	424	60.09	17.48	146.00	59463	13.86	-1.74	10.72	0.61
148	**ch4_nov_aircraft-flask_20_allvalid**	20	55.00	83.00	3418.85	3099	16.13	0.42	15.40	0.89
149	**ch4_noy_tower-insitu_20_allvalid-43magl**	20	63.43	75.78	151.00	33731	60.54	-19.32	56.16	0.96
150	**ch4_nsa_aircraft-pfp_1_allvalid**	1	68.97	-151.39	2595.17	378	12.08	3.61	8.43	0.66
151	**ch4_nwf_surface-pfp_1_allvalid-23magl**	1	40.03	-105.55	3072.99	658	18.72	-1.46	18.02	0.93

152	**ch4_nwp_surface-flask_8_allvalid**	8	-4.29	152.38	20.00	3604	19.64	-3.02	18.17	0.88
153	**ch4_nwr_surface-flask_1_representative**	1	40.05	-105.58	3526.00	1367	12.80	-0.32	11.89	0.86
154	**ch4_nwr_surface-pfp_1_allvalid-3magl**	1	40.05	-105.59	3526.20	3968	15.42	2.01	14.31	0.88
155	**ch4_nya_surface-flask_8_representative**	8	78.92	11.93	43.00	1097	9.24	-3.40	8.07	0.87
156	**ch4_obn_surface-flask_1_representative**	1	55.10	36.60	484.00	324	38.75	-13.46	37.75	1.07
157	**ch4_oil_aircraft-pfp_1_allvalid**	1	41.28	-88.94	4628.11	406	17.35	2.21	15.21	0.90
158	**ch4_ope_tower-insitu_11_allvalid-120magl**	11	48.56	5.50	510.00	103578	21.00	2.48	19.48	0.87
159	**ch4_orl_aircraft-flask_11_allvalid**	11	47.83	2.50	2382.45	2156	22.46	8.15	23.33	1.34
160	**ch4_ota_surface-flask_2_representative**	2	-38.52	142.82	50.00	217	50.92	-19.05	50.60	1.12
161	**ch4_oxk_surface-flask_1_representative**	1	50.03	11.81	1181.38	704	24.58	-6.30	25.04	1.10
162	**ch4_oxk_surface-flask_45_representative**	45	50.03	11.81	1185.00	702	21.68	-3.80	22.03	1.06
163	**ch4_oxk_tower-insitu_147_allvalid-163magl**	147	50.03	11.81	1185.00	34617	19.33	-5.83	18.20	0.98
164	**ch4_pal_surface-flask_1_representative**	1	67.97	24.12	570.00	1004	14.72	-3.45	12.45	0.77
165	**ch4_pal_surface-insitu_30_marine**	30	67.97	24.12	570.00	16034	7.36	-1.38	6.74	0.87
166	**ch4_pal_surface-insitu_30_nonlocal**	30	67.97	24.12	570.00	81677	13.52	-1.98	10.67	0.64
167	**ch4_pdm_surface-flask_11_allvalid**	11	42.94	0.14	2877.91	540	18.65	-10.66	16.12	1.78
168	**ch4_pdm_surface-insitu_11_allvalid**	11	42.94	0.14	2905.00	72954	11.78	1.11	10.06	0.74
169	**ch4_pfa_aircraft-pfp_1_allvalid**	1	65.02	-148.12	4080.71	5134	10.31	0.32	9.17	0.77
170	**ch4_poc_shipboard-flask_1_representative**	1	-1.53	-113.98	20.00	3717	11.87	-1.23	7.84	0.45
171	**ch4_poc_surface-flask_15_allvalid**	15	0.41	125.26	25.72	350	10.59	5.31	11.46	1.28
172	**ch4_prs_surface-insitu_21_allvalid**	21	45.93	7.70	3490.00	102468	16.85	5.95	16.02	1.03
173	**ch4_psa_surface-flask_1_representative**	1	-64.77	-64.05	15.00	1326	5.00	-0.44	2.21	0.20
174	**ch4_pta_surface-flask_1_representative**	1	38.95	-123.73	22.00	497	19.15	-4.23	13.58	0.55
175	**ch4_pui_tower-insitu_30_allvalid-84magl**	30	62.91	27.65	316.00	67647	15.59	-1.42	11.77	0.58
176	**ch4_puy_surface-flask_11_allvalid**	11	45.77	2.97	1470.00	728	29.76	-11.99	27.96	0.99
177	**ch4_puy_surface-insitu_11_allvalid**	11	45.77	2.97	1475.00	104365	17.75	-10.75	15.06	1.09
178	**ch4_rba-b_aircraft-pfp_433_representative**	433	-9.21	-66.16	2880.31	2287	19.32	-4.07	15.47	0.65
179	**ch4_rgl_tower-insitu_160_allvalid-90magl**	160	52.00	-2.54	297.00	98970	24.16	-6.48	21.51	0.86
180	**ch4_ric_surface-insitu_112_allvalid**	112	37.51	-77.58	154.00	24150	39.34	-2.58	36.66	0.87
181	**ch4_roc_tower-insitu_11_allvalid-140magl**	11	48.41	-3.89	502.00	10369	20.24	-10.23	17.05	0.96
182	**ch4_rpb_surface-flask_1_representative**	1	13.17	-59.43	20.00	1317	8.62	2.15	7.80	0.88
183	**ch4_rta_aircraft-pfp_1_allvalid**	1	-21.23	-159.79	3770.71	3100	6.65	-5.48	5.21	1.28
184	**ch4_run_surface-insitu_472_allvalid**	472	-21.08	55.38	2160.00	72547	6.83	-4.95	4.89	1.04
185	**ch4_ryo_surface-insitu_19_representative**	19	39.03	141.82	280.00	215527	18.66	-1.67	14.64	0.62
186	**ch4_sac_tower-insitu_11_allvalid-100magl**	11	48.72	2.14	260.00	72071	25.89	-0.57	23.32	0.81
187	**ch4_sah_aircraft-pfp_433_representative**	433	-0.87	-48.24	3828.22	354	11.14	-3.11	10.22	0.91
188	**ch4_san_aircraft-pfp_1_allvalid**	1	-2.86	-54.86	2486.70	335	19.59	-8.56	19.02	1.17

189	**ch4_san_aircraft-pfp_433_representative**	433	-2.85	-54.96	2623.24	3753	20.85	-10.24	20.42	0.96
190	**ch4_sca_aircraft-pfp_1_allvalid**	1	32.86	-79.53	4549.06	3973	13.86	5.97	11.53	0.89
191	**ch4_scs_shipboard-flask_1_representative**	1	11.75	110.34	20.00	364	21.59	3.77	23.01	1.16
192	**ch4_sct_surface-pfp_1_allvalid-305magl**	1	33.41	-81.83	420.00	3073	28.61	-7.38	24.73	0.81
193	**ch4_sct_tower-insitu_1_allvalid-305magl**	1	33.41	-81.83	420.00	60799	31.84	-9.68	26.86	0.80
194	**ch4_sdz_surface-flask_1_representative**	1	40.65	117.12	298.00	295	88.19	5.62	65.22	0.55
195	**ch4_sey_surface-flask_1_representative**	1	-4.68	55.53	7.00	1232	12.09	-1.97	8.92	0.57
196	**ch4_sgc_surface-insitu_431_allvalid**	431	36.70	-5.40	870.00	12540	13.81	1.20	12.68	0.85
197	**ch4_sgp_aircraft-pfp_1_allvalid**	1	36.62	-97.52	2952.60	6999	19.03	3.99	17.59	0.88
198	**ch4_sgp_surface-flask_1_representative**	1	36.67	-97.49	373.91	1228	49.99	-23.42	40.48	0.88
199	**ch4_sgp_surface-insitu_64_allvalid-60magl**	64	36.61	-97.49	374.00	78292	52.22	-16.92	43.11	0.79
200	**ch4_shm_surface-flask_1_representative**	1	52.72	174.11	28.00	1281	8.84	-4.91	8.84	1.31
201	**ch4_sig_surface-insitu_112_allvalid**	112	35.21	-85.29	676.75	31065	32.23	-4.76	26.32	0.69
202	**ch4_sis_surface-flask_2_representative**	2	60.09	-1.26	33.00	203	10.70	3.21	11.00	1.14
203	**ch4_sis_surface-flask_45_representative**	45	60.09	-1.26	35.00	987	14.64	4.69	17.55	1.54
204	**ch4_smo_surface-flask_1_representative**	1	-14.25	-170.57	53.50	2446	7.01	-2.98	5.18	0.73
205	**ch4_smr_tower-insitu_421_allvalid-125magl**	421	61.85	24.29	306.00	71155	14.70	-0.06	11.08	0.57
206	**ch4_snj_surface-insitu_112_allvalid**	112	41.14	-74.54	453.45	43122	33.24	-1.64	26.62	0.64
207	**ch4_sno_tower-insitu_464_allvalid-85magl**	464	81.36	-16.39	109.00	21798	8.89	-2.88	7.52	0.82
208	**ch4_sod_surface-insitu_30_allvalid**	30	67.36	26.64	227.00	46209	16.40	-5.21	13.44	0.77
209	**ch4_spo_surface-flask_1_representative**	1	-89.98	-24.80	2817.14	1973	5.00	-0.61	2.84	0.34
210	**ch4_spo_surface-flask_2_representative**	2	-89.98	-24.80	2847.00	1172	5.00	-1.34	3.09	0.45
211	**ch4_ste_tower-insitu_147_allvalid-252magl**	147	53.04	8.46	281.00	36918	41.61	-22.75	38.45	1.15
212	**ch4_stm_surface-flask_1_representative**	1	66.00	2.00	6.17	1229	11.15	0.49	12.33	1.22
213	**ch4_str_surface-pfp_1_allvalid-232magl**	1	37.76	-122.45	486.00	3766	31.94	8.47	29.88	0.94
214	**ch4_sum_surface-flask_1_representative**	1	72.60	-38.42	3214.54	1197	8.36	-0.83	7.18	0.75
215	**ch4_sur_aircraft-flask_20_allvalid**	20	61.20	73.20	3109.97	3076	16.64	-3.65	18.55	1.23
216	**ch4_svb_tower-insitu_440_allvalid-150magl**	440	64.26	19.77	419.00	53876	12.38	-3.27	9.77	0.69
217	**ch4_svv_tower-insitu_20_allvalid-52magl**	20	51.33	82.13	547.00	5992	57.98	-81.68	55.62	2.90
218	**ch4_syo_surface-flask_1_representative**	1	-69.01	39.58	17.23	643	5.00	-0.36	2.27	0.21
219	**ch4_syo_surface-insitu_8_representative**	8	-69.00	39.58	22.00	229069	5.00	-0.64	2.53	0.27
220	**ch4_tab_aircraft-pfp_433_representative**	433	-5.61	-69.84	2622.99	468	18.48	0.11	14.23	0.59
221	**ch4_tac_surface-flask_1_representative**	1	52.52	1.14	236.00	54	12.72	5.17	15.73	1.63
222	**ch4_tac_tower-insitu_160_allvalid-185magl**	160	52.52	1.14	249.00	89712	22.78	4.31	22.76	1.03
223	**ch4_tap_surface-flask_1_representative**	1	36.73	126.13	21.00	1918	42.25	1.54	35.08	0.69
224	**ch4_tef_aircraft-pfp_433_representative**	433	-3.48	-66.05	2667.70	641	20.89	2.34	16.80	0.62

225	**ch4_ter_surface-flask_55_allvalid**	55	69.20	35.10	42.00	940	18.34	-9.05	17.50	1.15
226	**ch4_tgc_aircraft-pfp_1_allvalid**	1	27.69	-96.74	4603.03	3186	13.03	4.67	11.84	0.89
227	**ch4_thd_aircraft-pfp_1_allvalid**	1	41.12	-124.25	4371.02	2944	12.13	3.28	11.19	0.92
228	**ch4_thd_surface-flask_1_representative**	1	41.05	-124.15	112.00	732	12.44	-5.65	11.38	1.04
229	**ch4_thd_surface-insitu_112_allvalid**	112	41.05	-124.15	197.00	55728	17.64	-4.04	13.07	0.60
230	**ch4_tik_surface-flask_1_representative**	1	71.60	128.89	29.00	343	18.87	-8.72	19.40	1.27
231	**ch4_tik_surface-insitu_55_allvalid**	55	71.80	128.97	29.00	79758	20.34	-8.88	19.90	1.15
232	**ch4_tll_surface-insitu_133_allvalid**	133	-30.17	-70.80	2159.00	48101	13.05	-1.93	7.85	0.38
233	**ch4_tll_surface-insitu_5_allvalid**	5	-30.17	-70.80	2225.00	18255	11.15	-1.17	6.39	0.34
234	**ch4_tmd_surface-pfp_1_allvalid-113magl**	1	39.58	-77.49	673.91	171	33.13	-13.93	27.25	0.85
235	**ch4_toh_tower-insitu_147_allvalid-147magl**	147	51.81	10.53	948.00	50667	18.90	-2.96	18.48	0.98
236	**ch4_tpi_surface-flask_1_representative**	1	10.38	114.37	9.00	212	15.27	-4.54	13.97	0.92
237	**ch4_trm_surface-flask_11_allvalid**	11	-15.88	54.52	10.00	130	10.84	2.56	10.67	1.01
238	**ch4_trn_tower-insitu_11_allvalid-180magl**	11	47.96	2.11	311.00	104503	22.18	0.99	20.79	0.88
239	**ch4_ulb_aircraft-pfp_1_allvalid**	1	47.40	106.04	3351.78	552	10.49	0.98	10.99	1.08
240	**ch4_uld_surface-insitu_61_allvalid**	61	37.48	130.90	230.90	27058	36.25	-7.90	29.83	0.72
241	**ch4_uny_surface-insitu_112_allvalid**	112	42.88	-74.79	523.01	28488	25.73	-1.46	19.66	0.59
242	**ch4_ush_surface-flask_1_representative**	1	-54.85	-68.31	32.00	797	5.23	0.58	2.55	0.25
243	**ch4_uta_surface-flask_1_representative**	1	39.90	-113.72	1332.00	1374	19.93	3.30	15.80	0.66
244	**ch4_uum_surface-flask_1_representative**	1	44.45	111.10	1012.00	1174	38.56	3.53	19.51	0.26
245	**ch4_vac_surface-insitu_431_allvalid**	431	42.88	-3.21	1122.00	26868	13.57	-2.32	13.12	0.96
246	**ch4_vgn_tower-insitu_20_allvalid-85magl**	20	54.50	62.32	277.00	25719	44.04	-15.16	34.28	0.72
247	**ch4_vkv_surface-insitu_55_allvalid**	55	59.95	30.70	76.00	26250	40.35	-10.95	37.84	0.95
248	**ch4_vrs_surface-flask_45_representative**	45	81.58	-16.64	34.00	116	8.95	-1.15	7.27	0.67
249	**ch4_wbi_aircraft-pfp_1_allvalid**	1	41.82	-91.41	4506.65	3370	13.12	4.94	12.44	1.06
250	**ch4_wbi_surface-pfp_1_allvalid-379magl**	1	41.72	-91.35	620.60	3853	31.00	-5.87	25.48	0.71
251	**ch4_wgc_tower-insitu_1_allvalid-483magl**	1	38.26	-121.49	486.00	118238	53.87	-16.03	50.52	0.97
252	**ch4_wis_surface-flask_1_representative**	1	30.72	34.82	431.91	1340	21.65	-0.71	17.30	0.64
253	**ch4_wkt_surface-flask_1_representative**	1	31.32	-97.32	426.00	366	42.92	-15.05	42.83	1.13
254	**ch4_wkt_surface-pfp_1_allvalid-457magl**	1	31.31	-97.33	708.00	2451	42.69	-8.95	40.71	0.95
255	**ch4_wlg_surface-flask_1_representative**	1	36.28	100.90	3823.30	1363	14.89	-6.75	13.55	1.04
256	**ch4_wpc_shipboard-flask_1_representative**	1	0.72	151.28	10.00	279	9.18	-0.40	8.35	0.83
257	**ch4_wsd_tower-insitu_60_allvalid**	60	44.05	-98.59	652.00	20496	46.20	-2.51	36.45	0.63
258	**ch4_yak_tower-insitu_20_allvalid-77magl**	20	62.09	129.36	341.00	12354	21.74	-9.92	22.15	1.25
259	**ch4_yon_surface-insitu_19_representative**	19	24.47	123.01	50.00	207655	20.30	0.10	18.94	0.87
260	**ch4_zep_surface-flask_1_representative**	1	78.91	11.89	479.00	1437	10.46	1.60	10.94	1.12
261	**ch4_zep_surface-insitu_56_allvalid**	56	78.91	11.89	489.00	45565	10.59	-0.28	10.54	0.99

262	**ch4_zgt_surface-insitu_25_allvalid**	25	54.43	12.73	7.50	23729	33.66	-5.21	28.03	0.72
263	**ch4_zot_surface-flask_45_representative**	45	64.48	89.21	414.00	805	27.49	3.34	31.69	1.34

Unassimilated

	Site Code	Laboratory	Latitude	Longitude	Elevation (MASL)	No. of Observation	Model-data mismatch	Mean bias	Standard deviation of bias	Chi-squared
1	**ch4 aao aircraft-pfp 1 allvalid**	1	40.14	-88.58	2000.09	3044	N/A	3.14	17.72	N/A
2	**ch4 above aircraft-insitu 1 allvalid**	1	64.02	-140.92	2260.40	95424	N/A	1.13	16.55	N/A
3	**ch4 above aircraft-pfp 1 allvalid**	1	65.18	-143.39	1974.67	344	N/A	-2.05	24.96	N/A
4	**ch4 abp surface-flask 1 representative**	1	-12.76	-38.16	6.00	113	N/A	0.68	2.58	N/A
5	**ch4 abp surface-flask 433 allvalid**	433	-12.77	-38.17	15.00	193	N/A	0.66	7.77	N/A
6	**ch4 abt surface-insitu 6 allvalid**	6	49.01	-122.34	93.00	57780	N/A	-111.31	117.45	N/A
7	**ch4 acg aircraft-pfp 1 allvalid**	1	68.06	-152.95	2305.13	1895	N/A	-0.77	17.48	N/A
8	**ch4 act aircraft-insitu 428 allvalid-b200**	428	37.32	-89.52	2272.25	350889	N/A	3.42	33.76	N/A
9	**ch4 act aircraft-insitu 428 allvalid-c130**	428	38.28	-88.44	3120.07	360820	N/A	4.81	23.40	N/A
10	**ch4 act aircraft-pfp 1 allvalid-b200**	1	36.73	-89.14	1892.90	615	N/A	0.88	31.84	N/A
11	**ch4 act aircraft-pfp 1 allvalid-c130**	1	37.86	-87.12	2183.92	544	N/A	3.08	27.34	N/A
12	**ch4 aia aircraft-flask 2 representative**	2	-40.30	144.42	3093.67	839	N/A	-3.36	7.54	N/A
13	**ch4 aircorenoaa aircore 1 allvalid**	1	37.57	-82.20	7793.86	81771	N/A	11.47	34.05	N/A
14	**ch4 ajax aircraft-insitu 429 allvalid**	429	37.56	-120.44	4381.23	289650	N/A	-9.18	171.76	N/A
15	**ch4 alf aircraft-pfp 433 representative**	433	-8.87	-56.75	1219.07	1920	N/A	1.51	17.76	N/A
16	**ch4 alk aircraft-flask 8 allvalid**	8	65.89	-152.10	2067.39	64	N/A	-8.83	11.88	N/A
17	**ch4 alt surface-flask 1 representative**	1	82.45	-62.51	190.00	1882	N/A	-3.58	18.36	N/A
18	**ch4 alt surface-flask 2 representative**	2	82.45	-62.51	210.00	1053	N/A	1.21	7.05	N/A
19	**ch4 alt surface-flask 45 representative**	45	82.45	-62.51	190.00	470	N/A	-2.83	14.72	N/A
20	**ch4 alt surface-insitu 6 allvalid**	6	82.45	-62.51	195.00	180832	N/A	2.04	9.94	N/A
21	**ch4 ams surface-insitu 11 allvalid**	11	-37.80	77.54	75.00	12793	N/A	0.35	2.03	N/A
22	**ch4 amt surface-flask 1 representative**	1	45.01	-68.66	157.00	268	N/A	-19.70	28.07	N/A
23	**ch4 amt surface-pfp 1 allvalid-107magl**	1	45.03	-68.68	160.40	2096	N/A	-6.83	19.93	N/A
24	**ch4 amy surface-flask 1 representative**	1	36.54	126.33	87.00	521	N/A	-73.98	83.94	N/A
25	**ch4 amy surface-insitu 61 allvalid**	61	36.54	126.33	67.00	165542	N/A	-12.57	89.95	N/A
26	**ch4 aoa aircraft-flask 19 allvalid**	19	27.96	147.80	5318.93	3291	N/A	1.11	15.46	N/A
27	**ch4 aoc shipboard-flask 1 allvalid**	1	-2.74	-25.05	12.37	238	N/A	-2.28	8.16	N/A
28	**ch4 ara surface-flask 2 representative**	2	-23.86	148.48	185.00	30	N/A	15.99	0.00	N/A
29	**ch4 arh surface-flask 15 allvalid**	15	-77.83	166.66	184.00	189	N/A	0.12	4.70	N/A
30	**ch4 arh surface-insitu 15 baseline**	15	-77.83	166.66	189.00	659	N/A	0.45	2.72	N/A
31	**ch4 asc surface-flask 1 representative**	1	-7.97	-14.40	90.00	2268	N/A	-3.95	5.96	N/A
32	**ch4 ask surface-flask 1 representative**	1	23.26	5.63	2715.00	1116	N/A	0.44	9.77	N/A

33	**ch4 azr surface-flask 1 representative**	1	38.76	-27.30	24.00	806	N/A	-5.75	26.06	N/A
34	**ch4 bal surface-flask 1 representative**	1	55.44	16.91	28.00	1342	N/A	-15.06	43.10	N/A
35	**ch4 bao aircraft-pfp 1 allvalid**	1	40.05	-105.01	3094.69	12	N/A	-23.46	48.60	N/A
36	**ch4 bao surface-pfp 1 allvalid-300magl**	1	40.05	-105.00	1884.00	3105	N/A	-56.11	102.70	N/A
37	**ch4 bao tower-insitu 1 allvalid**	1	40.05	-105.00	1719.61	4190	N/A	-38.56	72.60	N/A
38	**ch4 bck surface-insitu 6 allvalid**	6	62.80	-115.92	220.00	81945	N/A	-7.19	25.49	N/A
39	**ch4 bgi aircraft-pfp 1 allvalid**	1	42.82	-94.41	3347.49	339	N/A	-1.85	16.16	N/A
40	**ch4 bgu surface-flask 11 allvalid**	11	41.97	3.23	13.52	593	N/A	-3.19	81.15	N/A
41	**ch4 bhd surface-flask 15 allvalid**	15	-41.41	174.87	85.00	316	N/A	1.53	5.45	N/A
42	**ch4 bhd surface-flask 1 representative**	1	-41.41	174.87	92.12	336	N/A	-0.17	9.65	N/A
43	**ch4 bhd surface-insitu 15 baseline**	15	-41.41	174.87	95.00	2073	N/A	2.12	5.98	N/A
44	**ch4 bik surface-flask 45 representative**	45	53.20	22.75	483.00	418	N/A	-16.06	36.05	N/A
45	**ch4 bik tower-insitu 45 allvalid-180magl**	45	53.23	23.01	363.00	41522	N/A	-2.15	25.18	N/A
46	**ch4 bik tower-insitu 45 allvalid-300magl**	45	53.23	23.01	483.00	41516	N/A	-2.48	24.62	N/A
47	**ch4 bik tower-insitu 45 allvalid-30magl**	45	53.23	23.01	213.00	41527	N/A	-4.65	34.44	N/A
48	**ch4 bik tower-insitu 45 allvalid-5magl**	45	53.23	23.01	188.00	41525	N/A	-6.72	36.61	N/A
49	**ch4 bik tower-insitu 45 allvalid-90magl**	45	53.23	23.01	273.00	41532	N/A	-1.05	29.04	N/A
50	**ch4 bir tower-insitu 56 allvalid-10magl**	56	58.39	8.25	229.00	18739	N/A	1.10	18.87	N/A
51	**ch4 bir tower-insitu 56 allvalid-50magl**	56	58.39	8.25	269.00	18753	N/A	2.57	18.61	N/A
52	**ch4 bir tower-insitu 56 allvalid-75magl**	56	58.39	8.25	294.00	18945	N/A	2.82	18.92	N/A
53	**ch4 bis surface-insitu 11 allvalid**	11	44.38	-1.23	120.00	100871	N/A	2.52	20.93	N/A
54	**ch4 bkt surface-flask 1 representative**	1	-0.20	100.32	875.00	851	N/A	6.04	39.32	N/A
55	**ch4 bkt surface-insitu 5 allvalid**	5	-0.20	100.32	896.50	23400	N/A	-2.11	48.86	N/A
56	**ch4 blk surface-insitu 6 allvalid**	6	64.33	-96.01	61.00	19978	N/A	-9.18	11.32	N/A
57	**ch4 bme surface-flask 1 representative**	1	32.37	-64.65	17.00	396	N/A	-9.02	23.84	N/A
58	**ch4 bmw surface-flask 1 representative**	1	32.26	-64.88	55.78	1021	N/A	-3.33	17.45	N/A
59	**ch4 bne aircraft-pfp 1 allvalid**	1	40.80	-97.18	3424.00	1026	N/A	1.95	19.75	N/A
60	**ch4 bra surface-insitu 6 allvalid**	6	50.20	-104.71	630.00	90383	N/A	7.94	44.39	N/A
61	**ch4 brm tower-insitu 49 allvalid-12magl**	49	47.19	8.18	809.50	83403	N/A	-36.51	59.09	N/A
62	**ch4 brm tower-insitu 49 allvalid-132magl**	49	47.19	8.18	929.00	83211	N/A	1.96	49.74	N/A
63	**ch4 brm tower-insitu 49 allvalid-212magl**	49	47.19	8.18	1009.00	83439	N/A	19.64	48.52	N/A
64	**ch4 brm tower-insitu 49 allvalid-44magl**	49	47.19	8.18	841.60	83416	N/A	-17.00	52.87	N/A
65	**ch4 brm tower-insitu 49 allvalid-72magl**	49	47.19	8.18	869.00	83414	N/A	-8.55	51.30	N/A
66	**ch4 brw surface-flask 1 representative**	1	71.32	-156.61	21.63	2544	N/A	-36.35	55.89	N/A
67	**ch4 brw surface-insitu 1 allvalid**	1	71.32	-156.61	28.51	201512	N/A	-7.37	32.55	N/A
68	**ch4 bsc surface-flask 1 representative**	1	44.18	28.66	5.00	723	N/A	-129.11	161.00	N/A
69	**ch4 bsd tower-insitu 160 allvalid-108magl**	160	54.36	-1.15	490.00	60637	N/A	-8.51	23.97	N/A
70	**ch4 bsd tower-insitu 160 allvalid-248magl**	160	54.36	-1.15	630.00	60692	N/A	-5.97	19.82	N/A
71	**ch4 bsd tower-insitu 160 allvalid-42magl**	160	54.36	-1.15	424.00	60943	N/A	-10.10	27.07	N/A

72	**ch4 buc surface-insitu 112 allvalid**	112	38.46	-76.04	64.73	41497	N/A	19.40	41.21	N/A
73	**ch4 bwd surface-pfp 1 allvalid**	1	38.94	-76.95	69.56	79	N/A	-5.85	108.46	N/A
74	**ch4 car aircraft-pfp 1 allvalid**	1	40.82	-104.62	4893.95	8252	N/A	1.88	14.49	N/A
75	**ch4 carl surface-insitu 60 allvalid-9magl**	60	32.18	-104.44	1358.00	21506	N/A	-5.59	143.83	N/A
76	**ch4 cba surface-flask 1 representative**	1	55.21	-162.72	42.53	2318	N/A	-14.59	24.22	N/A
77	**ch4 cbw surface-insitu 118 allvalid**	118	51.97	4.93	37.00	2763	N/A	-123.61	162.68	N/A
78	**ch4 cbw tower-insitu 445 allvalid-127magl**	445	51.97	4.93	127.00	146885	N/A	-8.58	78.47	N/A
79	**ch4 cbw tower-insitu 445 allvalid-207magl**	445	51.97	4.93	207.00	155222	N/A	3.79	63.24	N/A
80	**ch4 cbw tower-insitu 445 allvalid-27magl**	445	51.97	4.93	27.00	150664	N/A	-110.52	165.57	N/A
81	**ch4 cbw tower-insitu 445 allvalid-67magl**	445	51.97	4.93	67.00	150825	N/A	-48.27	99.14	N/A
82	**ch4 cby surface-insitu 6 allvalid**	6	69.13	-105.06	47.00	66462	N/A	-9.45	12.43	N/A
83	**ch4 cdl surface-insitu 6 allvalid**	6	53.99	-105.12	630.00	31526	N/A	-4.57	36.92	N/A
84	**ch4 cea aircraft-flask 20 allvalid**	20	62.43	77.26	10824.90	887	N/A	40.12	50.72	N/A
85	**ch4 cfa surface-flask 2 representative**	2	-19.28	147.06	5.00	766	N/A	-2.38	6.83	N/A
86	**ch4 cgo surface-flask 1 representative**	1	-40.68	144.69	164.00	1055	N/A	4.11	14.32	N/A
87	**ch4 cgo surface-flask 2 representative**	2	-40.68	144.69	164.00	1787	N/A	0.88	2.15	N/A
88	**ch4 cgo surface-flask 45 representative**	45	-40.68	144.69	164.00	158	N/A	-21.56	93.38	N/A
89	**ch4 cgo surface-insitu 2 allvalid**	2	-40.68	144.69	164.00	89708	N/A	6.72	12.54	N/A
90	**ch4 chc surface-insitu 11 allvalid**	11	-16.20	-68.10	5355.00	49227	N/A	-13.54	17.31	N/A
91	**ch4 chl surface-insitu 6 allvalid**	6	58.74	-93.82	89.00	64043	N/A	0.85	28.22	N/A
92	**ch4 chm surface-insitu 6 allvalid**	6	49.69	-74.34	423.00	24019	N/A	-4.85	15.51	N/A
93	**ch4 chr surface-flask 1 representative**	1	1.70	-157.15	5.00	722	N/A	-2.94	14.93	N/A
94	**ch4 chs surface-insitu 1 allvalid**	1	68.51	161.53	46.35	109083	N/A	-14.38	35.02	N/A
95	**ch4 cib surface-flask 1 representative**	1	41.81	-4.93	850.00	607	N/A	-35.92	127.29	N/A
96	**ch4 cma aircraft-pfp 1 allvalid**	1	38.85	-74.33	2902.28	3273	N/A	3.85	17.62	N/A
97	**ch4 cmn surface-insitu 106 allvalid**	106	44.17	10.68	2172.00	78681	N/A	-11.02	30.27	N/A
98	**ch4 cmn surface-insitu 443 allvalid**	443	44.19	10.70	2173.00	77308	N/A	-5.23	25.28	N/A
99	**ch4 cmo surface-flask 1 representative**	1	45.48	-123.97	35.00	24	N/A	14.27	30.95	N/A
100	**ch4 cob2003b aircraft-insitu 59 allvalid**	59	43.46	-94.39	5183.07	935	N/A	64.18	217.86	N/A
101	**ch4 cob aircraft-flask 1 allvalid**	1	42.13	-89.20	3215.22	680	N/A	-0.23	66.42	N/A
102	**ch4 coi surface-insitu 20 allvalid**	20	43.16	145.50	94.00	136493	N/A	-5.95	17.01	N/A
103	**ch4 con aircraft-flask 42 allvalid**	42	29.25	108.73	9868.78	5279	N/A	15.52	53.23	N/A
104	**ch4 cpa surface-flask 2 representative**	2	-12.42	130.57	9.00	92	N/A	-5.42	10.54	N/A
105	**ch4 cpa surface-insitu 5 allvalid**	5	42.64	77.07	1623.00	30357	N/A	-10.86	33.63	N/A
106	**ch4 cps surface-insitu 6 allvalid**	6	49.82	-74.98	418.30	83738	N/A	-2.71	14.60	N/A
107	**ch4 cpt surface-flask 1 representative**	1	-34.35	18.49	260.00	422	N/A	-21.44	53.66	N/A
108	**ch4 cpt surface-insitu 36 marine**	36	-34.35	18.49	260.00	170647	N/A	2.43	4.73	N/A
109	**ch4 cra tower-insitu 188 allvalid-30magl**	188	43.13	0.37	630.00	30674	N/A	-0.04	26.31	N/A
110	**ch4 cra tower-insitu 188 allvalid-60magl**	188	43.13	0.37	660.00	31009	N/A	5.67	26.09	N/A

111	**ch4 cri surface-flask 2 representative**	2	15.08	73.83	66.00	342	N/A	-21.12	57.79	N/A
112	**ch4 crp surface-insitu 137 allvalid**	137	52.18	-6.37	23.00	61891	N/A	-2.29	41.11	N/A
113	**ch4 crv aircraft-pfp 1 allvalid**	1	64.27	-150.70	1360.35	2106	N/A	-18.90	55.72	N/A
114	**ch4 crv surface-pfp 1 allvalid-32magl**	1	64.99	-147.60	643.13	1703	N/A	-8.74	26.25	N/A
115	**ch4 crv tower-insitu 1 allvalid-17magl**	1	64.99	-147.60	628.53	77877	N/A	-0.22	14.76	N/A
116	**ch4 crv tower-insitu 1 allvalid-32magl**	1	64.99	-147.60	643.13	81117	N/A	-0.51	14.64	N/A
117	**ch4 crv tower-insitu 1 allvalid-5magl**	1	64.99	-147.60	616.33	78862	N/A	0.08	14.95	N/A
118	**ch4 crz surface-flask 1 representative**	1	-46.43	51.85	202.00	1010	N/A	-0.30	4.52	N/A
119	**ch4 cvo surface-flask 45 representative**	45	16.86	-24.87	40.00	700	N/A	3.26	7.76	N/A
120	**ch4 cvo surface-insitu 456 allvalid**	456	16.86	-24.87	40.00	70723	N/A	2.01	20.86	N/A
121	**ch4 cya surface-flask 2 representative**	2	-66.28	110.52	55.00	838	N/A	-1.00	2.20	N/A
122	**ch4 dec surface-insitu 431 allvalid**	431	40.74	0.79	10.00	30602	N/A	-128.58	319.68	N/A
123	**ch4 deu surface-insitu 25 allvalid**	25	49.77	7.05	480.00	33820	N/A	7.49	40.96	N/A
124	**ch4 dnd aircraft-pfp 1 allvalid**	1	47.86	-98.48	2964.01	1988	N/A	1.97	15.63	N/A
125	**ch4 dnh surface-insitu 112 allvalid**	112	43.71	-72.15	659.00	13947	N/A	2.47	14.57	N/A
126	**ch4 drp shipboard-flask 1 representative**	1	-58.64	-64.11	10.00	291	N/A	-0.16	3.55	N/A
127	**ch4 dsi surface-flask 1 representative**	1	20.70	116.73	8.00	597	N/A	-25.01	48.71	N/A
128	**ch4 dvv tower-insitu 60 allvalid**	60	36.71	-79.44	492.00	10584	N/A	9.57	34.78	N/A
129	**ch4 eco aircraft-insitu 1 allvalid**	1	40.18	-74.22	918.33	30473	N/A	0.64	21.67	N/A
130	**ch4 eec surface-insitu 431 allvalid**	431	36.06	-5.66	40.00	12816	N/A	7.75	32.99	N/A
131	**ch4 egb surface-insitu 6 allvalid**	6	44.23	-79.78	270.88	119570	N/A	-5.92	38.51	N/A
132	**ch4 eic surface-flask 1 representative**	1	-27.15	-109.44	61.37	807	N/A	-6.28	6.66	N/A
133	**ch4 ena surface-insitu 64 allvalid-10magl**	64	39.09	-28.03	40.48	38567	N/A	-6.45	27.88	N/A
134	**ch4 ers surface-insitu 11 allvalid**	11	42.97	9.38	573.00	58690	N/A	17.80	23.11	N/A
135	**ch4 esp aircraft-pfp 1 allvalid**	1	49.40	-126.49	2395.73	4934	N/A	-0.73	9.03	N/A
136	**ch4 esp surface-flask 2 representative**	2	49.38	-126.53	47.00	78	N/A	-13.92	1.87	N/A
137	**ch4 esp surface-insitu 6 allvalid**	6	49.38	-126.54	47.00	101002	N/A	-2.08	11.24	N/A
138	**ch4 est surface-insitu 6 allvalid**	6	51.67	-110.21	752.66	100403	N/A	-42.42	104.73	N/A
139	**ch4 etl aircraft-pfp 1 allvalid**	1	54.33	-104.95	1790.17	3255	N/A	-2.05	14.07	N/A
140	**ch4 etl surface-insitu 6 allvalid**	6	54.35	-104.99	598.00	128494	N/A	-9.30	29.33	N/A
141	**ch4 fam aircraft-flask 1 allvalid**	1	52.56	0.82	715.50	22	N/A	2.60	30.55	N/A
142	**ch4 fkl surface-flask 11 allvalid**	11	35.34	25.67	150.93	390	N/A	8.41	89.72	N/A
143	**ch4 fkl surface-insitu 11 allvalid**	11	35.34	25.67	265.00	67861	N/A	-0.49	12.08	N/A
144	**ch4 fne surface-insitu 6 allvalid**	6	58.84	-122.57	376.00	49280	N/A	20.83	49.47	N/A
145	**ch4 fort surface-insitu 60 allvalid-128magl**	60	30.87	-102.82	1115.00	21094	N/A	58.54	111.00	N/A
146	**ch4 fsd surface-insitu 6 allvalid**	6	49.88	-81.57	250.00	168316	N/A	2.36	27.60	N/A
147	**ch4 ftl aircraft-pfp 1 allvalid**	1	-4.15	-38.28	1477.26	159	N/A	-0.76	7.23	N/A
148	**ch4 fwi aircraft-pfp 1 allvalid**	1	44.71	-91.01	3536.32	361	N/A	2.94	21.10	N/A
149	**ch4 gat tower-insitu 147 allvalid-132magl**	147	53.07	11.44	202.00	53118	N/A	3.86	31.30	N/A

150	**ch4 gat tower-insitu 147 allvalid-216magl**	147	53.07	11.44	286.00	53141	N/A	3.26	28.12	N/A
151	**ch4 gat tower-insitu 147 allvalid-30magl**	147	53.07	11.44	100.00	53231	N/A	-3.63	35.54	N/A
152	**ch4 gat tower-insitu 147 allvalid-341magl**	147	53.07	11.44	411.00	53558	N/A	2.00	25.68	N/A
153	**ch4 gat tower-insitu 147 allvalid-60magl**	147	53.07	11.44	130.00	53226	N/A	2.36	35.12	N/A
154	**ch4 gci01 tower-insitu 60 allvalid**	60	32.47	-92.28	165.00	8373	N/A	44.65	81.73	N/A
155	**ch4 gci02 tower-insitu 60 allvalid**	60	33.75	-89.85	205.00	18498	N/A	41.87	68.65	N/A
156	**ch4 gci03 tower-insitu 60 allvalid**	60	31.89	-89.73	232.00	11163	N/A	-3.93	48.47	N/A
157	**ch4 gci04 tower-insitu 60 allvalid**	60	33.18	-85.89	428.00	5441	N/A	5.03	29.77	N/A
158	**ch4 ghg03 surface-insitu 112 allvalid**	112	32.65	-83.03	177.27	38120	N/A	7.73	47.48	N/A
159	**ch4 ghg06 surface-insitu 112 allvalid**	112	47.52	-95.43	528.37	62332	N/A	-9.45	32.53	N/A
160	**ch4 ghg09 surface-insitu 112 allvalid**	112	48.67	-98.84	559.88	86277	N/A	6.40	28.28	N/A
161	**ch4 ghg10 surface-insitu 112 allvalid**	112	33.85	-80.53	142.35	37715	N/A	-0.35	53.82	N/A
162	**ch4 gic surface-insitu 431 allvalid**	431	40.35	-5.18	1456.00	33885	N/A	-34.93	61.82	N/A
163	**ch4 gif surface-insitu 11 allvalid**	11	48.71	2.15	167.00	51250	N/A	-0.13	40.17	N/A
164	**ch4 gmi surface-flask 1 representative**	1	13.39	144.66	6.28	1673	N/A	-6.56	32.60	N/A
165	**ch4 goz surface-flask 1 representative**	1	36.05	14.89	6.00	26	N/A	-26.40	61.67	N/A
166	**ch4 gpa surface-flask 2 representative**	2	-12.25	131.04	37.00	87	N/A	-34.76	54.97	N/A
167	**ch4 gsn surface-insitu 61 allvalid**	61	33.28	126.15	78.00	77837	N/A	-17.06	46.69	N/A
168	**ch4 gvn surface-flask 45 representative**	45	-70.67	-8.27	44.00	208	N/A	0.20	2.10	N/A
169	**ch4 haa aircraft-pfp 1 allvalid**	1	21.23	-158.92	2962.34	1776	N/A	-0.99	9.39	N/A
170	**ch4 hat surface-insitu 20 allvalid**	20	24.06	123.81	47.30	134193	N/A	-6.49	18.83	N/A
171	**ch4 hba surface-flask 1 representative**	1	-75.61	-26.21	35.00	977	N/A	0.03	1.89	N/A
172	**ch4 hct surface-insitu 112 allvalid**	112	41.43	-72.95	277.00	17133	N/A	5.49	28.71	N/A
173	**ch4 hei surface-insitu 22 allvalid**	22	49.42	8.68	143.00	194338	N/A	3.76	51.82	N/A
174	**ch4 hel surface-insitu 147 allvalid**	147	54.18	7.88	153.00	19628	N/A	5.37	47.06	N/A
175	**ch4 hfm aircraft-pfp 1 allvalid**	1	42.54	-72.17	2399.60	1593	N/A	-3.73	17.77	N/A
176	**ch4 hfm surface-pfp 1 allvalid**	1	42.54	-72.17	369.00	12	N/A	-5.26	19.38	N/A
177	**ch4 hil aircraft-pfp 1 allvalid**	1	40.06	-87.92	3484.93	3424	N/A	4.98	15.61	N/A
178	**ch4 hip aircraft-insitu 59 allvalid**	59	17.58	-87.99	6936.72	110784	N/A	-0.10	25.29	N/A
179	**ch4 hip aircraft-pfp 1 allvalid**	1	14.22	-92.98	5331.94	1352	N/A	2.22	19.21	N/A
180	**ch4 hle surface-flask 11 allvalid**	11	32.78	78.96	4522.00	321	N/A	27.11	115.20	N/A
181	**ch4 hnp surface-insitu 6 allvalid**	6	43.61	-79.39	97.00	46026	N/A	-14.57	56.09	N/A
182	**ch4 hobb surface-insitu 60 allvalid-91magl**	60	32.71	-103.09	1194.00	24167	N/A	-57.13	258.26	N/A
183	**ch4 how aircraft-pfp 1 allvalid**	1	42.20	-68.13	1395.00	30	N/A	5.23	17.12	N/A
184	**ch4 hpb surface-flask 1 representative**	1	47.80	11.02	990.00	850	N/A	-39.89	84.33	N/A
185	**ch4 hpb tower-insitu 147 allvalid-131magl**	147	47.80	11.02	1065.00	61690	N/A	27.17	48.44	N/A
186	**ch4 hpb tower-insitu 147 allvalid-50magl**	147	47.80	11.02	984.00	58957	N/A	17.87	48.81	N/A
187	**ch4 hpb tower-insitu 147 allvalid-93magl**	147	47.80	11.02	1027.00	60448	N/A	23.45	48.56	N/A
188	**ch4 hsu surface-flask 1 representative**	1	41.05	-124.65	7.60	87	N/A	19.26	21.96	N/A

189	**ch4 htm tower-insitu 424 allvalid-150magl**	424	56.10	13.42	265.00	49652	N/A	-3.64	19.00	N/A
190	**ch4 htm tower-insitu 424 allvalid-30magl**	424	56.10	13.42	145.00	49170	N/A	-4.51	20.23	N/A
191	**ch4 htm tower-insitu 424 allvalid-70magl**	424	56.10	13.42	185.00	49154	N/A	-2.96	19.43	N/A
192	**ch4 hun surface-flask 1 representative**	1	46.96	16.65	344.00	1299	N/A	-48.29	64.14	N/A
193	**ch4 hun tower-insitu 35 allvalid-10magl**	35	46.96	16.65	258.00	24463	N/A	-5.97	39.60	N/A
194	**ch4 hun tower-insitu 35 allvalid-115magl**	35	46.96	16.65	363.00	23747	N/A	13.61	32.23	N/A
195	**ch4 hun tower-insitu 35 allvalid-48magl**	35	46.96	16.65	296.00	24448	N/A	1.79	32.19	N/A
196	**ch4 hun tower-insitu 35 allvalid-82magl**	35	46.96	16.65	330.00	53848	N/A	2.83	33.65	N/A
197	**ch4 iagos-caribic aircraft-flask 457 allvalid**	457	39.12	1.65	11060.98	8025	N/A	21.71	39.12	N/A
198	**ch4 iagos-caribic aircraft-insitu 457 allvalid**	457	39.87	-9.23	10740.86	749510	N/A	20.11	35.94	N/A
199	**ch4 iagos-core aircraft-insitu 45 allvalid**	45	46.06	8.83	10654.09	824383	N/A	30.75	41.70	N/A
200	**ch4 ice surface-flask 1 representative**	1	63.40	-20.29	126.06	1236	N/A	-6.37	17.88	N/A
201	**ch4 inu surface-insitu 6 allvalid**	6	68.32	-133.53	123.00	90548	N/A	-11.42	20.75	N/A
202	**ch4 inx01 surface-insitu 60 allhours-10magl**	60	39.58	-86.42	266.30	61267	N/A	4.60	46.59	N/A
203	**ch4 inx01 surface-insitu 60 allhours-121magl**	60	39.58	-86.42	377.30	65995	N/A	7.97	39.07	N/A
204	**ch4 inx01 surface-insitu 60 allhours-40magl**	60	39.58	-86.42	296.30	61326	N/A	8.40	49.05	N/A
205	**ch4 inx02 surface-insitu 60 allhours-10magl**	60	39.80	-86.02	276.90	25921	N/A	-22.07	68.79	N/A
206	**ch4 inx02 surface-insitu 60 allhours-136magl**	60	39.80	-86.02	402.90	88483	N/A	-0.98	39.56	N/A
207	**ch4 inx02 surface-insitu 60 allhours-40magl**	60	39.80	-86.02	306.90	25969	N/A	-5.92	47.94	N/A
208	**ch4 inx03 surface-insitu 60 allhours-10magl**	60	39.78	-86.17	236.00	3932	N/A	-54.33	284.86	N/A
209	**ch4 inx03 surface-insitu 60 allhours-20magl**	60	39.78	-86.17	246.00	3934	N/A	-51.51	279.97	N/A
210	**ch4 inx03 surface-insitu 60 allhours-40magl**	60	39.78	-86.17	266.00	3933	N/A	-45.46	264.90	N/A
211	**ch4 inx03 surface-insitu 60 allhours-54magl**	60	39.78	-86.17	280.00	3973	N/A	-41.37	228.81	N/A
212	**ch4 inx04 surface-insitu 60 allhours-60magl**	60	39.59	-86.11	309.00	36765	N/A	4.66	59.29	N/A
213	**ch4 inx05 surface-insitu 60 allhours-125magl**	60	39.89	-86.20	376.00	7608	N/A	-8.29	46.88	N/A
214	**ch4 inx07 surface-insitu 60 allhours-21magl**	60	39.77	-86.27	262.00	16082	N/A	-30.11	212.62	N/A
215	**ch4 inx07 surface-insitu 60 allhours-58magl**	60	39.77	-86.27	299.00	52744	N/A	-18.13	128.82	N/A
216	**ch4 inx08 surface-insitu 60 allhours-41magl**	60	40.04	-85.97	286.00	76021	N/A	-0.21	41.88	N/A
217	**ch4 inx09 surface-insitu 60 allhours-130magl**	60	39.86	-85.74	407.00	31804	N/A	3.99	37.75	N/A
218	**ch4 inx10 surface-insitu 60 allhours-40magl**	60	39.72	-86.14	263.00	77927	N/A	-30.65	147.39	N/A
219	**ch4 inx11 surface-insitu 60 allhours-130magl**	60	39.84	-86.18	344.00	49460	N/A	-1.26	56.74	N/A
220	**ch4 inx13 surface-insitu 60 allhours-87magl**	60	39.72	-85.94	335.00	60749	N/A	6.31	43.14	N/A
221	**ch4 inx14 surface-insitu 60 allhours-76magl**	60	40.00	-86.74	340.00	46351	N/A	12.64	39.38	N/A
222	**ch4 inx15 surface-insitu 60 allhours-75magl**	60	39.64	86.48	333.00	18637	N/A	-53.88	53.77	N/A
223	**ch4 inx aircraft-pfp 1 allvalid**	1	39.87	-86.20	1006.47	350	N/A	-3.58	25.92	N/A
224	**ch4 inx surface-pfp 1 allvalid-121magl**	1	39.58	-86.42	376.73	549	N/A	3.00	24.17	N/A
225	**ch4 inx surface-pfp 1 allvalid-125magl**	1	39.89	-86.20	373.99	171	N/A	-4.29	39.15	N/A
226	**ch4 inx surface-pfp 1 allvalid-129magl**	1	39.86	-85.74	407.82	303	N/A	-0.31	26.72	N/A
227	**ch4 inx surface-pfp 1 allvalid-130magl**	1	39.84	-86.18	344.12	12	N/A	-12.33	27.51	N/A
228	**ch4 inx surface-pfp 1 allvalid-137magl**	1	39.80	-86.02	402.95	598	N/A	-0.92	30.03	N/A
229	**ch4 inx surface-pfp 1 allvalid-39magl**	1	39.92	-86.03	290.78	141	N/A	-2.21	20.17	N/A

230	**ch4 inx surface-pfp 1 allvalid-40magl**	1	39.72	-86.14	263.96	99	N/A	-17.65	40.39	N/A
231	**ch4 inx surface-pfp 1 allvalid-54magl**	1	39.78	-86.17	279.81	377	N/A	-16.07	73.10	N/A
232	**ch4 ipr tower-insitu 103 allvalid-100magl**	103	45.81	8.64	310.00	43280	N/A	-6.07	97.62	N/A
233	**ch4 ipr tower-insitu 103 allvalid-40magl**	103	45.81	8.64	250.00	41496	N/A	-36.70	103.11	N/A
234	**ch4 ipr tower-insitu 103 allvalid-60magl**	103	45.81	8.64	270.00	41679	N/A	-24.28	100.48	N/A
235	**ch4 itn surface-flask 1 allvalid**	1	35.37	-77.39	456.63	268	N/A	-6.04	35.20	N/A
236	**ch4 ivi surface-insitu 11 allvalid**	11	61.21	-48.17	18.00	22218	N/A	-7.15	12.82	N/A
237	**ch4 izo surface-flask 1 representative**	1	28.31	-16.49	2377.90	1189	N/A	-2.80	19.58	N/A
238	**ch4 izo surface-insitu 27 allvalid**	27	28.31	-16.50	2401.90	202879	N/A	0.88	12.20	N/A
239	**ch4 jar tower-insitu 475 allvalid-110magl**	475	58.28	27.31	146.00	41678	N/A	-6.62	22.60	N/A
240	**ch4 jar tower-insitu 475 allvalid-30magl**	475	58.28	27.31	66.00	41677	N/A	-10.87	22.57	N/A
241	**ch4 jar tower-insitu 475 allvalid-50magl**	475	58.28	27.31	86.00	41677	N/A	-10.39	22.18	N/A
242	**ch4 jar tower-insitu 475 allvalid-70magl**	475	58.28	27.31	106.00	41678	N/A	-9.43	21.76	N/A
243	**ch4 jar tower-insitu 475 allvalid-90magl**	475	58.28	27.31	126.00	41675	N/A	-8.35	21.63	N/A
244	**ch4 jfj surface-flask 45 representative**	45	46.55	7.99	3570.00	341	N/A	-7.61	31.40	N/A
245	**ch4 jfj surface-insitu 5 allvalid**	5	46.55	7.99	3580.00	70681	N/A	0.87	15.14	N/A
246	**ch4 jfj tower-insitu 49 allvalid-13magl**	49	46.55	7.99	3585.70	139477	N/A	-1.44	16.99	N/A
247	**ch4 jfj tower-insitu 49 allvalid-5magl**	49	46.55	7.99	3576.80	7088	N/A	1.53	15.19	N/A
248	**ch4 jue tower-insitu 147 allvalid-120magl**	147	50.91	6.41	218.00	26460	N/A	16.97	60.06	N/A
249	**ch4 jue tower-insitu 147 allvalid-50magl**	147	50.91	6.41	148.00	26308	N/A	1.40	64.24	N/A
250	**ch4 jue tower-insitu 147 allvalid-80magl**	147	50.91	6.41	178.00	26364	N/A	7.57	60.84	N/A
251	**ch4 kas surface-insitu 53 allvalid**	53	49.23	19.98	1994.00	144606	N/A	0.29	27.87	N/A
252	**ch4 kco surface-flask 1 allvalid**	1	4.97	73.47	6.00	89	N/A	0.92	7.57	N/A
253	**ch4 key surface-flask 1 representative**	1	25.67	-80.18	6.00	1061	N/A	-60.05	67.73	N/A
254	**ch4 kit tower-insitu 147 allvalid-100magl**	147	49.09	8.42	210.00	49217	N/A	3.78	37.39	N/A
255	**ch4 kit tower-insitu 147 allvalid-200magl**	147	49.09	8.42	310.00	50377	N/A	16.64	37.38	N/A
256	**ch4 kit tower-insitu 147 allvalid-30magl**	147	49.09	8.42	140.00	48336	N/A	-0.86	37.47	N/A
257	**ch4 kit tower-insitu 147 allvalid-60magl**	147	49.09	8.42	170.00	49247	N/A	-1.26	41.15	N/A
258	**ch4 kjn surface-flask 45 representative**	45	70.85	29.23	10.00	176	N/A	-13.84	18.42	N/A
259	**ch4 kmp surface-insitu 30 allvalid**	30	60.20	24.96	56.00	64738	N/A	-0.37	24.86	N/A
260	**ch4 korus-aq aircraft-insitu 428 allvalid-dc8**	428	37.78	96.24	3456.24	64394	N/A	-13.71	55.59	N/A
261	**ch4 kre tower-insitu 441 allvalid-10magl**	441	49.57	15.08	544.00	36382	N/A	-20.66	56.69	N/A
262	**ch4 kre tower-insitu 441 allvalid-125magl**	441	49.57	15.08	659.00	37935	N/A	-4.68	25.59	N/A
263	**ch4 kre tower-insitu 441 allvalid-250magl**	441	49.57	15.08	784.00	40392	N/A	-3.04	23.36	N/A
264	**ch4 kre tower-insitu 441 allvalid-50magl**	441	49.57	15.08	584.00	38989	N/A	-8.80	32.91	N/A
265	**ch4 krk surface-insitu 118 allvalid**	118	50.07	19.91	255.00	3585	N/A	-128.99	156.44	N/A
266	**ch4 kum surface-flask 1 representative**	1	19.54	-154.84	8.83	2560	N/A	0.16	15.26	N/A
267	**ch4 kzd surface-flask 1 representative**	1	44.30	76.11	489.95	575	N/A	-38.04	53.52	N/A

268	**ch4 kzm surface-flask 1 representative**	1	43.25	77.88	2524.00	566	N/A	-12.51	30.58	N/A
269	**ch4 lac surface-pfp 1 allvalid**	1	34.07	-118.21	229.83	843	N/A	-58.34	90.25	N/A
270	**ch4 lau surface-flask 15 allvalid**	15	-45.03	169.67	380.00	435	N/A	0.30	8.62	N/A
271	**ch4 lau surface-insitu 15 allvalid**	15	-45.04	169.68	380.00	1273	N/A	0.88	9.81	N/A
272	**ch4 lau surface-insitu 15 baseline**	15	-45.04	169.68	380.00	473	N/A	-11.73	13.84	N/A
273	**ch4 lef aircraft-pfp 1 allvalid**	1	45.96	-90.20	1645.92	4585	N/A	3.57	18.33	N/A
274	**ch4 lef surface-flask 1 representative**	1	45.94	-90.27	868.00	1159	N/A	-2.22	33.51	N/A
275	**ch4 lef surface-pfp 1 allvalid-244magl**	1	45.95	-90.27	716.00	1516	N/A	6.46	26.24	N/A
276	**ch4 lef surface-pfp 1 allvalid-396magl**	1	45.95	-90.27	868.00	2980	N/A	-12.63	32.98	N/A
277	**ch4 lef tower-insitu 1 allvalid-122magl**	1	45.95	-90.27	594.00	87131	N/A	-1.24	23.49	N/A
278	**ch4 lef tower-insitu 1 allvalid-30magl**	1	45.95	-90.27	502.00	86354	N/A	-1.80	28.79	N/A
279	**ch4 lef tower-insitu 1 allvalid-396magl**	1	45.95	-90.27	868.00	87608	N/A	-4.44	20.89	N/A
280	**ch4 lew surface-insitu 112 allvalid**	112	40.94	-76.88	238.13	49151	N/A	3.36	62.53	N/A
281	**ch4 lew surface-pfp 1 allvalid-95magl**	1	40.94	-76.88	261.00	998	N/A	-36.23	77.97	N/A
282	**ch4 lhw surface-insitu 5 allvalid**	5	47.48	8.40	872.00	81331	N/A	0.44	40.67	N/A
283	**ch4 lin tower-insitu 147 allvalid-10magl**	147	52.17	14.12	83.00	54924	N/A	-12.85	46.63	N/A
284	**ch4 lin tower-insitu 147 allvalid-2.5magl**	147	52.17	14.12	75.50	54662	N/A	-14.05	48.64	N/A
285	**ch4 lin tower-insitu 147 allvalid-40magl**	147	52.17	14.12	113.00	57326	N/A	-4.27	30.90	N/A
286	**ch4 lin tower-insitu 147 allvalid-98magl**	147	52.17	14.12	171.00	58091	N/A	4.51	30.31	N/A
287	**ch4 llb surface-flask 1 representative**	1	54.95	-112.45	567.05	212	N/A	-166.98	171.82	N/A
288	**ch4 llb surface-insitu 6 allvalid**	6	54.95	-112.47	584.42	112344	N/A	-25.85	84.11	N/A
289	**ch4 lln surface-flask 1 representative**	1	23.47	120.87	2867.00	853	N/A	-14.27	31.99	N/A
290	**ch4 lmp surface-flask 1 representative**	1	35.52	12.62	50.00	733	N/A	2.81	17.54	N/A
291	**ch4 lmp surface-flask 28 allvalid**	28	35.52	12.63	47.00	1042	N/A	9.63	27.14	N/A
292	**ch4 lmp surface-insitu 28 allvalid**	28	35.52	12.63	47.00	1042	N/A	9.63	27.14	N/A
293	**ch4 lmu surface-insitu 431 allvalid**	431	41.60	-1.10	3079.00	38650	N/A	-36.58	35.63	N/A
294	**ch4 lpo surface-flask 11 allvalid**	11	48.80	-3.58	20.00	272	N/A	-4.10	134.11	N/A
295	**ch4 lut surface-insitu 118 allvalid**	118	53.40	6.35	61.00	2460	N/A	-54.81	99.44	N/A
296	**ch4 lut surface-insitu 44 allvalid**	44	53.40	6.35	61.00	119019	N/A	-31.15	91.53	N/A
297	**ch4 maa surface-flask 2 representative**	2	-67.62	62.87	42.00	951	N/A	-0.79	1.54	N/A
298	**ch4 malj surface-insitu 60 allvalid-134magl**	60	32.87	-103.76	1444.00	10718	N/A	-9.94	84.99	N/A
299	**ch4 man aircraft-insitu 1 allvalid**	1	-2.49	-59.82	2712.78	5187	N/A	-9.91	14.62	N/A
300	**ch4 man aircraft-pfp 433 representative**	433	-2.43	-59.55	1050.07	587	N/A	-7.30	22.14	N/A
301	**ch4 mbc surface-flask 1 representative**	1	76.25	-119.35	35.00	35	N/A	-13.28	23.51	N/A
302	**ch4 mbo surface-pfp 1 allvalid-11magl**	1	43.98	-121.69	2742.30	2177	N/A	-6.48	29.06	N/A
303	**ch4 mci aircraft-pfp 1 allvalid**	1	41.05	-89.88	1247.36	128	N/A	-14.43	18.88	N/A
304	**ch4 mdm surface-flask 28 allvalid**	28	37.88	14.03	1653.00	400	N/A	-12.60	22.58	N/A
305	**ch4 mex surface-flask 1 representative**	1	18.98	-97.31	4469.00	540	N/A	-12.66	23.68	N/A

306	**ch4 mhd surface-flask 11 allvalid**	11	53.33	-9.90	29.56	780	N/A	-10.12	109.05	N/A
307	**ch4 mhd surface-flask 1 representative**	1	53.33	-9.90	26.10	1155	N/A	-19.22	41.40	N/A
308	**ch4 mhd surface-insitu 11 allvalid**	11	53.33	-9.90	29.00	109929	N/A	-0.64	18.60	N/A
309	**ch4 mid surface-flask 1 representative**	1	28.21	-177.37	10.81	1283	N/A	1.99	8.10	N/A
310	**ch4 mkn surface-flask 1 representative**	1	-0.06	37.30	3649.00	156	N/A	-3.84	32.67	N/A
311	**ch4 mkn surface-insitu 701 allvalid**	701	-0.06	37.30	3688.00	21193	N/A	-9.25	14.81	N/A
312	**ch4 mlh surface-insitu 468 allvalid**	468	55.35	-7.33	69.00	71608	N/A	-7.65	34.85	N/A
313	**ch4 mlo surface-flask 1 representative**	1	19.53	-155.58	3419.08	2680	N/A	4.76	9.46	N/A
314	**ch4 mlo surface-flask 2 representative**	2	19.54	-155.58	3435.00	1313	N/A	3.37	8.47	N/A
315	**ch4 mlo surface-insitu 1 allvalid**	1	19.54	-155.58	3437.00	217423	N/A	2.75	9.33	N/A
316	**ch4 mnc surface-insitu 112 allvalid**	112	35.83	-78.15	205.99	42124	N/A	11.88	35.88	N/A
317	**ch4 mnm surface-insitu 19 representative**	19	24.29	153.98	27.10	207073	N/A	2.16	9.59	N/A
318	**ch4 mqa surface-flask 2 representative**	2	-54.48	158.97	13.00	961	N/A	-0.38	3.14	N/A
319	**ch4 mrc aircraft-pfp 1 allvalid**	1	41.70	-76.22	1264.79	77	N/A	-12.89	15.92	N/A
320	**ch4 mrc surface-pfp 1 allvalid-east**	1	41.77	-75.68	509.02	179	N/A	-19.83	106.87	N/A
321	**ch4 mrc surface-pfp 1 allvalid-south**	1	41.47	-76.42	651.99	816	N/A	-9.57	27.73	N/A
322	**ch4 mrc tower-insitu 60 allvalid-south**	60	41.47	-76.42	652.00	77010	N/A	-7.22	34.67	N/A
323	**ch4 msh surface-pfp 1 allvalid-46magl**	1	41.66	-70.50	78.30	605	N/A	-12.85	32.72	N/A
324	**ch4 mvy surface-pfp 1 allvalid-16magl**	1	41.33	-70.57	16.00	210	N/A	0.91	25.29	N/A
325	**ch4 mwo surface-pfp 1 allvalid-46magl**	1	34.22	-118.06	1775.23	4889	N/A	-39.79	50.19	N/A
326	**ch4 nam surface-flask 45 representative**	45	-23.56	15.05	431.00	282	N/A	-5.47	10.25	N/A
327	**ch4 nat surface-flask 1 representative**	1	-5.64	-35.23	50.92	385	N/A	-12.38	17.50	N/A
328	**ch4 ndao surface-insitu 45 allvalid-21magl**	45	-23.56	15.05	429.00	7872	N/A	-1.13	9.62	N/A
329	**ch4 neb surface-pfp 1 allvalid**	1	39.32	-76.58	110.95	102	N/A	-27.83	47.99	N/A
330	**ch4 ngm shipboard-flask 8 allvalid**	8	3.34	147.62	20.00	629	N/A	-44.41	131.51	N/A
331	**ch4 nha aircraft-pfp 1 allvalid**	1	42.93	-70.59	2515.36	4201	N/A	2.18	13.41	N/A
332	**ch4 nmb surface-flask 1 representative**	1	-23.58	15.03	461.00	744	N/A	-8.04	28.33	N/A
333	**ch4 nor tower-insitu 424 allvalid-100magl**	424	60.09	17.48	146.00	50877	N/A	-1.90	12.82	N/A
334	**ch4 nor tower-insitu 424 allvalid-32magl**	424	60.09	17.48	78.00	50535	N/A	-3.27	13.64	N/A
335	**ch4 nor tower-insitu 424 allvalid-58magl**	424	60.09	17.48	104.00	50530	N/A	-2.76	13.04	N/A
336	**ch4 notr surface-insitu 60 allvalid-91magl**	60	31.97	102.77	1106.00	22240	N/A	-51.21	126.68	N/A
337	**ch4 nov aircraft-flask 20 allvalid**	20	55.00	83.00	1821.78	3099	N/A	-1.24	31.66	N/A
338	**ch4 noy tower-insitu 20 allvalid-21magl**	20	63.43	75.78	129.00	33645	N/A	-51.99	106.20	N/A
339	**ch4 noy tower-insitu 20 allvalid-43magl**	20	63.43	75.78	151.00	33731	N/A	-33.99	82.28	N/A
340	**ch4 nsa aircraft-pfp 1 allvalid**	1	68.99	-150.78	712.51	379	N/A	-12.88	25.77	N/A
341	**ch4 nsk aircraft-pfp 1 allvalid**	1	58.80	-104.59	2929.37	47	N/A	-4.63	30.80	N/A
342	**ch4 nwb surface-pfp 1 allvalid**	1	39.34	-76.69	189.89	96	N/A	-26.14	55.81	N/A
343	**ch4 nwf surface-pfp 1 allvalid-23magl**	1	40.03	-105.55	3072.99	658	N/A	-9.49	34.71	N/A
344	**ch4 nwf surface-pfp 1 allvalid-2magl**	1	40.03	-105.55	3051.96	222	N/A	-0.30	20.25	N/A

345	**ch4 nwp surface-flask 8 allvalid**	8	-3.85	151.11	20.00	3604	N/A	-10.26	34.02	N/A
346	**ch4 nwr surface-flask 1 representative**	1	40.05	-105.58	3526.00	1314	N/A	-18.29	30.25	N/A
347	**ch4 nwr surface-pfp 1 allvalid-3magl**	1	40.05	-105.59	3526.20	3968	N/A	-10.01	33.42	N/A
348	**ch4 nya surface-flask 8 representative**	8	78.92	11.93	43.00	1097	N/A	-14.44	352.14	N/A
349	**ch4 obn surface-flask 1 representative**	1	55.10	36.60	484.00	324	N/A	-71.77	105.32	N/A
350	**ch4 ohp tower-insitu 468 allvalid-100magl**	468	43.93	5.71	750.00	67604	N/A	12.82	18.18	N/A
351	**ch4 ohp tower-insitu 468 allvalid-10magl**	468	43.93	5.71	660.00	67928	N/A	16.49	19.67	N/A
352	**ch4 ohp tower-insitu 468 allvalid-50magl**	468	43.93	5.71	700.00	62943	N/A	14.50	19.04	N/A
353	**ch4 oil aircraft-pfp 1 allvalid**	1	41.28	-88.94	4161.12	406	N/A	1.97	14.47	N/A
354	**ch4 oli surface-insitu 64 allvalid-10magl**	64	70.50	-149.89	12.00	48720	N/A	-33.14	86.49	N/A
355	**ch4 ope tower-insitu 11 allvalid-10magl**	11	48.56	5.50	400.00	92131	N/A	8.67	30.72	N/A
356	**ch4 ope tower-insitu 11 allvalid-120magl**	11	48.56	5.50	510.00	95371	N/A	6.39	25.32	N/A
357	**ch4 ope tower-insitu 11 allvalid-50magl**	11	48.56	5.50	440.00	91310	N/A	11.06	29.23	N/A
358	**ch4 orc aircraft-insitu 3 allvalid-merge10**	3	-46.22	-72.33	7310.62	35908	N/A	10.46	34.70	N/A
359	**ch4 orl aircraft-flask 11 allvalid**	11	47.83	2.50	856.66	2156	N/A	12.40	132.33	N/A
360	**ch4 ota surface-flask 2 representative**	2	-38.52	142.82	50.00	217	N/A	-499.45	509.81	N/A
361	**ch4 oxk surface-flask 1 representative**	1	50.03	11.81	1181.07	659	N/A	-31.45	73.83	N/A
362	**ch4 oxk surface-flask 45 representative**	45	50.03	11.81	1185.00	659	N/A	-26.98	45.10	N/A
363	**ch4 oxk tower-insitu 147 allvalid-163magl**	147	50.03	11.81	1185.00	26868	N/A	-7.08	20.40	N/A
364	**ch4 oxk tower-insitu 147 allvalid-23magl**	147	50.03	11.81	1045.00	27595	N/A	-14.86	26.90	N/A
365	**ch4 oxk tower-insitu 147 allvalid-90magl**	147	50.03	11.81	1112.00	27433	N/A	-10.42	23.12	N/A
366	**ch4 pal surface-flask 1 representative**	1	67.97	24.12	570.00	958	N/A	-17.90	28.10	N/A
367	**ch4 pal surface-insitu 30 allvalid**	30	67.97	24.12	577.00	149612	N/A	-6.78	14.14	N/A
368	**ch4 pal surface-insitu 30 continental**	30	67.97	24.12	570.00	20725	N/A	-3.69	13.43	N/A
369	**ch4 pal surface-insitu 30 marine**	30	67.97	24.12	570.00	16034	N/A	-4.04	7.43	N/A
370	**ch4 pal surface-insitu 30 nonlocal**	30	67.97	24.12	570.00	81677	N/A	-4.97	12.55	N/A
371	**ch4 pao shipboard-flask 1 allvalid**	1	18.07	-72.97	10.00	178	N/A	-1.17	12.22	N/A
372	**ch4 pco surface-flask 1 allvalid**	1	38.47	-28.40	2230.00	12	N/A	13.51	11.97	N/A
373	**ch4 pdi surface-insitu 5 allvalid**	5	21.57	103.52	1478.00	15978	N/A	-30.55	41.49	N/A
374	**ch4 pdm surface-flask 11 allvalid**	11	42.94	0.14	2880.27	540	N/A	-6.46	200.28	N/A
375	**ch4 pdm surface-insitu 11 allvalid**	11	42.94	0.14	2905.00	68098	N/A	-0.09	11.06	N/A
376	**ch4 pfa aircraft-pfp 1 allvalid**	1	64.89	-148.26	2343.69	4893	N/A	-0.68	11.25	N/A
377	**ch4 pip aircraft-flask 8 allvalid**	8	37.81	141.35	1911.49	2044	N/A	-1.59	24.67	N/A
378	**ch4 poc shipboard-flask 1 representative**	1	-1.06	-117.03	20.00	3717	N/A	-3.31	15.49	N/A
379	**ch4 poc surface-flask 15 allvalid**	15	-5.14	154.20	27.26	350	N/A	3.02	12.03	N/A
380	**ch4 prs surface-insitu 21 allvalid**	21	45.93	7.70	3490.00	94740	N/A	7.62	18.55	N/A
381	**ch4 psa surface-flask 1 representative**	1	-64.77	-64.05	15.00	1275	N/A	-1.62	9.40	N/A
382	**ch4 pta surface-flask 1 representative**	1	38.95	-123.73	22.00	497	N/A	-9.18	37.67	N/A
383	**ch4 pui tower-insitu 30 allvalid-47magl**	30	62.91	27.65	279.00	22813	N/A	0.53	14.51	N/A

384	**ch4 pui tower-insitu 30 allvalid-84magl**	30	62.91	27.65	316.00	59082	N/A	0.62	14.02	N/A
385	**ch4 puy surface-flask 11 allvalid**	11	45.77	2.97	1469.31	728	N/A	-18.26	205.14	N/A
386	**ch4 puy surface-insitu 11 allvalid**	11	45.77	2.97	1475.00	49999	N/A	-10.37	18.19	N/A
387	**ch4 rba-b aircraft-pfp 433 representative**	433	-9.19	-65.89	1051.16	2287	N/A	-18.87	93.85	N/A
388	**ch4 rgl tower-insitu 160 allvalid-45magl**	160	52.00	-2.54	252.00	89082	N/A	-10.80	32.36	N/A
389	**ch4 rgl tower-insitu 160 allvalid-90magl**	160	52.00	-2.54	297.00	90490	N/A	-9.06	33.73	N/A
390	**ch4 ric surface-insitu 112 allvalid**	112	37.51	-77.58	154.00	24150	N/A	-11.48	114.34	N/A
391	**ch4 roc tower-insitu 11 allvalid-140magl**	11	48.41	-3.89	502.00	7737	N/A	-12.30	23.35	N/A
392	**ch4 roc tower-insitu 11 allvalid-25magl**	11	48.41	-3.89	387.00	8942	N/A	-22.64	30.53	N/A
393	**ch4 roc tower-insitu 11 allvalid-80magl**	11	48.41	-3.89	442.00	7741	N/A	-15.87	24.62	N/A
394	**ch4 rpb surface-flask 1 representative**	1	13.16	-59.43	20.00	1267	N/A	-13.63	85.72	N/A
395	**ch4 rta aircraft-pfp 1 allvalid**	1	-21.24	-159.78	2605.10	2899	N/A	-5.80	5.20	N/A
396	**ch4 run surface-insitu 472 allvalid**	472	-21.08	55.38	2160.00	64604	N/A	-3.79	5.92	N/A
397	**ch4 ryo surface-insitu 19 representative**	19	39.03	141.82	280.00	207471	N/A	-1.84	16.36	N/A
398	**ch4 s2k aircraft-pfp 1 allvalid**	1	-23.93	29.30	4268.61	183	N/A	-10.23	71.20	N/A
399	**ch4 sac tower-insitu 11 allvalid-100magl**	11	48.72	2.14	260.00	63335	N/A	7.95	37.44	N/A
400	**ch4 sac tower-insitu 11 allvalid-15magl**	11	48.72	2.14	175.00	53616	N/A	-5.65	42.55	N/A
401	**ch4 sac tower-insitu 11 allvalid-60magl**	11	48.72	2.14	220.00	52723	N/A	2.68	36.50	N/A
402	**ch4 sah aircraft-pfp 433 representative**	433	-0.81	-48.06	1984.19	354	N/A	2.20	15.94	N/A
403	**ch4 san aircraft-pfp 1 allvalid**	1	-2.86	-54.87	1102.78	335	N/A	-30.27	40.28	N/A
404	**ch4 san aircraft-pfp 433 representative**	433	-2.86	-54.95	1240.39	3753	N/A	-30.09	36.37	N/A
405	**ch4 sca aircraft-pfp 1 allvalid**	1	32.83	-79.48	3393.90	3777	N/A	6.84	18.84	N/A
406	**ch4 scs shipboard-flask 1 representative**	1	13.04	110.89	20.00	364	N/A	-23.13	63.14	N/A
407	**ch4 sct surface-pfp 1 allvalid-305magl**	1	33.41	-81.83	420.00	3073	N/A	-12.41	47.43	N/A
408	**ch4 sct tower-insitu 1 allvalid-305magl**	1	33.41	-81.83	420.00	58756	N/A	5.95	31.40	N/A
409	**ch4 sct tower-insitu 1 allvalid-31magl**	1	33.41	-81.83	146.20	53598	N/A	-18.46	66.65	N/A
410	**ch4 sct tower-insitu 1 allvalid-61magl**	1	33.41	-81.83	176.20	58172	N/A	-10.02	54.67	N/A
411	**ch4 sdz surface-flask 1 representative**	1	40.65	117.12	298.00	295	N/A	-32.30	119.41	N/A
412	**ch4 seac4rs aircraft-insitu 428 allvalid-ER2**	428	32.53	-95.97	17996.62	41999	N/A	52.47	37.88	N/A
413	**ch4 seac4rs aircraft-insitu 428 allvalid-dc8**	428	33.60	-95.73	5253.35	17279	N/A	12.61	32.30	N/A
414	**ch4 sey surface-flask 1 representative**	1	-4.68	55.53	7.00	1186	N/A	-5.23	18.60	N/A
415	**ch4 sgc surface-insitu 431 allvalid**	431	36.70	-5.40	870.00	12540	N/A	-5.30	16.26	N/A
416	**ch4 sgp aircraft-pfp 1 allvalid**	1	36.62	-97.51	1657.27	6786	N/A	-7.86	31.46	N/A
417	**ch4 sgp surface-flask 1 representative**	1	36.67	-97.49	373.55	1151	N/A	-79.66	96.59	N/A
418	**ch4 sgp surface-insitu 64 allvalid-60magl**	64	36.61	-97.49	374.00	69588	N/A	-25.12	96.40	N/A
419	**ch4 sgp surface-pfp 1 allvalid-60magl**	1	36.61	-97.49	374.00	345	N/A	-78.82	92.33	N/A
420	**ch4 sgp surface-pfp 1 allvalid-9magl**	1	36.61	-97.49	323.10	16	N/A	-6.49	55.98	N/A
421	**ch4 shm surface-flask 1 representative**	1	52.71	174.11	28.00	1244	N/A	-5.91	15.26	N/A

422	**ch4 sig surface-insitu 112 allvalid**	112	35.21	-85.29	676.71	31065	N/A	-1.64	29.08	N/A
423	**ch4 sis surface-flask 2 representative**	2	60.09	-1.25	33.00	203	N/A	11.37	15.87	N/A
424	**ch4 sis surface-flask 45 representative**	45	60.09	-1.25	35.00	940	N/A	3.75	24.50	N/A
425	**ch4 smo surface-flask 1 representative**	1	-14.25	-170.57	53.32	2359	N/A	-4.23	8.05	N/A
426	**ch4 smr tower-insitu 421 allvalid-125magl**	421	61.85	24.29	306.00	62730	N/A	0.65	12.69	N/A
427	**ch4 smr tower-insitu 421 allvalid-16magl**	421	61.85	24.29	197.80	63020	N/A	3.75	13.69	N/A
428	**ch4 smr tower-insitu 421 allvalid-67magl**	421	61.85	24.29	248.20	62715	N/A	1.49	12.79	N/A
429	**ch4 snj surface-insitu 112 allvalid**	112	41.14	-74.54	453.45	43122	N/A	-1.70	33.89	N/A
430	**ch4 sno tower-insitu 464 allvalid-20magl**	464	81.36	-16.39	44.00	13437	N/A	0.51	8.62	N/A
431	**ch4 sno tower-insitu 464 allvalid-50magl**	464	81.36	-16.39	74.00	13526	N/A	0.57	8.60	N/A
432	**ch4 sno tower-insitu 464 allvalid-85magl**	464	81.36	-16.39	109.00	13738	N/A	0.47	8.75	N/A
433	**ch4 sod surface-insitu 30 allvalid**	30	67.36	26.64	227.00	46209	N/A	-12.82	29.27	N/A
434	**ch4 spo surface-flask 1 representative**	1	-89.98	-24.80	2817.27	1900	N/A	-0.33	2.77	N/A
435	**ch4 spo surface-flask 2 representative**	2	-89.98	-24.80	2847.00	1129	N/A	-0.73	2.79	N/A
436	**ch4 ssl tower-insitu 23 allvalid-12magl**	23	47.92	7.92	1217.00	195662	N/A	4.10	22.22	N/A
437	**ch4 ssl tower-insitu 23 allvalid-35magl**	23	47.92	7.92	1240.00	10895	N/A	5.09	18.14	N/A
438	**ch4 start08 aircraft-insitu 59 allvalid**	59	44.73	-101.87	9908.37	20412	N/A	21.74	41.16	N/A
439	**ch4 ste tower-insitu 147 allvalid-127magl**	147	53.04	8.46	156.00	28728	N/A	-14.83	65.03	N/A
440	**ch4 ste tower-insitu 147 allvalid-187magl**	147	53.04	8.46	216.00	28745	N/A	-13.94	52.82	N/A
441	**ch4 ste tower-insitu 147 allvalid-252magl**	147	53.04	8.46	281.00	29089	N/A	-10.99	45.59	N/A
442	**ch4 ste tower-insitu 147 allvalid-32magl**	147	53.04	8.46	61.00	28818	N/A	-69.90	104.45	N/A
443	**ch4 ste tower-insitu 147 allvalid-82magl**	147	53.04	8.46	111.00	28737	N/A	-28.23	72.15	N/A
444	**ch4 stm surface-flask 1 representative**	1	66.00	2.00	6.28	1229	N/A	-6.15	23.12	N/A
445	**ch4 str surface-pfp 1 allvalid-232magl**	1	37.76	-122.45	486.00	3766	N/A	4.61	45.54	N/A
446	**ch4 sum surface-flask 1 representative**	1	72.60	-38.42	3214.54	1146	N/A	-2.31	14.29	N/A
447	**ch4 sur aircraft-flask 20 allvalid**	20	61.20	73.20	2662.12	3076	N/A	-3.33	33.52	N/A
448	**ch4 svb tower-insitu 440 allvalid-150magl**	440	64.26	19.77	419.00	45605	N/A	-3.60	10.69	N/A
449	**ch4 svb tower-insitu 440 allvalid-35magl**	440	64.26	19.77	304.00	45410	N/A	-3.62	11.16	N/A
450	**ch4 svb tower-insitu 440 allvalid-85magl**	440	64.26	19.77	354.00	45651	N/A	-3.66	10.81	N/A
451	**ch4 svv tower-insitu 20 allvalid-27magl**	20	51.33	82.13	522.00	5990	N/A	-88.76	78.71	N/A
452	**ch4 svv tower-insitu 20 allvalid-52magl**	20	51.33	82.13	547.00	5992	N/A	-91.63	84.21	N/A
453	**ch4 syo surface-flask 1 representative**	1	-69.00	39.58	16.97	620	N/A	0.37	2.55	N/A
454	**ch4 syo surface-insitu 8 representative**	8	-69.00	39.58	22.00	220703	N/A	-0.09	2.57	N/A
455	**ch4 tab aircraft-pfp 433 representative**	433	-5.65	-69.87	1513.59	468	N/A	-19.95	26.52	N/A
456	**ch4 tac surface-flask 1 representative**	1	52.52	1.14	236.00	54	N/A	-5.95	22.91	N/A
457	**ch4 tac tower-insitu 160 allvalid-100magl**	160	52.52	1.14	164.00	84683	N/A	6.62	34.68	N/A
458	**ch4 tac tower-insitu 160 allvalid-185magl**	160	52.52	1.14	249.00	81442	N/A	4.34	28.26	N/A
459	**ch4 tac tower-insitu 160 allvalid-54magl**	160	52.52	1.14	118.00	83474	N/A	7.98	39.22	N/A
460	**ch4 tao surface-insitu 6 allvalid**	6	43.66	-79.40	274.00	16901	N/A	-23.40	49.96	N/A

461	**ch4 tap surface-flask 1 representative**	1	36.73	126.13	21.00	1863	N/A	-71.76	109.52	N/A
462	**ch4 tda aircraft-flask 8 allvalid**	8	36.02	135.65	7084.95	2690	N/A	-8.48	29.22	N/A
463	**ch4 tef aircraft-pfp 433 representative**	433	-3.48	-66.06	1070.50	641	N/A	4.76	191.02	N/A
464	**ch4 ter surface-flask 55 allvalid**	55	69.20	35.10	42.00	940	N/A	-14.82	26.86	N/A
465	**ch4 tgc aircraft-pfp 1 allvalid**	1	27.69	-96.75	2919.61	2959	N/A	4.32	21.33	N/A
466	**ch4 thd aircraft-pfp 1 allvalid**	1	41.06	-124.18	3096.49	2685	N/A	3.48	13.56	N/A
467	**ch4 thd surface-flask 1 representative**	1	41.05	-124.15	112.00	732	N/A	2.40	17.00	N/A
468	**ch4 thd surface-insitu 112 allvalid**	112	41.05	-124.15	197.00	55728	N/A	0.47	16.14	N/A
469	**ch4 tik surface-flask 1 representative**	1	71.60	128.89	29.00	343	N/A	-38.79	56.60	N/A
470	**ch4 tik surface-flask 55 allvalid**	55	71.59	128.92	18.00	241	N/A	-3.44	26.46	N/A
471	**ch4 tik surface-insitu 55 allvalid**	55	71.80	128.97	29.00	53286	N/A	-4.39	26.84	N/A
472	**ch4 tll surface-insitu 133 allvalid**	133	-30.17	-70.80	2159.00	48101	N/A	-3.53	8.17	N/A
473	**ch4 tll surface-insitu 5 allvalid**	5	-30.17	-70.80	2225.00	18255	N/A	-3.02	7.58	N/A
474	**ch4 tmd surface-pfp 1 allvalid**	1	39.58	-77.49	673.91	162	N/A	-38.52	69.51	N/A
475	**ch4 toh tower-insitu 147 allvalid-10magl**	147	51.81	10.53	811.00	42655	N/A	-6.91	22.96	N/A
476	**ch4 toh tower-insitu 147 allvalid-110magl**	147	51.81	10.53	911.00	42699	N/A	-6.20	21.32	N/A
477	**ch4 toh tower-insitu 147 allvalid-147magl**	147	51.81	10.53	948.00	42640	N/A	-6.41	21.25	N/A
478	**ch4 toh tower-insitu 147 allvalid-76magl**	147	51.81	10.53	877.00	42692	N/A	-6.81	22.10	N/A
479	**ch4 tom aircraft-insitu 1 allvalid**	1	10.65	-78.41	6828.28	140383	N/A	7.29	26.74	N/A
480	**ch4 tom aircraft-pfp 1 allvalid**	1	11.22	-82.32	5281.65	1229	N/A	2.81	22.61	N/A
481	**ch4 tpd surface-insitu 6 allvalid**	6	42.64	-80.56	266.00	68235	N/A	16.50	47.45	N/A
482	**ch4 tpi surface-flask 1 allvalid**	1	10.38	114.37	9.00	297	N/A	-6.44	21.48	N/A
483	**ch4 trm surface-flask 11 allvalid**	11	-15.88	54.52	10.00	130	N/A	-9.14	45.85	N/A
484	**ch4 trn tower-insitu 11 allvalid-100magl**	11	47.96	2.11	231.00	92936	N/A	10.84	31.84	N/A
485	**ch4 trn tower-insitu 11 allvalid-180magl**	11	47.96	2.11	311.00	96075	N/A	13.95	31.30	N/A
486	**ch4 trn tower-insitu 11 allvalid-50magl**	11	47.96	2.11	181.00	94206	N/A	6.13	32.96	N/A
487	**ch4 trn tower-insitu 11 allvalid-5magl**	11	47.96	2.11	136.00	63948	N/A	4.61	31.49	N/A
488	**ch4 ugd aircraft-insitu 1 allvalid**	1	2.22	31.68	3758.35	19699	N/A	-27.33	51.52	N/A
489	**ch4 ulb aircraft-pfp 1 allvalid**	1	47.40	106.04	2057.83	552	N/A	-0.64	9.99	N/A
490	**ch4 uld surface-insitu 61 allvalid**	61	37.48	130.90	230.90	67773	N/A	-3.02	28.84	N/A
491	**ch4 uny surface-insitu 112 allvalid**	112	42.88	-74.79	523.00	28488	N/A	1.74	22.80	N/A
492	**ch4 ush surface-flask 1 representative**	1	-54.85	-68.31	32.00	757	N/A	-1.96	6.24	N/A
493	**ch4 uta surface-flask 1 representative**	1	39.90	-113.72	1332.00	1323	N/A	-33.72	78.08	N/A
494	**ch4 uto surface-insitu 30 allvalid**	30	59.78	21.37	64.00	43800	N/A	5.90	15.16	N/A
495	**ch4 uum surface-flask 1 representative**	1	44.45	111.10	1012.00	1174	N/A	-17.52	35.79	N/A
496	**ch4 vac surface-insitu 431 allvalid**	431	42.88	-3.21	1122.00	26868	N/A	-3.77	13.72	N/A
497	**ch4 vgn tower-insitu 20 allvalid-42magl**	20	54.50	62.32	234.00	25731	N/A	-19.52	41.67	N/A
498	**ch4 vgn tower-insitu 20 allvalid-85magl**	20	54.50	62.32	277.00	25719	N/A	-14.60	42.62	N/A
499	**ch4 vkv surface-insitu 55 allvalid**	55	59.95	30.70	76.00	26250	N/A	-49.51	106.84	N/A

500	**ch4 vrs surface-flask 45 representative**	45	81.58	-16.64	34.00	116	N/A	-14.37	25.74	N/A
501	**ch4 wao surface-insitu 13 allvalid**	13	52.95	1.12	41.00	73684	N/A	12.89	36.09	N/A
502	**ch4 wbi aircraft-pfp 1 allvalid**	1	41.95	-91.50	3629.01	3094	N/A	4.16	16.76	N/A
503	**ch4 wbi surface-pfp 1 allvalid-379magl**	1	41.72	-91.35	620.60	3853	N/A	-15.44	39.26	N/A
504	**ch4 wes surface-insitu 25 allvalid**	25	54.92	8.31	26.00	12208	N/A	-9.65	50.78	N/A
505	**ch4 wgc aircraft-pfp 1 allvalid**	1	38.18	-119.80	901.79	165	N/A	-20.27	30.91	N/A
506	**ch4 wgc surface-pfp 1 allvalid-484magl**	1	38.26	-121.49	486.00	61	N/A	-37.35	74.68	N/A
507	**ch4 wgc surface-pfp 1 allvalid-89magl**	1	38.26	-121.49	91.10	3088	N/A	-65.87	135.80	N/A
508	**ch4 wgc tower-insitu 1 allvalid-30magl**	1	38.26	-121.49	32.00	119657	N/A	-119.29	218.10	N/A
509	**ch4 wgc tower-insitu 1 allvalid-483magl**	1	38.26	-121.49	486.00	117907	N/A	10.81	72.07	N/A
510	**ch4 wgc tower-insitu 1 allvalid-91magl**	1	38.26	-121.49	91.10	121265	N/A	-74.98	163.03	N/A
511	**ch4 wis surface-flask 1 representative**	1	30.50	34.89	351.02	1299	N/A	-21.76	42.75	N/A
512	**ch4 wkt surface-flask 1 representative**	1	31.32	-97.33	401.24	366	N/A	-28.09	60.19	N/A
513	**ch4 wkt surface-pfp 1 allvalid-122magl**	1	31.31	-97.33	373.00	924	N/A	-8.87	43.47	N/A
514	**ch4 wkt surface-pfp 1 allvalid-457magl**	1	31.31	-97.33	708.00	2451	N/A	-28.04	82.49	N/A
515	**ch4 wlg surface-flask 1 representative**	1	36.28	100.90	3822.64	1311	N/A	-14.65	26.09	N/A
516	**ch4 wpc shipboard-flask 1 representative**	1	8.06	147.47	10.00	279	N/A	3.46	7.96	N/A
517	**ch4 wsa surface-insitu 6 allvalid**	6	43.93	-60.01	24.05	107103	N/A	-3.21	13.89	N/A
518	**ch4 wsd tower-insitu 60 allvalid**	60	44.05	-98.59	652.00	20496	N/A	-8.26	33.79	N/A
519	**ch4 yak tower-insitu 20 allvalid-11magl**	20	62.09	129.36	275.00	13413	N/A	-18.43	44.86	N/A
520	**ch4 yak tower-insitu 20 allvalid-77magl**	20	62.09	129.36	341.00	12354	N/A	-5.68	29.96	N/A
521	**ch4 yon surface-insitu 19 representative**	19	24.47	123.01	50.00	199272	N/A	0.33	20.68	N/A
522	**ch4 zep surface-flask 1 representative**	1	78.91	11.89	479.00	1385	N/A	-9.56	20.50	N/A
523	**ch4 zep surface-insitu 56 allvalid**	56	78.91	11.89	489.00	100084	N/A	3.09	24.25	N/A
524	**ch4 zgt surface-insitu 25 allvalid**	25	54.43	12.73	7.50	23729	N/A	-11.93	55.97	N/A
525	**ch4 zot surface-flask 45 representative**	45	60.75	89.38	411.00	805	N/A	-8.31	42.43	N/A
526	**ch4 zsf surface-insitu 25 allvalid**	25	47.42	10.98	2669.00	1	N/A	-13.24	0.00	N/A

Table 7. Summary of statistics of observational Sites for $\delta^{13}C$-CH_4 used in CarbonTracker-CH_4.

[Download Here]

Assimilated										
	Site Code	**Laboratory**	**Latitude**	**Longitude**	**Elevation (MASL)**	**No. of Observation**	**Model-data mismatch**	**Mean bias**	**Standard deviation of bias**	**Chi-squared**
1	**ch4_acg_aircraft-pfp_1_allvalid**	1	68.50	-153.42	3897.74	809	0.20	0.06	0.22	3.27
2	**ch4_alt_surface-flask_1_representative**	1	82.45	-62.51	190.00	1037	0.17	0.01	0.10	0.72

3	ch4_alt_surface-flask_45_representative	45	82.45	-62.51	190.00	285	0.37	0.07	0.13	0.16
4	ch4_amy_surface-flask_1_representative	1	36.54	126.33	87.00	224	1.50	-0.15	0.17	0.03
5	ch4_asc_surface-flask_1_representative	1	-7.97	-14.40	90.00	1292	0.19	-0.06	0.09	0.85
6	ch4_azr_surface-flask_1_representative	1	38.76	-27.33	24.00	387	0.20	-0.06	0.11	0.93
7	ch4_bal_surface-flask_1_representative	1	55.35	17.22	28.00	206	0.89	-0.09	0.16	0.11
8	ch4_bhd_surface-flask_1_representative	1	-41.41	174.87	92.72	150	0.24	-0.09	0.09	0.54
9	ch4_bhd_surface-insitu_15_baseline	15	-41.41	174.87	95.00	376	0.21	-0.10	0.06	0.47
10	ch4_bik_surface-flask_45_representative	45	53.20	22.75	483.00	144	0.90	-0.02	0.16	0.06
11	ch4_cba_surface-flask_1_representative	1	55.21	-162.72	57.04	969	0.19	0.05	0.13	1.12
12	ch4_cgo_surface-flask_1_representative	1	-40.68	144.68	164.00	643	0.14	-0.08	0.09	1.31
13	ch4_con_aircraft-flask_42_allvalid	42	9.38	133.32	11126.07	394	0.32	0.00	0.10	0.16
14	ch4_crv_surface-pfp_1_allvalid-32magl	1	64.99	-147.60	643.13	1121	0.57	0.03	0.22	1.00
15	ch4_cvo_surface-flask_45_representative	45	16.86	-24.87	40.00	481	0.37	-0.05	0.12	0.13
16	ch4_eic_surface-flask_1_representative	1	-27.16	-109.43	69.00	77	0.11	-0.10	0.07	2.15
17	ch4_gmi_surface-flask_1_representative	1	13.39	144.66	5.00	215	0.25	-0.07	0.11	0.60
18	ch4_gvn_surface-flask_45_representative	45	-70.67	-8.27	44.00	195	0.33	-0.06	0.12	0.16
19	ch4_jfj_surface-flask_45_representative	45	46.55	7.99	3570.00	190	0.40	-0.02	0.14	0.14
20	ch4_kjn_surface-flask_45_representative	45	70.85	29.23	10.00	171	0.41	0.06	0.13	0.14
21	ch4_kum_surface-flask_1_representative	1	19.54	-154.85	8.23	894	0.21	-0.07	0.09	0.85
22	ch4_llb_surface-flask_1_representative	1	54.95	-112.45	574.74	133	0.97	0.05	0.39	0.28
23	ch4_mex_surface-flask_1_representative	1	18.98	-97.31	4469.00	398	0.37	-0.06	0.10	0.41
24	ch4_mhd_surface-flask_1_representative	1	53.32	-9.90	25.43	591	0.28	-0.07	0.10	0.46
25	ch4_mid_surface-flask_1_representative	1	28.21	-177.37	12.69	296	0.19	-0.06	0.10	0.94
26	ch4_mlo_surface-flask_1_representative	1	19.53	-155.57	3437.00	1595	0.31	-0.07	0.09	0.60
27	ch4_nam_surface-flask_45_representative	45	-23.56	15.05	431.00	286	0.43	-0.05	0.11	0.09
28	ch4_ngm_shipboard-flask_8_allvalid	8	-0.31	148.20	20.00	463	0.37	-0.06	0.12	0.25
29	ch4_nwr_surface-flask_1_representative	1	40.05	-105.58	3526.00	815	0.29	-0.10	0.09	0.58
30	ch4_nya_surface-flask_8_representative	8	78.92	11.93	43.00	893	0.32	0.09	0.10	0.25
31	ch4_oxk_surface-flask_45_representative	45	50.03	11.81	1185.00	205	0.65	0.01	0.18	0.12
32	ch4_pfa_aircraft-pfp_1_allvalid	1	64.93	-148.83	3850.52	1597	0.22	0.01	0.23	2.40
33	ch4_psa_surface-flask_1_representative	1	-64.77	-64.05	15.00	6	0.09	0.07	0.15	3.43
34	ch4_sis_surface-flask_45_representative	45	60.09	-1.26	35.00	561	0.47	0.03	0.16	0.16
35	ch4_smo_surface-flask_1_representative	1	-14.25	-170.57	53.32	1457	0.15	-0.05	0.08	0.92
36	ch4_spo_surface-flask_1_representative	1	-89.98	-24.80	2817.14	1256	0.10	-0.07	0.09	2.20
37	ch4_sum_surface-flask_1_representative	1	72.60	-38.42	3214.54	493	0.14	-0.03	0.12	1.20
38	ch4_sur_aircraft-flask_20_allvalid	20	61.20	73.20	1375.00	9	0.41	-0.10	0.20	0.27
39	ch4_syo_surface-insitu_8_representative	8	-69.00	39.58	22.00	1089	0.20	-0.04	0.09	0.23
40	ch4_tac_surface-flask_1_representative	1	52.52	1.14	236.00	40	0.65	-0.18	0.14	0.17
41	ch4_tap_surface-flask_1_representative	1	36.73	126.13	21.00	539	1.31	-0.11	0.18	0.04

42	**ch4_vrs_surface-flask_45_representative**	45	81.58	-16.64	34.00	55	0.39	0.08	0.20	0.33
43	**ch4_wlg_surface-flask_1_representative**	1	36.29	100.90	3815.00	631	0.51	-0.02	0.11	0.17
44	**ch4_wpc_shipboard-flask_1_representative**	1	0.83	151.22	10.00	118	0.21	-0.03	0.13	0.67
45	**ch4_zep_surface-flask_1_representative**	1	78.91	11.89	479.00	571	0.22	0.01	0.13	0.74
46	**ch4_zot_surface-flask_45_representative**	45	64.48	89.21	414.00	610	0.72	0.16	0.29	0.39

Unassimilated

	Site Code	Laboratory	Latitude	Longitude	Elevation (MASL)	No. of Observation	Model-data mismatch	Mean bias	Standard deviation of bias	Chi-squared
1	**ch4_above_aircraft-pfp_1_allvalid**	1	65.35	-142.58	1985.71	299	N/A	0.00	0.23	N/A
2	**ch4_acg_aircraft-pfp_1_allvalid**	1	68.75	-150.99	2039.44	809	N/A	0.04	0.23	N/A
3	**ch4_act_aircraft-pfp_1_allvalid-b200**	1	36.85	-89.17	1828.73	448	N/A	-0.09	0.23	N/A
4	**ch4_act_aircraft-pfp_1_allvalid-c130**	1	38.25	-87.21	2269.72	632	N/A	-0.10	0.19	N/A
5	**ch4_alk_aircraft-flask_8_allvalid**	8	65.88	-152.16	2092.95	63	N/A	-0.09	0.13	N/A
6	**ch4_alt_surface-flask_1_representative**	1	82.45	-62.51	190.00	1037	N/A	0.00	0.14	N/A
7	**ch4_alt_surface-flask_45_representative**	45	82.45	-62.51	190.00	285	N/A	0.32	0.44	N/A
8	**ch4_amy_surface-flask_1_representative**	1	36.54	126.33	87.00	224	N/A	-0.11	0.20	N/A
9	**ch4_asc_surface-flask_1_representative**	1	-7.97	-14.40	90.00	1292	N/A	-0.07	0.11	N/A
10	**ch4_azr_surface-flask_1_representative**	1	38.76	-27.34	24.00	387	N/A	-0.02	0.19	N/A
11	**ch4_bal_surface-flask_1_representative**	1	55.35	17.22	28.00	206	N/A	-0.05	0.17	N/A
12	**ch4_bhd_surface-flask_1_representative**	1	-41.41	174.87	93.75	150	N/A	-0.11	0.07	N/A
13	**ch4_bhd_surface-insitu_15_baseline**	15	-41.41	174.87	95.00	376	N/A	-0.12	0.06	N/A
14	**ch4_bik_surface-flask_45_representative**	45	53.20	22.75	483.00	144	N/A	0.05	0.31	N/A
15	**ch4_bmw_surface-flask_1_representative**	1	32.26	-64.88	51.30	17	N/A	-0.06	0.08	N/A
16	**ch4_brw_surface-flask_1_representative**	1	71.32	-156.61	22.53	1407	N/A	0.04	0.13	N/A
17	**ch4_bsc_surface-flask_1_representative**	1	44.18	28.66	5.00	10	N/A	0.01	0.15	N/A
18	**ch4_cba_surface-flask_1_representative**	1	55.21	-162.72	57.04	969	N/A	0.08	0.13	N/A
19	**ch4_cbw_surface-insitu_118_allvalid**	118	51.97	4.93	37.00	1969	N/A	0.53	0.82	N/A
20	**ch4_cgo_surface-flask_1_representative**	1	-40.68	144.68	164.00	643	N/A	-0.08	0.10	N/A
21	**ch4_chr_surface-flask_1_representative**	1	1.70	-157.15	5.00	8	N/A	-0.06	0.08	N/A
22	**ch4_cib_surface-flask_1_representative**	1	41.81	-4.93	850.00	2	N/A	-0.17	0.15	N/A
23	**ch4_con_aircraft-flask_42_allvalid**	42	8.40	149.05	11313.42	394	N/A	-0.04	0.22	N/A
24	**ch4_crv_aircraft-pfp_1_allvalid**	1	65.64	-152.47	1284.20	1425	N/A	0.21	0.40	N/A
25	**ch4_crv_surface-pfp_1_allvalid-32magl**	1	64.99	-147.60	643.13	1121	N/A	0.01	0.37	N/A
26	**ch4_cvo_surface-flask_45_representative**	45	16.86	-24.87	40.00	481	N/A	-0.01	0.25	N/A
27	**ch4_eic_surface-flask_1_representative**	1	-27.16	-109.43	69.00	77	N/A	-0.09	0.07	N/A
28	**ch4_gmi_surface-flask_1_representative**	1	13.39	144.66	5.00	215	N/A	-0.12	0.11	N/A
29	**ch4_gvn_surface-flask_45_representative**	45	-70.67	-8.27	44.00	195	N/A	0.06	0.22	N/A
30	**ch4_hip_aircraft-pfp_1_allvalid**	1	19.74	-91.17	5122.98	210	N/A	0.08	0.31	N/A

31	**ch4_inx_aircraft-pfp_1_allvalid**	1	39.86	-86.06	801.16	149	N/A	0.03	0.27	N/A
32	**ch4_inx_surface-pfp_1_allvalid-121magl**	1	39.58	-86.42	376.73	6	N/A	-0.05	0.10	N/A
33	**ch4_inx_surface-pfp_1_allvalid-129magl**	1	39.86	-85.74	407.82	3	N/A	-0.01	0.16	N/A
34	**ch4_inx_surface-pfp_1_allvalid-39magl**	1	39.92	-86.03	290.78	5	N/A	-0.03	0.11	N/A
35	**ch4_jfj_surface-flask_45_representative**	45	46.55	7.99	3570.00	190	N/A	0.22	0.41	N/A
36	**ch4_kjn_surface-flask_45_representative**	45	70.85	29.23	10.00	171	N/A	0.15	0.19	N/A
37	**ch4_krk_surface-insitu_118_allvalid**	118	50.07	19.91	255.00	3008	N/A	-0.33	0.37	N/A
38	**ch4_kum_surface-flask_1_representative**	1	19.54	-154.85	8.55	894	N/A	-0.06	0.10	N/A
39	**ch4_llb_surface-flask_1_representative**	1	54.95	-112.45	567.83	133	N/A	0.10	0.44	N/A
40	**ch4_lut_surface-insitu_118_allvalid**	118	53.40	6.35	61.00	1617	N/A	0.10	0.59	N/A
41	**ch4_mex_surface-flask_1_representative**	1	18.98	-97.31	4469.00	398	N/A	-0.07	0.15	N/A
42	**ch4_mhd_surface-flask_1_representative**	1	53.32	-9.90	25.33	591	N/A	-0.09	0.13	N/A
43	**ch4_mid_surface-flask_1_representative**	1	28.21	-177.37	12.99	296	N/A	-0.03	0.10	N/A
44	**ch4_mlo_surface-flask_1_representative**	1	19.53	-155.58	3419.12	1595	N/A	-0.07	0.10	N/A
45	**ch4_mrc_aircraft-pfp_1_allvalid**	1	41.73	-76.26	1285.30	65	N/A	-0.23	0.16	N/A
46	**ch4_mrc_surface-pfp_1_allvalid-east**	1	41.77	-75.68	509.02	141	N/A	-0.20	0.21	N/A
47	**ch4_mrc_surface-pfp_1_allvalid-south**	1	41.47	-76.42	651.99	631	N/A	-0.16	0.20	N/A
48	**ch4_nam_surface-flask_45_representative**	45	-23.56	15.05	431.00	286	N/A	0.03	0.29	N/A
49	**ch4_ngm_shipboard-flask_8_allvalid**	8	-8.18	152.70	20.00	463	N/A	-0.10	0.28	N/A
50	**ch4_nsa_aircraft-pfp_1_allvalid**	1	70.02	-151.02	1083.82	112	N/A	0.00	0.43	N/A
51	**ch4_nwr_surface-flask_1_representative**	1	40.05	-105.58	3526.00	815	N/A	-0.10	0.12	N/A
52	**ch4_nya_surface-flask_8_representative**	8	78.92	11.93	43.00	893	N/A	-1.62	15.72	N/A
53	**ch4_oxk_surface-flask_45_representative**	45	50.03	11.81	1185.00	205	N/A	0.02	0.22	N/A
54	**ch4_pfa_aircraft-pfp_1_allvalid**	1	64.83	-148.63	1723.19	1597	N/A	-0.03	0.73	N/A
55	**ch4_sdz_surface-flask_1_representative**	1	40.65	117.12	298.00	4	N/A	-0.38	0.25	N/A
56	**ch4_sgp_aircraft-pfp_1_allvalid**	1	36.61	-97.49	2407.51	12	N/A	-0.03	0.09	N/A
57	**ch4_sis_surface-flask_45_representative**	45	60.09	-1.26	35.00	561	N/A	0.03	0.28	N/A
58	**ch4_smo_surface-flask_1_representative**	1	-14.25	-170.56	53.02	1457	N/A	-0.05	0.10	N/A
59	**ch4_spo_surface-flask_1_representative**	1	-89.98	-24.80	2817.16	1256	N/A	-0.09	0.11	N/A
60	**ch4_sum_surface-flask_1_representative**	1	72.60	-38.42	3214.54	493	N/A	-0.01	0.14	N/A
61	**ch4_sur_aircraft-flask_20_allvalid**	20	61.20	73.20	2000.00	9	N/A	-0.89	0.00	N/A
62	**ch4_syo_surface-insitu_8_representative**	8	-69.00	39.58	22.00	1089	N/A	-3.38	22.03	N/A
63	**ch4_tac_surface-flask_1_representative**	1	52.52	1.14	236.00	40	N/A	-0.18	0.16	N/A
64	**ch4_tap_surface-flask_1_representative**	1	36.73	126.13	21.00	539	N/A	-0.08	0.20	N/A
65	**ch4_tom_aircraft-pfp_1_allvalid**	1	11.25	-79.52	5236.41	1090	N/A	-0.06	0.22	N/A
66	**ch4_vrs_surface-flask_45_representative**	45	81.58	-16.64	34.00	55	N/A	0.15	0.43	N/A
67	**ch4_wgc_surface-pfp_1_allvalid-89magl**	1	38.26	-121.49	91.10	132	N/A	-0.22	0.36	N/A
68	**ch4_wlg_surface-flask_1_representative**	1	36.29	100.90	3815.00	631	N/A	-0.03	0.13	N/A
69	**ch4_wpc_shipboard-flask_1_representative**	1	25.07	139.23	10.00	118	N/A	-0.04	0.21	N/A

70	**ch4_zep_surface-flask_1_representative**	1	78.91	11.89	479.00	571	N/A	0.01	0.16	N/A
71	**ch4_zot_surface-flask_45_representative**	45	64.48	89.21	414.00	610	N/A	0.22	0.44	N/A

C. Atmospheric inversion setup

1. The TM5 Atmospheric Transport Model

The global chemistry Transport Model, version 5 (TM5) is developed and maintained jointly by the Institute for Marine and Atmospheric Research Utrecht (IMAU, the Netherlands), the Joint Research Centre (JRC, Italy), the Royal Netherlands Meteorological Institute (KNMI, the Netherlands), and the National Oceanic & Atmospheric Administration (NOAA) Global Monitoring Laboratory (GML, USA) (Krol et al. 2005; Bruhwiler et al. 2014; Peters et al. 2007). The model simulates atmospheric transport using input from the European Center for Medium range Weather Forecast (ECMWF) model. TM5 has detailed treatments of advection, convection (deep and shallow), and vertical diffusion in the planetary boundary layer and free troposphere.

The winds which drive TM5 come from the ECMWF operational forecast model. This "parent" model currently runs with ~25 km horizontal resolution and 60 layers in the vertical before 2006 (and 91 layers in the vertical from 2006 onwards). Since the ERA-interim product is not available after September 2019, we switched meteorological inputs from ERA-interim to ERA-5, which covers the Earth on a 30 km grid and resolves the atmosphere using 137 levels from the surface up to a height of 80km (Hersbach et al. 2020).

For use in TM5, the ECMWF meteorological data are preprocessed into mass fluxes at coarser horizontal and vertical resolution. In this release of CarbonTracker-CH_4, TM5 is run at a global 3°x 2° spatial resolution and 30-minute temporal resolution. The vertical resolution of TM5 in CarbonTracker-CH_4 is 25 hybrid sigma-pressure levels. The approximate heights of the mid-levels (in meters, with a surface pressure of 1012 hPa) are summarized in Table 8.

Table 8. Approximate heights of the vertical model layers.

Level	Height (m)	Level	Height (m)
1	34.5	14	9076.6
2	111.9	15	10533.3
3	256.9	16	12108.3
4	490.4	17	13874.2
5	826.4	18	15860.1
6	1274.1	19	18093.2
7	1839	20	20590
8	2524	21	24247.3

9	3329.9	22	29859.6
10	4255.6	23	35695
11	5298.5	24	42551.5
12	6453.8	25	80000
13	7715.4		

2. 4DVAR inversion setup

2.1. Inversion framework

We use the TM5-4DVAR inversion framework (Meirink et al. 2008), which has been used to estimate surface fluxes of CO, CO_2, and CH_4 (Hooghiemstra & van Ees 2011; Bergamaschi et al. 2013; Krol et al. 2013; Basu et al. 2014) in single-tracer inversions, as well as source-specific CO_2 fluxes in multi-tracer inversions (Ma et al. 2021; Basu et al. 2020; Basu et al. 2022).

Two tracers are simulated in our inversion: total CH_4 or *C* and the artificial tracer *Cxδ'*, where $\delta' = (^{13}CH_4/CH_4)/r_{std}-1$. More details can be found in (Basu et al. 2022). TM5-4DVAR minimizes a cost function *J* in equation below, as a function of surface fluxes *x* by balancing fits to atmospheric observations *y* with deviations from the prior fluxes x_0,

$$J(x) = 1/2\ (Hx-y)^T R^{-1}(Hx-y) + 1/2(x-x_0)^T B^{-1}(x-x_0)$$

where *H* is the transport, chemistry, and observation operator connecting surface fluxes with atmospheric measurements, and *R* and *B* are the error covariances of *Hx−y* and prior fluxes, respectively, and R was set based on the model-data mismatch setup (Tables 6-7). From the inversion, we optimize monthly surface fluxes (*x*, posterior flux) for microbial, fossil, and pyrogenic sources at 3°x 2° spatial resolution.

2.2. Prior error covariance

For each source type (pyrogenic, fossil, and microbial), the diagonal elements of *B* per time step and lateral grid cell are proportional (f in Table 7) to the prior flux (x_0), or $f \times x_0$. Off-diagonal elements of *B* are constructed assuming an exponential decay of the prior error correlation in space and time with source-specific scales *λ* and *τ*, respectively. By following Basu et al. (2022), we also followed the source-specific scales to be the same as Table 9.

Table 9. Parameters for constructing the prior flux error covariance.

	Diagonal uncertainty (f, %)	Off-diagonal spatial (λ, km)	Off-diagonal temporal (τ, months)
Microbial	120	500	2
Fossil	150	700	6
Pyrogenic	100	300	1

2.3. Simulation setup

The cost function J is minimized over 65-100 iterations by an M1QN3 minimizer, which utilizes a limited memory quasi-Newton technique (the L-BFGS method of J. Nocedal) with a dynamically updated scalar or diagonal preconditioner. Due to the long computation time for inversion, we split our simulation periods into 8 inversions that were run in parallel. Eight 5-year inversions were run simultaneously with 2 years of overlap (first and last years) between inversions, starting in 1997, 2000, 2003, 2006, 2009, 2012, 2015, and 2018. After all eight inversions finished, the fluxes from the middle 3-year period of each inversion were considered for analysis. For simulating prior and posterior mole fractions, fluxes from the non-overlapping periods were stitched together and a single forward run was done with those long-term posterior fluxes.

2.4. Uncertainty estimation

We estimated the uncertainty of our simulation using 100 ensemble members with different random uncertainties in prior flux and observations. The random uncertainties are associated with components of the inversion system whose errors are assumed to be zero on average. We construct the ensembles with prior fluxes and observations perturbed according to the covariances specified by B and R, respectively. With 100 ensemble members, our estimate is expected to be within 10 % of the exact analytical solution. More information can be found in (Basu et al. 2022).

D. Outputs

Spatial flux maps and bar charts of optimized emissions can be found at https://gml.noaa.gov/ccgg/carbontracker-ch4/fluxes.html. These pages give access to maps and bar charts illustrating the estimated microbial, fossil, and pyrogenic CH_4 emission fluxes. On the flux maps page, users may select the entire time period, a single month, or a year at different regions to see prior and posterior CH_4 fluxes of microbial, fossil, and pyrogenic sources. Flux bar charts pages show long-term prior and posterior CH_4 fluxes of microbial, fossil, and pyrogenic sources at monthly and yearly timescale.

Second, evaluation and observation tabs are available to compare the simulated atmospheric CH_4 and $\delta^{13}C\text{-}CH_4$ with observations using various metrics: https://gml.noaa.gov/ccgg/carbontracker-ch4/network_map3.html and https://gml.noaa.gov/ccgg/carbontracker-ch4/evaluation.html. Specifically, we provide interactive plots of time series of atmospheric CH_4 and $\delta^{13}C\text{-}CH_4$, prior, post-assimilation (posterior), withheld, and observed, at each observation site and aircraft profile. We provide three diagnostics to evaluate this version of inversion system: (1) Comparison of prior, posterior, and observed atmospheric CH_4 and $\delta^{13}C\text{-}CH_4$ from all assimilated and un-assimilated sites, (2) Comparison of posterior and observed CH_4 and $\delta^{13}C\text{-}CH_4$ for independent Aircraft Profiles, and (3) Large-scale averages and growth rates of prior, posterior, and observed atmospheric CH_4 and $\delta^{13}C\text{-}CH_4$.

Third, three-dimensional atmospheric methane concentrations simulated with optimized emissions by CarbonTracker-CH_4 are visualized as sphere and 3-D volume plots at monthly timescale: https://gml.noaa.gov/ccgg/carbontracker-ch4/visualization.html.

Lastly, users can download the optimized (posterior) surface emissions from microbial, fossil, and pyrogenic sources (1x1°, monthly) and optimized 4-dimensional atmospheric CH_4 mole fractions (3x2° horizontal grids and 25 vertical layers, 3-hourly) globally from this page: https://gml.noaa.gov/ccgg/carbontracker-ch4/download.html.

E. References

Abbott, D.W. et al., 2020. Seaweed and Seaweed Bioactives for Mitigation of Enteric Methane: Challenges and Opportunities. *Animals : an open access journal from MDPI*, 10(12). Available at: http://dx.doi.org/10.3390/ani10122432.

Basu, S. et al., 2022. Estimating emissions of methane consistent with atmospheric measurements of methane and δ 13 C of methane. *Atmospheric Chemistry and Physics*, 22(23), pp.15351–15377.

Basu, S. et al., 2014. The seasonal variation of the CO2 flux over Tropical Asia estimated from GOSAT, CONTRAIL, and IASI. *Geophysical research letters*, 41(5), pp.1809–1815.

Bergamaschi, P. et al., 2013. Atmospheric CH4 in the first decade of the 21st century: Inverse modeling analysis using SCIAMACHY satellite retrievals and NOAA surface measurements. *Journal of Geophysical Research, D: Atmospheres*, 118(13), pp.7350–7369.

Bergamaschi, P. et al., 2005. Inverse modelling of national and European CH4 emissions using the atmospheric zoom model TM5 To cite this version : HAL Id : hal-00328403 and Physics Inverse modelling of national and European CH 4 emissions using the atmospheric zoom model TM5.

Bruhwiler, L. et al., 2014. CarbonTracker-CH4: An assimilation system for estimating emissions of atmospheric methane. *Atmospheric Chemistry and Physics*, 14(16), pp.8269–8293.

Calle, L. & Poulter, B., 2020. Ecosystem age-class dynamics and distribution in the LPJ-wsl v2. 0 global ecosystem model. *Geoscientific Model Development Discussions*, 2020, pp.1–44.

Cantrell, C.A. et al., 1990. Carbon kinetic isotope effect in the oxidation of methane by the hydroxyl radical. *Journal of Geophysical Research, D: Atmospheres*, 95(D13), pp.22455–22462.

Chang, J. et al., 2019. Revisiting enteric methane emissions from domestic ruminants and their δ 13 C CH4 source signature. *Nature communications*, 10(1), pp.1–14.

Crippa, M. et al., 2020. Fossil CO2 emissions of all world countries. *Luxembourg: European Commission*, pp.1–244.

Etiope, G. et al., 2019. Gridded maps of geological methane emissions and their isotopic signature. *Earth System Science Data*, 11(1), pp.1–22.

European Commission et al., 2023. *GHG emissions of all world countries – 2023*, Publications Office of the European Union.

Ganesan, A.L. et al., 2018. Spatially Resolved Isotopic Source Signatures of Wetland Methane Emissions. *Geophysical research letters*, 45(8), pp.3737–3745.

Gromov, S., Brenninkmeijer, C.A.M. & Jöckel, P., 2018. A very limited role of tropospheric chlorine as a sink of the greenhouse gas methane. *Atmospheric Chemistry and Physics*, 18(13), pp.9831–9843.

Hersbach, H. et al., 2020. The ERA5 global reanalysis. *Quarterly Journal of the Royal Meteorological Society*, 146(730), pp.1999–2049.

Hmiel, B. et al., 2020. Preindustrial 14CH4 indicates greater anthropogenic fossil CH4 emissions. *Nature*, 578, pp.409–412.

Hooghiemstra, R. & van Ees, H., 2011. Uniformity as response to soft law: Evidence from compliance and non-compliance with the Dutch corporate governance code. *Regulation & Governance*, 5(4), pp.480–498.

Janssens-Maenhout, G. et al., 2019. EDGAR v4. 3.2 Global Atlas of the three major greenhouse gas emissions for the period 1970--2012. *Earth System Science Data*, 11(3), pp.959–1002.

Jöckel, P. et al., 2006. The atmospheric chemistry general circulation model ECHAM5/MESSy1: consistent simulation of ozone from the surface to the mesosphere. *Atmospheric Chemistry and Physics*, 6(12), pp.5067–5104.

Judd, A.G., 2004. Natural seabed gas seeps as sources of atmospheric methane. *Environmental geology*, 46(8), pp.988–996.

King S. L. Quay P. D. Lansdown J., M., 1989. The 13C /12C Kinetic Isotope Effect for Soil Oxidation of Methane increase. *Journal of geophysical research*, 94, pp.273–277.

Krol, M. et al., 2013. How much CO was emitted by the 2010 fires around Moscow? *Atmospheric Chemistry and Physics*, 13(9), pp.4737–4747.

Krol, M. et al., 2005. The two-way nested global chemistry-transport zoom model TM5: algorithm and applications. *Atmospheric Chemistry and Physics*, 5(2), pp.417–432.

Krol, M., van Leeuwen, P.J. & Lelieveld, J., 1998. Global OH trend inferred from methylchloroform measurements. *Journal of geophysical research*, 103(D9), pp.10697–10711.

Lan, X. et al., 2021. Improved constraints on global methane emissions and sinks using $\delta^{13}C\text{-}CH_4$. *Global biogeochemical cycles*.

Lee, J. et al., 2023. Soil organic carbon is a key determinant of CH4 sink in global forest soils. *Nature communications*, 14(1), p.3110.

Le Mer, J. & Roger, P., 2001. Production, oxidation, emission and consumption of methane by soils: a review. *European journal of soil biology*, 37(1), pp.25–50.

Liu, L. et al., 2020. Uncertainty Quantification of Global Net Methane Emissions from Terrestrial Ecosystems Using a Mechanistically-based Biogeochemistry Model. *Journal of Geophysical Research: Biogeosciences*, 125(6), p.e2019JG005428.

Masarie, K.A. et al., 2014. ObsPack: a framework for the preparation, delivery, and attribution of atmospheric greenhouse gas measurements. *Earth System Science Data*, 6(2), pp.375–384.

McNicol, G. et al., 2023. Upscaling wetland methane emissions from the FLUXNET‐CH4 eddy covariance network (UpCH4 v1.0): Model development, network assessment, and budget comparison. *AGU Advances*, 4(5). Available at: https://agupubs.onlinelibrary.wiley.com/doi/abs/10.1029/2023AV000956.

Meirink, J.F., Bergamaschi, P. & Krol, M.C., 2008. Four-dimensional variational data assimilation for inverse modelling of atmospheric methane emissions: method and comparison with synthesis inversion. *Atmospheric Chemistry and Physics*, 8(21), pp.6341–6353.

Miller, J.B. et al., 2002. Development of analytical methods and measurements of 13C/12C in atmospheric CH4 from the NOAA Climate Monitoring and Diagnostics Laboratory Global Air Sampling Network. *Journal of Geophysical Research, D: Atmospheres*, 107(13).

Montzka, S.A. et al., 2011. Small interannual variability of global atmospheric hydroxyl. *Science*, 331(6013), pp.67–69.

Oh, Y. et al., 2020. Reduced net methane emissions due to microbial methane oxidation in a warmer Arctic. *Nature climate change*, 10(4), pp.317–321.

Patra, P.K. et al., 2014. Observational evidence for interhemispheric hydroxyl-radical parity. *Nature*, 513(7517), pp.219–223.

Peters, W. et al., 2007. An atmospheric perspective on North American carbon dioxide exchange: CarbonTracker. *Proceedings of the National Academy of Sciences of the United States of America*, 104(48), pp.18925–18930.

Randerson, J.T. et al., 2012. Global burned area and biomass burning emissions from small fires. *Journal of Geophysical Research: Biogeosciences*, 117(G4).

Randerson, J.T. et al., 2018. Global Fire Emissions Database, Version 4.1 (GFEDv4). *ORNL DAAC, Oak Ridge, Tennessee, USA*.

Ren, T. & Patel, M.K., 2009. Basic petrochemicals from natural gas, coal and biomass: Energy use and CO2 emissions. *Resources, Conservation and Recycling*, 53(9), pp.513–528.

Rosentreter, J.A. et al., 2021. Half of global methane emissions come from highly variable aquatic ecosystem sources. *Nature geoscience*, 14(4), pp.225–230.

Saueressig, G. et al., 2001. Carbon 13 and D kinetic isotope effects in the reactions of CH4 with O (1 D) and OH: new laboratory measurements and their implications for the isotopic composition of stratospheric methane. *Journal of Geophysical Research, D: Atmospheres*, 106(D19), pp.23127–23138.

Saunois, M. et al., 2020. The Global Methane Budget 2000 – 2017. , pp.1561–1623.

Schuur, E.A.G. et al., 2022. Permafrost and Climate Change: Carbon Cycle Feedbacks From the Warming Arctic. *Annual review of environment and resources*, 47(1), pp.343–371.

Sherwood, O.A. et al., 2017. Global inventory of gas geochemistry data from fossil fuel, microbial and burning sources, version 2017. *Earth System Science Data*, 9(2), pp.639–656.

Sherwood, O.A., Schwietzke, S. & Lan, X., 2021. Global δ13C-CH4 source signature inventory 2020. *Monitoring Laboratory Data Repository [data set ….*

Spivakovsky, C.M. et al., 2000. Three‐dimensional climatological distribution of tropospheric OH: Update and evaluation. *Journal of Geophysical Research, D: Atmospheres*, 105(D7), pp.8931–8980.

Still, C.J. et al., 2003. Global distribution of C 3 and C 4 vegetation: Carbon cycle implications. *Global biogeochemical cycles*, 17(1), pp.6–1–6–14.

Strode, S.A. et al., 2020. Strong sensitivity of the isotopic composition of methane to the plausible range of tropospheric chlorine. *Atmospheric Chemistry and Physics*, 20(14), pp.8405–8419.

Themelis, N.J. & Bourtsalas, A.C., 2021. Methane generation and capture of US landfills. *J. Environ. Sci. Eng. A*, 10, pp.199–206.

Umezawa, T. et al., 2012. Carbon and hydrogen isotopic ratios of atmospheric methane in the upper troposphere over the Western Pacific. *Atmospheric Chemistry and Physics*, 12(17), pp.8095–8113.

Van Der Werf, G.R. et al., 2017. Global fire emissions estimates during 1997--2016. *Earth System Science Data*, 9(2), pp.697–720.

Wang, X. et al., 2019. The role of chlorine in global tropospheric chemistry. *Atmospheric Chemistry and Physics*, 19(6), pp.3981–4003.

Zhang, Z. et al., 2017. Emerging role of wetland methane emissions in driving 21st century climate change. *Proceedings of the National Academy of Sciences of the United States of America*, 114(36), pp.9647–9652.

Zhang, Z. et al., 2025. Ensemble estimates of global wetland methane emissions over 2000–2020. *Biogeosciences*, 22(1), pp.305–321.

Zhang, Z. et al., 2015. Modeling spatiotemporal dynamics of global wetlands: comprehensive evaluation of a new sub-grid TOPMODEL parameterization and uncertainties. *Biogeosciences*, 13, pp.1387–1408.

Zhang, Z. et al., 2023. Recent intensification of wetland methane feedback. *Nature climate change*, 13(5), pp.430–433.

Zhou, L. et al., 2023. Spatiotemporal Variability of Global Atmospheric Methane Observed from Two Decades of Satellite Hyperspectral Infrared Sounders. *Remote Sensing*, 15(12), p.2992.

Zhuang, Q. et al., 2023. Current and future global lake methane emissions: A process‐based modeling analysis. *Journal of geophysical research. Biogeosciences*, 128(3). Available at: https://agupubs.onlinelibrary.wiley.com/doi/10.1029/2022JG007137.

Zhuang, Q. et al., 2013. Response of global soil consumption of atmospheric methane to changes in atmospheric climate and nitrogen deposition. *Global biogeochemical cycles*, 27(3), pp.650–663.